



Risk-based optimal inspection strategy of structural systems using dynamic Bayesian networks

Jesus Humberto Luque Jimenez

Vollständiger Abdruck der von der TUM School of Engineering and Design der Technischen Universität München zur Erlangung des akademischen Grades eines Doktors der Ingenieurwissenschaften genehmigten Dissertation.

Vorsitzender: Prof. Dr.-Ing. habil. Fabian Duddeck

Prüfende der Dissertation:

1. Prof. Dr. sc. techn. Daniel Straub
2. Prof. Michael Havbro Faber Nielsen, Ph.D.
Aalborg University / Dänemark

Die Dissertation wurde am 07.04.2022 bei der Technischen Universität München eingereicht und durch die TUM School of Engineering and Design am 29.09.2022 angenommen.

Contents

Acknowledgements	i
Abstract	iii
List of publications	v
1 Introduction	1
1.1 Overview	1
1.2 State of the art	3
1.3 Statement of purpose and proposed solution	5
1.4 Thesis structure	6
2 Bayesian networks and influence diagrams	7
2.1 Bayesian Networks	7
2.2 Bayesian inference	8
2.3 Dynamic BNs	9
2.4 Hierarchical BNs	10
2.5 Influence diagrams	12
3 Risk-based inspection planning	15
3.1 Mathematical formulation of the optimization problem	15
3.2 Optimization at the component level	16
3.3 Optimization at the system level	17
3.3.1 Heuristic strategy approach (to reduce the number of strategies)	18
3.3.2 Simulation-based approach (to approximate the expected cost of a strategy) ..	19
3.3.3 DBN deterioration model	19
3.3.4 The inference algorithm (to compute the updated probabilities given the	
inspection outcomes)	21
3.3.5 Flowchart of the optimization methodology	21
4 Case studies / Results	23
4.1 Hierarchical model for uniform corrosion in ship vessels	23
4.2 Reliability analysis of a Daniels system	29
4.3 Reliability analysis of a 2D tubular structure – the Zayas frame	33
4.4 Full optimization vs heuristic rules	37
4.5 Integral risk-based inspection planning	41
5 Paper A	45
A.1 Introduction	46
A.2 Dynamic Bayesian networks and influence diagrams	47
A.2.1 Bayesian networks	47
A.2.2 Dynamic Bayesian networks	48
A.2.3 Influence diagrams	48
A.2.4 Policies and strategies	49
A.3 Risk-based planning of inspections using influence diagrams for a structural element	
subject to fatigue	50
A.3.1 Fatigue crack growth model	50
A.3.2 Influence diagram for modeling inspections	51
A.3.3 Memory assumptions in the ID model	53
A.3.4 Finding optimal inspection times with the ID	54
A.4 Numerical investigations	55
A.5 Conclusions and outlook	60
6 Paper B	61
B.1 Introduction	62
B.2 Dynamic Bayesian network for assessing component deterioration	65
B.2.1 DBN model of a single component	65

B.2.2	Computation of the posterior distribution.....	66
B.2.3	Discretization of continuous random variables.....	66
B.3	Bayesian network model of system deterioration.....	67
B.3.1	Hierarchical models.....	68
B.3.2	Hierarchical model based on correlation models.....	68
B.3.3	DBN model of the system.....	70
B.3.4	Inference algorithm.....	72
B.3.5	Computational complexity of the algorithm.....	75
B.4	Numerical investigation.....	76
B.4.1	Daniels system.....	76
B.4.2	Steel frame.....	85
B.5	Discussion.....	90
B.6	Conclusions.....	92
7	Paper C.....	93
C.1	Introduction.....	94
C.2	Spatio-temporal corrosion models for ship structures.....	97
C.2.1	Hierarchical Bayesian models.....	97
C.2.2	Hierarchical structure of the corrosion model.....	99
C.2.3	Thickness measurements.....	101
C.2.4	Corrosion model.....	102
C.2.5	Thickness margin.....	102
C.2.6	Coating life.....	103
C.2.7	Parameters of the corrosion model.....	104
C.2.8	Measurement model.....	107
C.2.9	Complete hierarchical corrosion model.....	107
C.2.10	Parameter estimation.....	108
C.3	Numerical investigations.....	108
C.3.1	Case study 1: Simulated scenario.....	109
C.3.2	Case study 2: Corrosion in tanker floors.....	111
C.3.3	Analysis of a specific vessel.....	113
C.4	Discussion.....	116
C.5	Conclusions.....	118
8	Paper D.....	119
D.1	Introduction.....	120
D.2	Methodology.....	122
D.2.1	The inspection optimization problem.....	122
D.2.2	Optimization at the component level.....	125
D.2.3	Optimization at the system level.....	130
D.2.4	DBN framework.....	132
D.2.5	Summary of the proposed methodology.....	134
D.3	Numerical investigations.....	135
D.3.1	System definition.....	135
D.3.2	Deterioration and inspection model.....	136
D.3.3	Costs and failure risk.....	139
D.3.4	Optimization.....	140
D.3.5	Results.....	141
D.4	Discussion.....	146
D.5	Conclusions.....	147
9	Concluding remarks.....	149
9.1	Discussion.....	149

9.2 Future research..... 153
9.3 Conclusions..... 157
References..... 159

Acknowledgements

To the patience of Daniel Straub.

This work was supported by the Deutsche Forschungsgemeinschaft (DFG) through Grant STR 1140/3-1 and the Consejo Nacional de Ciencia y Tecnología (CONACYT) through Grant No. 311700.

Abstract

In most structural systems, it is neither possible nor optimal to inspect all system components regularly. An optimal inspection-repair strategy controls deterioration in structural systems efficiently with limited cost and acceptable reliability. At present, an integral risk-based optimization procedure for entire structural systems is not available; existing risk-based inspection methods are limited to optimizing inspections component by component. The challenges to an integral approach lie in the large number of optimization parameters in the inspection-repair process of a structural system, and the need to perform probabilistic inference for the entire system at once to address interdependencies among all components. This thesis presents solutions to some of those challenges.

A multi-level hierarchical Bayesian network (BN) model is developed to represent complex spatio-temporal deterioration processes. The model provides a flexible and general framework to include dependencies in the deterioration states among different locations in the structural system. Its implementation in a real-life structure is shown with a case study on corrosion in ship vessels, where the deterioration process and other variables involved are estimated based on a set of measurements. To obtain such estimations, Markov Chain Monte Carlo is used as inference algorithm.

Performing inference in multi-level hierarchical BNs can be computationally expensive, mainly due to the large number of model parameters to estimate. To address this computational challenge of the inspection planning problem, a hierarchical dynamic Bayesian network (DBN) framework with a tailor-made inference algorithm is proposed. The simpler spatial representation (through a single hierarchical level) and the customized inference algorithm allow computing rapidly and efficiently the system reliability conditional on inspection results. The DBN framework uses a heuristic approach for reducing the number of possible inspection/maintenance strategies and nests the DBN inside a Monte Carlo simulation for computing the expected cost associated with a system-wide inspection strategy. In contrast to existing methods, the DBN framework can simultaneously account for system effects arising from (a) the dependence among the deterioration at different components, (b) the joint effect of deterioration at multiple components on the system reliability, and (c) the interaction among inspection costs, i.e. the reduction in the marginal cost of an inspection if these are grouped in larger inspection campaigns. The DBN framework is applicable to a wide variety of structures subject to deterioration processes including offshore platforms, bridges, ships, and aircraft structures. The accuracy and robustness of the approach is demonstrated in a theoretical structure (Daniels system) and a laboratory structure (Zayas frame) subject to fatigue.

List of publications

This cumulative thesis is based on the papers listed below.

- PAPER A:** Luque J., Straub D. (2013). Algorithms for optimal risk-based planning of inspections using influence diagrams. *Proc. 11th International Probabilistic Workshop*, Brno, Czech Republic.
- PAPER B:** Luque J., Straub D. (2016). Reliability analysis and updating of deteriorating structural systems with dynamic Bayesian networks. *Structural Safety*, **62**, 34–46.
- PAPER C:** Luque J., Hamann R., Straub D. (2017). Spatial probabilistic modeling of corrosion in ship structures. *ASCE-ASME Journal of Risk and Uncertainty in Engineering Systems Part B: Mechanical Engineering*, 2017; **3(3)**: 031001-12
- PAPER D:** Luque J., Straub D. (2019). Risk-based optimal inspection strategies for structural systems using dynamic Bayesian networks. *Structural Safety* **76**, 68-80.

The following conference papers are the antecedent of some of the journal papers from above, and are not explicitly included in this thesis.

- PAPER E:** Luque J., Hamann R., Straub D., (2014). Spatial model for corrosion in ships and FPSOs. *Proceedings of OMAE, 33rd International Conference on Offshore Mechanics and Arctic Engineering*, San Francisco, CA.
- PAPER F:** Luque J., Straub D., (2015). Reliability analysis of monitored deteriorating structural systems with dynamic Bayesian networks. *Proc. 12th International Conference on Applications of Statistics and Probability in Civil Engineering*, Vancouver, Canada.

1 Introduction

1.1 Overview

Engineering structures are subject to deterioration, which reduces their service lives and can endanger the operation of the structure, workers' and other people's lives, and can impact the environment. Deterioration processes like corrosion and metal fatigue affect the capacity of the components and of the whole structural system, making the latter more vulnerable to conditions that were not considered as potentially risky during the first years of the structure's operation. This can lead to wrong or catastrophic decisions. Figure 1 shows a timeline of some of the most known catastrophic structural failures caused by metal corrosion and fatigue deterioration. NACE International reports that the global cost of corrosion for 2013 is estimated to be US\$2.5 trillion, equivalent to 3.4% of the global Gross Domestic Product of that year (NACE International 2016). The same report estimates that between 15% and 35% of the total cost of corrosion could be saved by using optimal corrosion management strategies. For this reason, significant resources are invested to identify, model, quantify, mitigate, and prevent deterioration processes in structures.

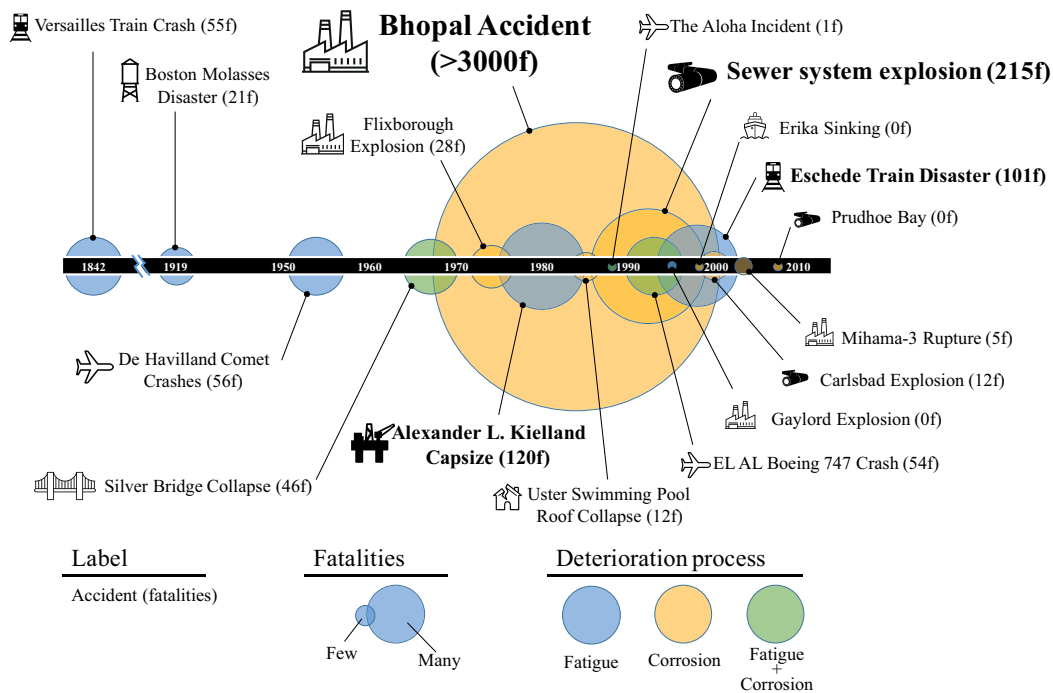


Figure 1. Timeline of some of the most known catastrophic structural failures caused by metal corrosion and/or fatigue deterioration.

Accurate modeling of structural deterioration processes remains a challenge today, due to their complexity and inherent uncertainties. To explicitly address the uncertainties in the predictions, probabilistic approaches are suitable for deterioration modeling in an engineering context (Lin and Yang 1985, Madsen et al. 1985, Ellingwood and Mori 1993, Melchers 1999, Qin and Cui 2003, Melchers and Jeffrey 2007, Kumar et al. 2015).

To reduce the uncertainty in deterioration processes, regular inspections are common practice for most engineering structures. Ideally, engineers and stakeholders define in advance an inspection strategy for the structural system, which specifies when, where, what and how to inspect. However, in many cases inspections are carried out in a static or less planned manner. In general, static inspection regimes (i.e. those that do not change in time and adapt to new circumstances) are not optimal; instead, one should account for results from previous inspections and maintenance activities when deciding upon new inspections. In general, an inspection strategy should be optimal in the sense it balances the cost of inspections with the achieved risk reduction (Figure 2).

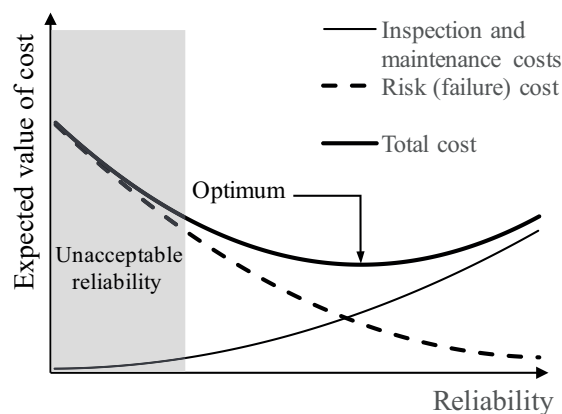


Figure 2. Graphical description of the optimal inspection strategy.

Risk-based optimization of inspection strategies for large engineering systems entails multiple challenges in practice. Firstly, the deterioration model should be able to incorporate the correlation among deterioration states at different locations. However, most probabilistic deterioration models are only developed at the structural component level or for relatively simple and small systems. Secondly, one needs to perform probabilistic inference for the entire system to address the impact that deterioration at one location has on the rest of the structure. Finally, when considering systems, the outcome space of the random variables and the number of decision alternatives increase exponentially with the number of time steps T , and with complexity $O(n^T)$ with the number of components n , as can be visualized in the decision tree

of Figure 3. This is one of the main reasons why previous work on risk-based inspection planning has focused mainly on individual components.

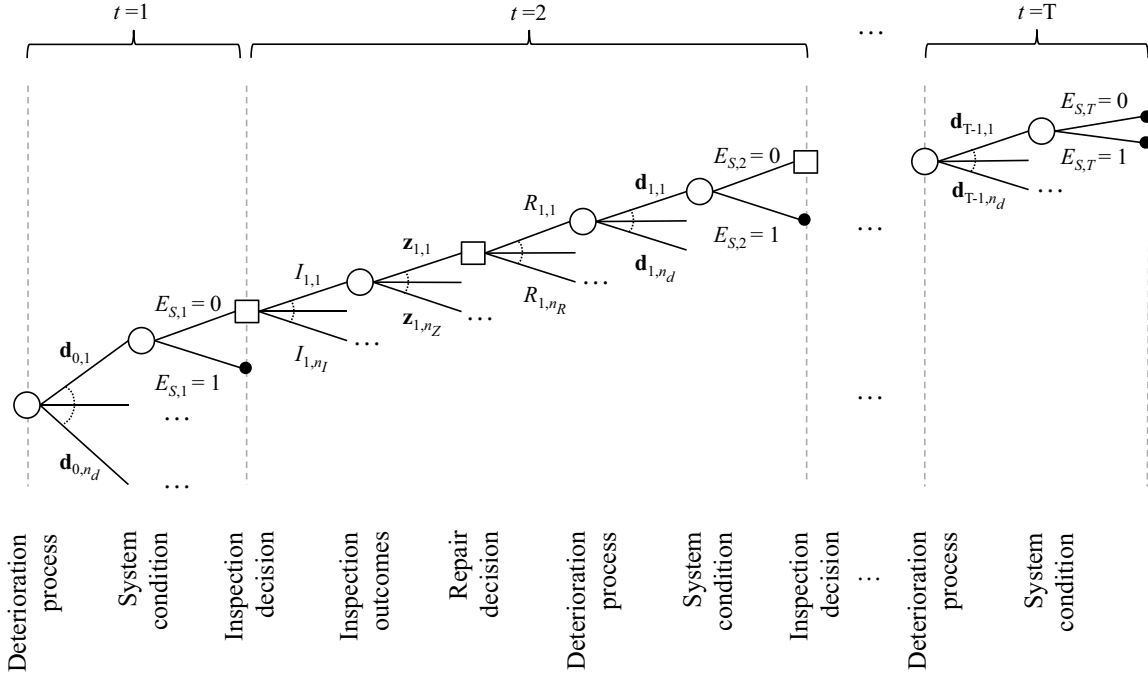


Figure 3. Example of a decision tree with deterioration vector $\mathbf{D}_{t,i}$ for all system components, system performance $E_{s,t}$ (0: safe, 1: fail), inspection $I_{t,i}$ and repair $R_{t,i}$ decisions at each time step $t = 1, \dots, T$, and a set of observations $\mathbf{Z}_{t,i}$ after each inspection decision. A black dot marks the end of a branch, which corresponds to either a system failure or the end of service life.

Prior to this research, an integral risk-based optimization procedure for entire structural systems using detailed physics-based deterioration models was not available.

1.2 State of the art

Methods for risk-based optimization of inspections of structural systems have been developed during the past 40 years (Yang and Trapp 1974, 1975, Thoft-Christensen and Sørensen 1987, Madsen et al. 1989, Sørensen et al. 1991, Straub and Faber 2005, Straub and Faber 2006, Nielsen and Sørensen 2015). The scientific literature documents a number of industrial applications of inspection planning on offshore structures, aircrafts, bridges or ships (e.g., Skjong and Torhaug 1991, Pedersen et al. 1992, Faber et al. 1992b, Lotsberg et al. 2000, Faber et al. 2005, Moan 2005, Dong and Frangopol 2015). The theory and the applications have focused almost exclusively on the optimization at component level, with a simplified treatment of the system (Straub and Faber 2005). Only limited research efforts have been directed towards optimization procedures for entire systems, accounting for the statistical dependence among the

deterioration states of individual structural details (Faber et al. 1992a, Straub and Faber 2004a, Straub and Faber 2005, Straub et al. 2009, Papakonstantinou and Shinozuka 2014, Memarzadeh and Pozzi 2015)

There are several challenges when risk-based inspection strategies for large engineering systems are to be computed:

- Firstly, the interdependence among stochastic deterioration processes for all the system components must be modeled. The two most common approaches to such an integral probabilistic deterioration modeling are random fields (Guedes Soares and Garbatov 1998, Vrouwenvelder 2004, Stewart and Mullard 2007, Ying and Vrouwenvelder 2007, Keßler et al. 2014) and hierarchical models (e.g. Maes and Dann 2007, Maes et al. 2008, Qin and Faber 2012, Banerjee et al. 2015, Paper C).
- Secondly, Bayesian updating is required for computing the probability of failure of all components and the system conditional on a potentially large number of inspection results. This represents a computationally challenging problem in itself (e.g. Schneider et al. 2017, Straub et al. 2020), but is particularly severe in the context of risk-based inspection (RBI), where these computations must be performed multiple times for the optimization of the inspection strategies.
- Thirdly, the inspection optimization must consider strategies at the system level, which in general leads to a number of optimization parameters that increases considerably with the number of components (Straub and Faber 2005).

Bayesian networks (BNs) can facilitate the solution of the probabilistic modeling and inference problem. BNs enable incorporating information from inspections into probabilistic deterioration models to quantify the reduction in uncertainty and to update the reliability estimate (Tang 1973, Madsen 1987, Moan et al. 2000, Straub et al. 2016). They have been applied to engineering risk analysis problems for the last two decades (Torres-Toledano and Sucar 1998, Friis-Hansen 2001, Mahadevan et al. 2001, Faber et al. 2002, Grêt-Regamey and Straub 2006, Nielsen and Sørensen 2010, Fenton and Neil 2012, Weber et al. 2012, Bensi et al. 2013).

A key computational aspect of BNs is performing inference, i.e. Bayesian updating. Through the graphical structure of the BN, the conditional independence among model parameters can facilitate Bayesian updating. If the deterioration process can be represented by discrete random variables (e.g. by discretizing all continuous random variables), exact inference algorithms can provide fast and robust solutions to Bayesian updating. These properties have been exploited

in Straub (2009) and Paper B, where dynamic Bayesian networks (DBNs) are applied to evaluate deterioration at component and system levels. Bespoke exact inference algorithms ensure rapid computation of the conditional probability of system failure given all inspection results, which is essential for solving the optimal inspection problem.

The next section summarizes the proposed solution by this thesis to the optimal inspection problem and it is based on the results from Paper A, Paper B, Paper C, and Paper D.

1.3 Statement of purpose and proposed solution

The goal of this thesis is to outline a methodology for an integral risk-based optimization of inspections in large structural systems using a dynamic Bayesian network (DBN) framework. The thesis develops a multi-level hierarchical BN model able to represent complex spatio-temporal deterioration processes (e.g., corrosion in ship vessels), and a hierarchical DBN framework with a tailor-made inference algorithm. On the one hand, the multi-level model provides a flexible and general framework to represent spatio-temporal dependencies among locations in the structural system, but with a high price when performing inference. This makes it computationally expensive (and in some cases impractical) for solving the inspection planning problem. On the other hand, the single-level hierarchical DBN framework utilizes a customized rapid inference algorithm to update the system reliability conditional on inspection results with a simpler spatial representation. The inference algorithm combined with a heuristic approach to reduce the number of considered inspection/maintenance strategies allows solving the optimization problem for large structural systems. The optimization problem is solved by nesting the DBN inside a Monte Carlo simulation for computing the expected cost associated with a system-wide inspection strategy.

In contrast to existing methods, the DBN framework can simultaneously account for system effects arising from (a) the dependence among the deterioration at different components, (b) the joint effect of deterioration at multiple components on the system reliability, and (c) the interaction among inspection costs, i.e. the reduction in the marginal cost of an inspection if these are grouped in larger inspection campaigns.

The developed framework is applicable to a wide variety of structures subject to deterioration processes including offshore platforms, bridges, wind turbines structures, ships, and aircraft structures. The accuracy and robustness of the approach is demonstrated in several structural systems: (a) a ship vessel subject to uniform corrosion, (b) a theoretical structure (Daniels system) subject to fatigue, and (c) a laboratory structure (Zayas frame) subject to fatigue.

1.4 Thesis structure

Chapter 2 summarizes the main concepts related to Bayesian networks and influence diagrams required to follow the proposed DBN framework and optimization approach. This chapter can be skipped if the reader is already familiar with these concepts.

Chapter 3 outlines the mathematical formulation of the risk-based inspection (RBI) problem and the main characteristics of the DBN deterioration framework proposed in this thesis. This is a summary of the proposed framework developed in Paper B and Paper D.

Chapter 4 presents five case studies that summarize the results from the publications that support this thesis. Section 4.1 shows how a hierarchical DBN can be used to model uniform corrosion deterioration in ship vessels (Paper C). Sections 4.2 and 4.3 show how to apply the DBN framework from Paper B to model fatigue deterioration in two different types of structures: 1) the Daniels system (a theoretical structure), and b) the Zayas frame (a laboratory structure). These cases demonstrate the accuracy and robustness of the inference algorithm to solve the reliability problem. Section 4.4 compares heuristic-based strategies against other approaches such as LIMIDs to approximate the optimal inspection strategy of a simplified system model (Paper A). Finally, Section 4.5 demonstrates how to combine the DBN framework from Paper B with heuristic rules and a simulation-based approach to solve the optimal inspection planning problem (Paper D).

Chapters 5 to 8 present the complete content of papers A to D, respectively. References to equations, tables, and figures from these papers are preceded by the letter of the article (e.g. Section A.2.2 corresponds to section 2.2. from Paper A) to keep the original numbering of the paper as it was published.

Chapter 9 discusses the advantages and limitations of the proposed DBN framework and some recommendations when putting it into practice. Then it continues with suggestions for extending the results of the thesis, and finally it presents the thesis' conclusion.

2 Bayesian networks and influence diagrams

This chapter summarizes the main concepts related to Bayesian networks and influence diagrams required to follow the proposed DBN framework and optimization approach. If the reader is already familiar with these concepts, it is suggested skipping this section and to go directly to Chapter 3, where the proposed DBN deterioration framework is explained.

2.1 Bayesian Networks

Bayesian Networks (BN) have become popular in engineering risk analysis due to their intuitive nature and their ability to handle many dependent random variables in a Bayesian analysis (Jensen and Nielsen 2007, Straub and Der Kiureghian 2010, Weber et al. 2012).

The graphical structure of the BN is formed by nodes and directed links. The nodes represent random variables or deterministic parameters, and the links represent the dependence among nodes. Ideally, the link between two nodes is based on a causal relation, but this is not necessary. As an example, if deterioration at a certain point in time D is modeled as a function of an external random load S and a material parameter M , then a corresponding BN may look like the one in Figure 4. Here, an additional node Z is included to represent the outcome of an inspection.

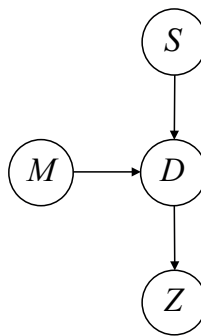


Figure 4. Example of a simple Bayesian network deterioration model with deterioration state D , external load S , material parameter M , and inspection outcome Z .

Since each random variable in the BN is specified by its conditional probability distribution given its parents, the inspection outcome is defined by $p(z|d)$, i.e. the probability of the inspection outcome $Z = z$ given the damage state $D = d$. This is known as the likelihood function and corresponds to classical models used for describing inspection or monitoring performance, such as probability of detection (POD).

The links in the BN provide information on the dependence between random variables in the model. For example, in the BN of Figure 4 M and S are assumed to be independent a-priori, and hence no direct link between them is present. The link from D to Z indicates that the inspection provides information on the damage state. In this example, the joint probability mass function (PMF) of M , S , D , and Z (assuming they all are discrete random variables) is

$$p(m, s, d, z) = p(m) \cdot p(s) \cdot p(d|m, s) \cdot p(z|d) \quad (1)$$

Even though Z provides no direct information on S and M , it does so indirectly because the information obtained on D also updates the probability distribution of S and M , as long as D is not known with certainty. In this way, by observing one random variable, potentially all others are updated.

2.2 Bayesian inference

Using BNs it is possible to obtain the posterior distribution of a set of random variables given a set of observations; this task is called inference. For example, if an inspection result is included in the model of Figure 4, i.e. if Z is given, then the (joint) probability distribution of the random variables S , M , and D conditional on the observed realization of Z is calculated using inference algorithms.

For the BN of Figure 4, the joint PMF of M , S , and D conditional on the realization $Z = z$ can be obtained analytically and it is equal to

$$p(m, s, d|z) = \frac{p(m, s, d, z)}{p(z)} = \frac{p(m) \cdot p(s) \cdot p(d|m, s) \cdot p(z|d)}{\sum_{m, s, d} p(m, s, d, z)} \propto p(m) \cdot p(s) \cdot p(d|m, s) \cdot p(z|d) \quad (2)$$

where $p(m) \cdot p(s) \cdot p(d|m, s) = p(m, s, d)$ represents the prior distribution when no observation of Z is available. As can be seen, the inference step simply reduces to computing (marginalizing) joint probabilities.

For efficient computation, all BN inference algorithms make use of the graphical structure by performing computations locally, exploiting the conditional independence assumptions encoded in the graph. These can be formally described by the d -separation property (Pearl 1988), where d stands for dependence. Basically, if two variables X_1 and X_2 are independent conditional on Y (i.e. an observation from X_1 gives no additional information about X_2 once Y is known) then X_1 and X_2 are called d -separated for given Y .

As already stated in Section 1.3, this thesis focuses on BN with discrete random variables, for which exact inference algorithms exist.

2.3 Dynamic BNs

In some cases, BNs contain a repetitive sequence of nodes which are associated with multiple times or spatial locations. Such a BN is called dynamic Bayesian network (DBN) and is useful for modeling time-dependent processes, such as deterioration.

Modeling of deterioration often involves random processes, which can be represented in a discrete-time manner by a DBN as proposed in Straub (2009). Figure 5 shows an extension of the BN in Figure 4 for multiple time steps. The resulting DBN includes a time-variant load S_t , deterioration state D_t , and inspection results Z_t at points in time $t = 1, 2, \dots, T$. Each vertical “slice” of the DBN represents a time step in the deterioration process.

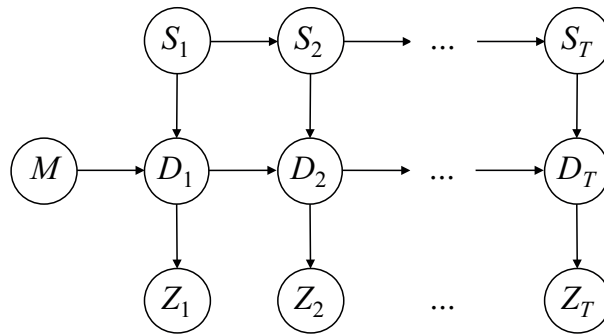


Figure 5. Extension of the BN deterioration model from Figure 4 to a dynamic Bayesian Network. Each set of random variables $\{S_t, D_t, Z_t\}$ corresponds to a single time step $t = 1, 2, \dots, T$.

In this example, the random process $\{S_1, S_2, \dots, S_T\}$ is a Markov chain, where each random variable is defined conditionally on the random variables of the previous time step. The deterioration D_t at time t is a stochastic function of the previous deterioration state D_{t-1} and the current load S_t . The probability distributions of the material parameter M , loads $\{S_1, S_2, \dots, S_T\}$, and the deterioration states $\{D_1, D_2, \dots, D_T\}$ are all updated once inspection outcomes Z_1, Z_2, \dots, Z_T , or a subset thereof, are observed.

To perform inference in DBNs, there exist exact, deterministic approximate, and stochastic approximate algorithms (Murphy 2002). All of them require computing $P(X_t^i | y_{1:\tau})$, i.e. the marginal probability of random variable X^i at time step t given some observations up to time step τ . For the case when $\tau = t$, the inference problem is called filtering; if $\tau < t$ it is called prediction; and if $\tau > t$ it is called smoothing. Depending on the characteristics of the DBN and the amount of observed data, some of the inference algorithms are more convenient than others

in terms of the computational effort and accuracy when computing such marginal probabilities. The computational cost of exact inference algorithms for discrete random variables is strongly affected by the size of the largest conditional probability table in the network (making the updating step intractable for some large DBNs) but insensitive to the number of included observations; in contrast, stochastic approximate algorithms such as Markov Chain Monte Carlo (MCMC) are less sensitive to the size of the network, but affected by the number of included observations. An extensive analysis of the complexity of several inference algorithms can be found in Murphy (2002). In this thesis, the developed DBN deterioration framework (Section 3.3) is based on exact inference algorithms for discrete random variables to perform filtering and prediction, where its performance and accuracy are compared to MCMC.

2.4 Hierarchical BNs

One challenging aspect of modeling deterioration in structural systems is the representation of the interrelation among the system components. Only a limited number of investigations can be found in literature that account for the dependence among component deterioration states (e.g. Hergenröder and Rackwitz 1992, Faber and Sørensen 2000, Straub and Faber 2004b, Vrouwenvelder 2004, Maes et al. 2008, Malioka 2009, Paper C). The two most common mathematical representations of such dependence are hierarchical models and random field models. The latter are suitable for systems where dependence among component deterioration is a function of the geometrical location (Maes 2003, Stewart and Mullard 2007). Hierarchical models are suitable when the dependence among component deterioration depends on common features and common influencing factors (Maes and Dann 2007, Maes et al. 2008, Banerjee et al. 2015). They also have computational advantages over random fields, in particular in the context of DBN modeling.

Because of their simplicity and computational efficiency, hierarchical models are commonly used in spatio-temporal system models for representing dependencies among system components. Their application to deterioration modeling is reported for deterioration in pipelines (Zhang et al. 2014, Qin et al. 2015) and in concrete structures (Qin and Faber 2012, Schneider et al. 2015). Hierarchical models can provide efficient probabilistic representations of large systems with correlated elements (Raudenbush and Bryk 2008). The observed correlation among system components is incorporated in the model through the definition of multiple levels, which group components with similar properties. For example, plate elements in ship vessels might be grouped according to their structural element type (e.g., main deck and bulkhead). These groups can be subdivided again into lower-level groups, which are based on

the spatial location in the structure (e.g., compartments inside vessels) and so on. At each level in the hierarchy, a group must contain elements with similar characteristics among them but different from other groups.

Probabilistic hierarchical models can be conveniently represented as BNs. In a hierarchical Bayesian model, the probability distributions of the random variables at each level are defined conditional on the random variables of the next higher level. The parameters of these conditional probability distributions, which are themselves random variables, are typically located at the highest level and are called hyperparameters (Gelman et al. 2004). The hyperparameters define the local and global correlation among the system components. In the Bayesian framework, these hyperparameters are learned jointly with the other random variables based on the available observations from the system.

Two distinct graphical representations of the same simple hierarchical Bayesian model with two levels are shown in Figure 6. Figure 6a depicts an explicit representation of the problem, where all random variables and their dependencies are indicated. However, the number of random variables soon becomes prohibitive for such a representation. In contrast, Figure 6b shows a compact representation, where each level in the hierarchy is indicated by a corresponding box.

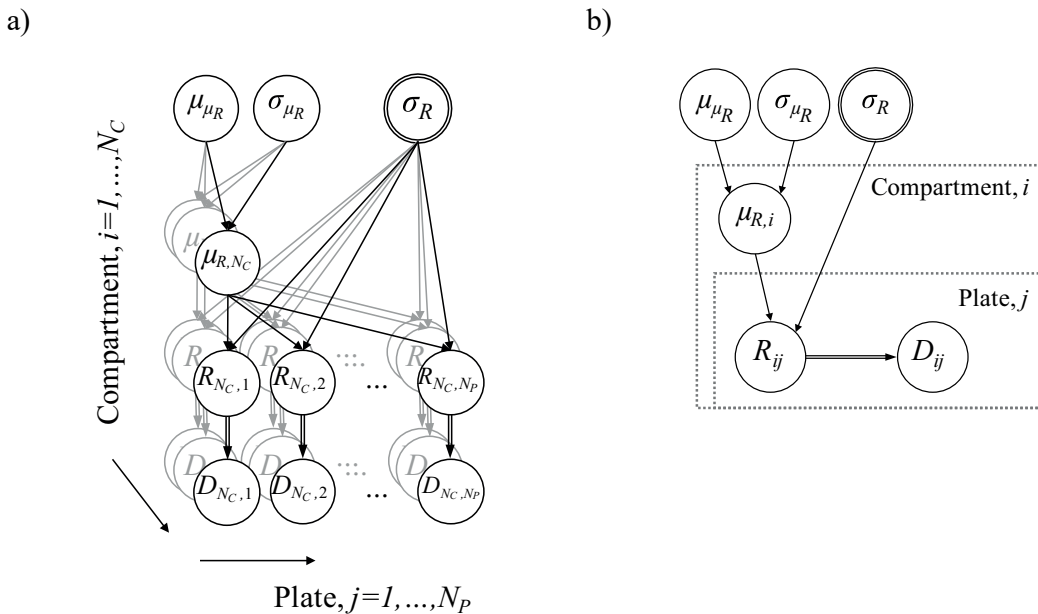


Figure 6. Example of a hierarchical Bayesian deterioration model (D : deterioration, R : corrosion rate, μ_X : mean of X , σ_X : standard deviation of X , N_C : number of compartments, N_P : number of plates) using (a) explicit and (b) compact representations.

In general, the main goal in the analysis of hierarchical Bayesian models is the estimation of the hyperparameters' posterior distribution. The benefit of knowing the distribution of the hyperparameters is that they can transfer knowledge either among different sections inside a structure or among structures with similar characteristics. This property is demonstrated and exploited in the case studies of Sections 4.1, 4.2, and 4.3.

2.5 Influence diagrams

An influence diagram (ID) is an extension of a Bayesian network to represent graphically a decision problem including decision and utility nodes (Jensen and Nielsen 2007). In an ID, decisions are shown as squared nodes and utilities as diamond-shaped nodes. Utility nodes assign a utility value to each combination of states of the parent nodes, which can be either random variables or decision nodes, but not utility nodes. In case there are several utility nodes, the total utility is the sum of the individual utilities.

Decision nodes describe different decision options, which influence the random variables that are children of the decision node. This influence is quantified through the conditional PMF of these child nodes. Links pointing towards the decision nodes represent the available information at the time of making the decision. All parents of the decision nodes are known when making the decision. However, there exist different versions of IDs, which differ in the way information is handled. Figure 7 shows an example of an ID applied to structural health monitoring (SHM) proposed by Straub et al. (2017).

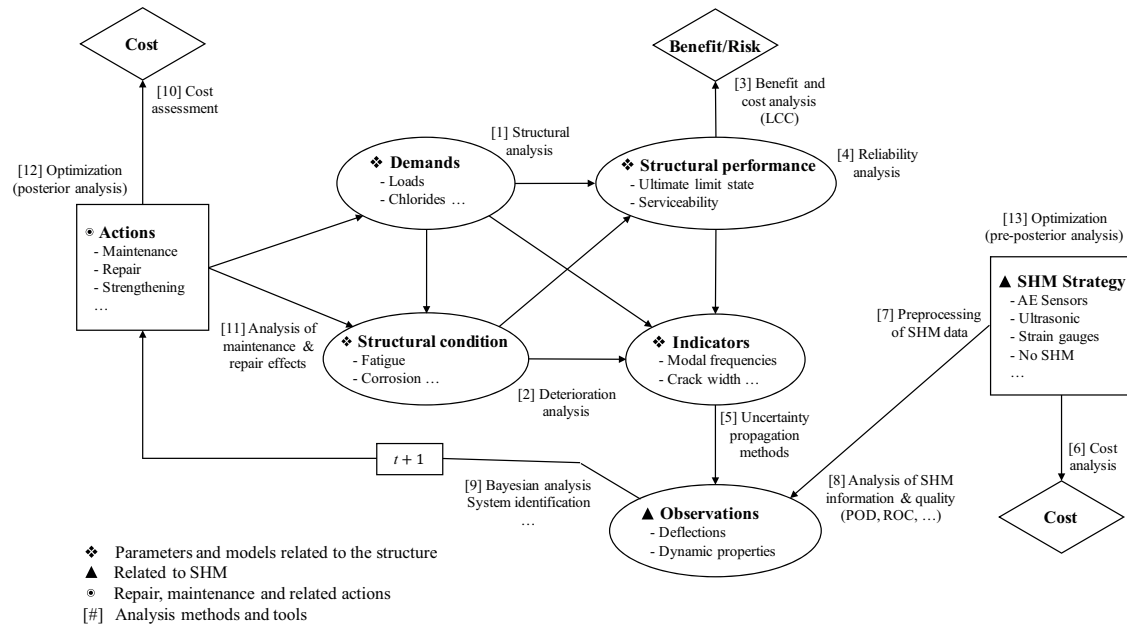


Figure 7. ID of an SHM analysis process with: a) parameters and models related to the structure, b) aspects related to the SHM, c) repair, maintenance and related actions, and d) analysis methods and tools used in the different parts of the process. The box [t + 1] indicates that the link is from a single time step to the next one, hence this ID represents a decision process in time (Straub et al. 2017).

A set of rules defining which decision to make as a function of the available information is called a policy. A set of policies of all decision nodes in an ID is called a strategy. The main goal in a decision analysis is to find the optimal strategy, i.e. the one that maximizes the total expected utility, based on the available information. The more information is used for making a decision, the larger the strategy domain and consequently the computational demand. In general, IDs are based on the no-forgetting assumption, i.e. when making a decision, all previous decisions as well as previous observations are known. The no-forgetting assumption leads to significant computational challenges and some assumptions are typically made to simplify the decision problem and giving an approximate solution.

One approach for approximating the optimal strategy is to consider only a subset of the past observations (e.g. the n most recent ones) at each decision step. This approach is known as limited memory influence diagram (LIMID) (Lauritzen and Nilsson 2001, Jensen and Nielsen 2007). LIMID makes an explicit link between the nodes that are known before taking the decision and the decision node. Additionally, only direct parents of a decision node are assumed to be known at the time of making the decision. This reduces (or limits) the number of nodes that will be considered for the decision, decreases the size of the policy domain and facilitates the computation of the optimal strategy. However, the size of the solution domain can still become intractable as the number of decision nodes increases.

Depending on the type of application, some characteristics (e.g. symmetry) can be used to reduce the computational demands of the decision problem (Jensen and Nielsen 2007). Alternatively, approximate solutions can be obtained. In particular, single policy updating (SPU) is an iterative algorithm for solving LIMIDs that runs over each decision node, obtaining its locally optimum policy that maximizes the expected utility of the decision problem by keeping the remaining policies fixed (Lauritzen and Nilsson 2001). An iteration is completed when all decision nodes are locally maximized, and the algorithm stops when the next iteration does not further reduce the expected utility. Due to its local nature, the solution obtained with SPU is likely to be suboptimal.

Sections 4.4 and 4.5 show examples of IDs and the optimization of strategies.

3 Risk-based inspection planning

This chapter outlines the mathematical formulation of the risk-based inspection (RBI) problem and the main characteristics of the DBN deterioration framework proposed in this thesis. This is a summary of the proposed framework developed in Paper B and Paper D.

3.1 Mathematical formulation of the optimization problem

The RBI problem belongs to the class of sequential decision problems (see Section D.2.1). Solutions to this type of problems can be found through the definition of policies. As already mentioned, a policy for a decision at time t defines where, what and how to inspect and repair, considering the full history of the structure up to t (i.e., past inspection outcomes, decisions, and repair actions). The set of policies at all times t defines a strategy \mathcal{S} . If the policies are the same for all t , the strategy is called stationary (Jensen and Nielsen 2007).

For a structural system with N components subject to deterioration, the inspection optimization problem of Figure 2 can be formalized as follows. The joint deterioration state \mathbf{D} of all components is represented through a probabilistic system deterioration model with random parameters \mathbf{X}_D . Each component can be inspected and/or repaired at discrete times t from 0 to the end of service life T . The strategy \mathcal{S} defines for each component at each time step if and how that component is inspected and repaired, based on all previous inspection outcomes \mathbf{Z} and the repair history of the structure.

Inspections, repairs and system failure are associated with consequences. These are quantified by the present value of total life-cycle cost C_T in function of the strategy \mathcal{S} and the inspection outcomes \mathbf{Z} . It is defined as the sum of the life-time inspection cost C_I , repair cost C_R , and failure risk R_F :

$$C_T(\mathcal{S}, \mathbf{Z}) = C_I(\mathcal{S}, \mathbf{Z}) + C_R(\mathcal{S}, \mathbf{Z}) + R_F(\mathcal{S}, \mathbf{Z}) \quad (3)$$

The failure risk is a function, among other values, of the conditional probability of system failure given the inspection outcomes, and it is defined as:

$$\begin{aligned} R_F(\mathcal{S}, \mathbf{Z}) &= \sum_{t=1}^T c_F \cdot \gamma(t) \cdot \Pr(F_t | \mathbf{Z}_{0:t-1}) \\ &= c_F \cdot \sum_{t=1}^T \gamma(t) \cdot [\Pr(E_{S,t} = Fail | \mathbf{Z}_{0:t-1}) - \Pr(E_{S,t-1} = Fail | \mathbf{Z}_{0:t-1})] \end{aligned} \quad (4)$$

where c_F is the undiscounted cost of a system failure event, $\gamma(t)$ is a discount factor, F_t is the event of a system failure during time step t , and $E_{S,t}$ is the system condition at time step t .

The conditional probability $\Pr(E_{S,t} = \text{Fail} | \mathbf{Z}_{0:t-1})$ is the probability of a system failure up to time t for given inspection outcomes $\mathbf{Z}_{0:t-1}$. Its computation defines a structural reliability problem, which is formulated and solved in Sections 3.3.3 and 3.3.4, and it is explained in detail in Paper D. Its solution is not trivial, particularly when the number of system components and the number of observations is large. Solving the RBI problem requires evaluating the conditional probabilities of Equation (4) multiple times (in the order of $10^4 - 10^5$), for which an efficient and robust solution as the one proposed in Paper B is indispensable.

Because the inspection outcomes Z are random variables themselves and are not known in advance, the total cost is also a random variable. Then the optimal strategy \mathcal{S}^* is defined as the one that minimizes the expected total cost with respect to the possible inspection scenarios:

$$\mathcal{S}^* = \arg \min_{\mathcal{S}} E_{\mathbf{Z}}[C_T(\mathcal{S}, \mathbf{Z})] \quad (5)$$

The two main challenges in finding the optimal strategy are:

1. The large number of possible inspection strategies \mathcal{S} , which increases exponentially with the number of time steps and system components (as shown in Figure 2)
2. The expectation operations in Equations D.3 and D.5 required to solve the structural reliability problem with respect to each possible inspection outcome.

In the following sections of this chapter, it is demonstrated how the proposed DBN deterioration framework and heuristic strategies can deal with these challenges to solve the RBI problem.

3.2 Optimization at the component level

Risk-based optimization of inspection planning for individual components has been studied extensively (e.g. Straub and Faber 2006, Nielsen and Sørensen 2015). In Paper D, some of the most common approaches used for RBI at component level are reviewed (limited memory influence diagrams LIMIDs, partially observable Markov decision processes and heuristic strategies). Sophisticated approaches like LIMIDs (combined with the SPU algorithm) have been used to estimate the optimal strategy obtaining near optimal solutions (e.g. Nielsen and Sørensen 2011, Paper A). However, its application has been limited to simplified deterioration models or using component-based approaches, making it impractical for application to large structural systems with more complex deterioration processes and component interaction.

For the inspection planning problem at the component level, simple heuristics were defined in the past to reduce the solution space (see e.g. Englund et al. 2000). The two most common heuristics are:

- *Periodic inspections* (also known as equidistant inspections): Inspections are performed with a predefined periodicity.
- *Reliability/Probability threshold*: For a given threshold β_{th} , an inspection is planned at time t if reliability of the system or component without inspection is smaller than β_{th} .

Heuristic-based strategies provide simple rules (and in many cases can be defined by a single parameter) that can be easily evaluated to estimate their expected cost. In Paper A two heuristics are used to define the times to inspect (periodic inspections and reliability threshold) and one to define repair actions (rule: all detected defects are to be repaired).

The results from Paper A show that the heuristic approach offers a simple and computationally convenient approach to simplify the RBI problem at the component level, which can be extended for solving the problem at the system level.

3.3 Optimization at the system level

The identification of the optimal inspection strategy is significantly more challenging for structural systems than for individual components. Firstly, the number of possible inspection strategies \mathcal{S} considerably increases with the number of components; e.g. in a system with N components and considering T time steps, there are $2^{N \cdot T}$ different ways of defining which components to inspect and when to do it. Secondly, the computation of the conditional reliabilities is more demanding as the number of components, time steps, and inspection observations increase.

Paper D shows that defining inspection strategies using heuristics provides a computationally feasible approach to solving the RBI problem at the system level. This considerably reduces the size of the solution space (i.e. possible strategies \mathcal{S}) to a few number of optimization parameters, whose combinations are considerably less than the set of general strategies.

The following sections explain the most important aspects of the developed DBN deterioration framework, which are:

- Defining heuristic strategies at the system level to reduce the number of potential solutions (from Paper D)

- Using a simulation-based approach to approximate the expected cost of a strategy (from Paper D)
- Definition of a DBN to model deterioration in large structural systems (from Paper B)
- Developing a robust, efficient, and accurate inference algorithm to compute the updated probabilities given the inspection outcomes (from Paper B)

3.3.1 Heuristic strategy approach (to reduce the number of strategies)

At the system level, identifying heuristics is less straightforward than at the component level. On the one hand, some heuristics applied at the component level (e.g. periodic inspections, reliability threshold, fixed repair criterion) can be extended to the system level. On the other hand, defining the locations of the inspections, i.e. where to inspect, must be defined more carefully to avoid strongly suboptimal strategies.

Paper D proposes the following set of heuristic rules:

- *When to inspect*
 - Inspection campaigns are performed at regular time intervals. The time between regular campaigns is Δt_I .
 - Whenever the updated system probability of failure exceeds a threshold value p_{th} , additional inspections must be carried out, either within the existing campaign or through an additional inspection campaign.
- *Where to inspect*
 - The initial number of inspected components during each inspection campaign is fixed at n_I . Additional components might be inspected if the probability threshold is exceeded during the inspection campaign.
 - The components to inspect during a campaign are determined based on the value of information (VoI) associated with the component inspection (Raiffa and Schlaifer 1961, Straub and Faber 2005). Here the probability of failure of the component is taken as a proxy of the VoI.
- *What/when to repair*
 - Repairs are performed according to a fixed repair criterion, e.g., any identified defect with a size larger than d_R is repaired.

A heuristic strategy \mathcal{S}_k is then a combination of the above stationary rules and is defined by the parameters Δt_I , n_I , p_{th} , and d_R . The combination of these parameters that minimizes the expected cost defines the optimal strategy.

3.3.2 Simulation-based approach (to approximate the expected cost of a strategy)

To estimate the total expected life-cycle cost of a strategy \mathcal{S}_k , a Monte Carlo (MC) approach is used (Paper D). The expected value is approximated as the average of the total cost associated to the strategy \mathcal{S}_k and a set of n_s simulated samples of inspection outcomes $\{\mathbf{z}_{k,1}, \mathbf{z}_{k,2}, \dots, \mathbf{z}_{k,n_s}\}$,

$$E_{\mathbf{Z}}[C_T(\mathcal{S}_k, \mathbf{Z})] \approx \frac{1}{n_s} \sum_{j=1}^{n_s} C_T(\mathcal{S}_k, \mathbf{z}_{k,j}) \quad (6)$$

The number of samples n_s required to ensure sufficient accuracy is a function of the coefficient of variation of the total cost δ_{C_T} . To ensure a relative error in the estimate of less than ε with a confidence of $1 - \alpha$, the required number of samples is

$$n_s \geq \left(\frac{\Phi^{-1}(\alpha)}{\varepsilon} \delta_{C_T} \right)^2 \quad (7)$$

In all the investigated cases, the value of δ_{C_T} was around 1.5. If one requires a relative error less than 10% (i.e. $\varepsilon = 0.1$) with a confidence of 95% (i.e. $\alpha = 0.05$), the required number of samples is $n_s \geq 271 \cdot \delta_{C_T}^2 = 609$. Typically, the requirements on the accuracy of the estimated total expected life-cycle cost are not as strict, and a number of samples in the order of 200 is expected to be sufficient for most practical applications. Note that the reason for this relatively small number lies in the fact that the conditional probability of failure is computed within each MC sample through the DBN.

3.3.3 DBN deterioration model

As already mentioned in Section 1.1, to perform reliability analysis of structural systems it is essential that the model incorporates the correlation among deterioration states at different locations. At the same time, performing inference for such model must be computationally efficient and accurate.

The backbone of this thesis is the extension of the deterioration framework developed in Straub (2009). He developed a DBN deterioration model at the component level combined with a robust exact inference algorithm. It requires discretizing all continuous random variables, but the inference algorithm achieves very good accuracy for standard deterioration models. In contrast to other Bayesian analysis methods, this framework combined with the exact inference algorithm is not affected by increasing the amount of inspection data.

In Paper B the component-level framework from Straub (2009) is extended to the system level. The extended framework includes the effect of inspection and monitoring results to update the reliability of the system and its components. It accounts for the dependence among deterioration parameters of different components and for the complex structural system behavior through a hierarchical approach. The DBN uses a set of hyperparameters α that model the correlation among deterioration parameters. These hyperparameters α are the link among the other parameters $\theta_{i,t}$, $\omega_{i,t}$, and deterioration states $D_{i,t}$ in all components (Figure 8).

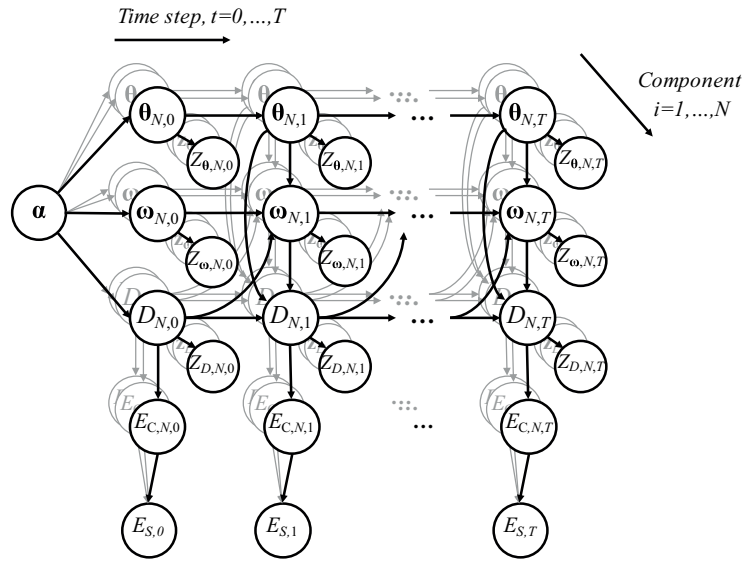


Figure 8. Hierarchical DBN system deterioration model (Paper B). Node $D_{i,t}$ represents the deterioration state of the i -th component at time step t as function of the previous deterioration $D_{i,t-1}$, time-independent parameters $\theta_{i,t}$, a time-dependent parameters $\omega_{i,t}$; $Z_{\theta,i,t}$, $Z_{\omega,i,t}$, and $Z_{D,i,t}$ are observations (from inspections or monitoring); $E_{C,i,t}$ and $E_{S,t}$ represent the condition (e.g. safe or failed) of the component and the system; α is the set of hyperparameters that links all components.

Most approximate methods to perform inference in DBNs are sampling based; the most popular among these belong to the family of Markov Chain Monte Carlo (MCMC) methods. MCMC using Gibb's sampler is particularly effective, as it exploits the conditional independence properties of the BN. Nevertheless, the computational cost of MCMC increases considerably as the number of observations included in the model increases and/or the probability of failure of interest decreases. This motivates the use of exact inference algorithms with discretized random variables, whose performance does not deteriorate with increasing the number of observations and is independent of the magnitude of the probabilities of interest.

For DBN models consisting exclusively of discrete random variables, exact inference algorithms exist. In particular the forward-backward algorithm is effective for DBNs. Straub (2009) develops a variant of the forward-backward algorithm, which is tailored towards

evaluating the generic DBN for deterioration modeling. The next section explains how this algorithm is extended to the system level and its computational complexity is kept at a feasible level through the hierarchical definition of the system DBN model.

3.3.4 The inference algorithm (to compute the updated probabilities given the inspection outcomes)

A key element in the proposed framework is the efficiency of the inference algorithm that computes the conditional probabilities of failure at the component and system level given the inspection outcomes.

In Paper B an exact inference algorithm is provided for solving the hierarchical DBN from Figure 8 based on the results from Straub (2009). The algorithm is formulated in a recursive manner for each time step exploiting the d-separability (Pearl 1988) of the hierarchical BN when the hyperparameters are given, i.e.

$$p(d_{i_1,t}, d_{i_2,t} | \alpha) = p(d_{i_1,t} | \alpha) \cdot p(d_{i_2,t} | \alpha) \quad (8)$$

Because of the hierarchical structure of the model, the computation time increases approximately linearly with the number of components and is independent of the number of included observations. Additionally, the algorithm can easily be parallelized per component computation.

The inference algorithm is composed of three main steps:

1. First, the joint probability distribution of a single component is updated using only inspection results from the same component and for a given set of hyperparameter values α . This step is repeated for every component and can be done in parallel due to Equation (8).
2. Then, the joint distribution of hyperparameters α is updated with the inspection results from all components.
3. Finally, the results of the first and second steps are combined to obtain the probability distributions of all components conditional on all inspection results in the system

Section B3.5 provides a detailed analysis of the complexity of the algorithm.

3.3.5 Flowchart of the optimization methodology

Putting all together, the complete optimization methodology is summarized with the flowchart in Figure 9.

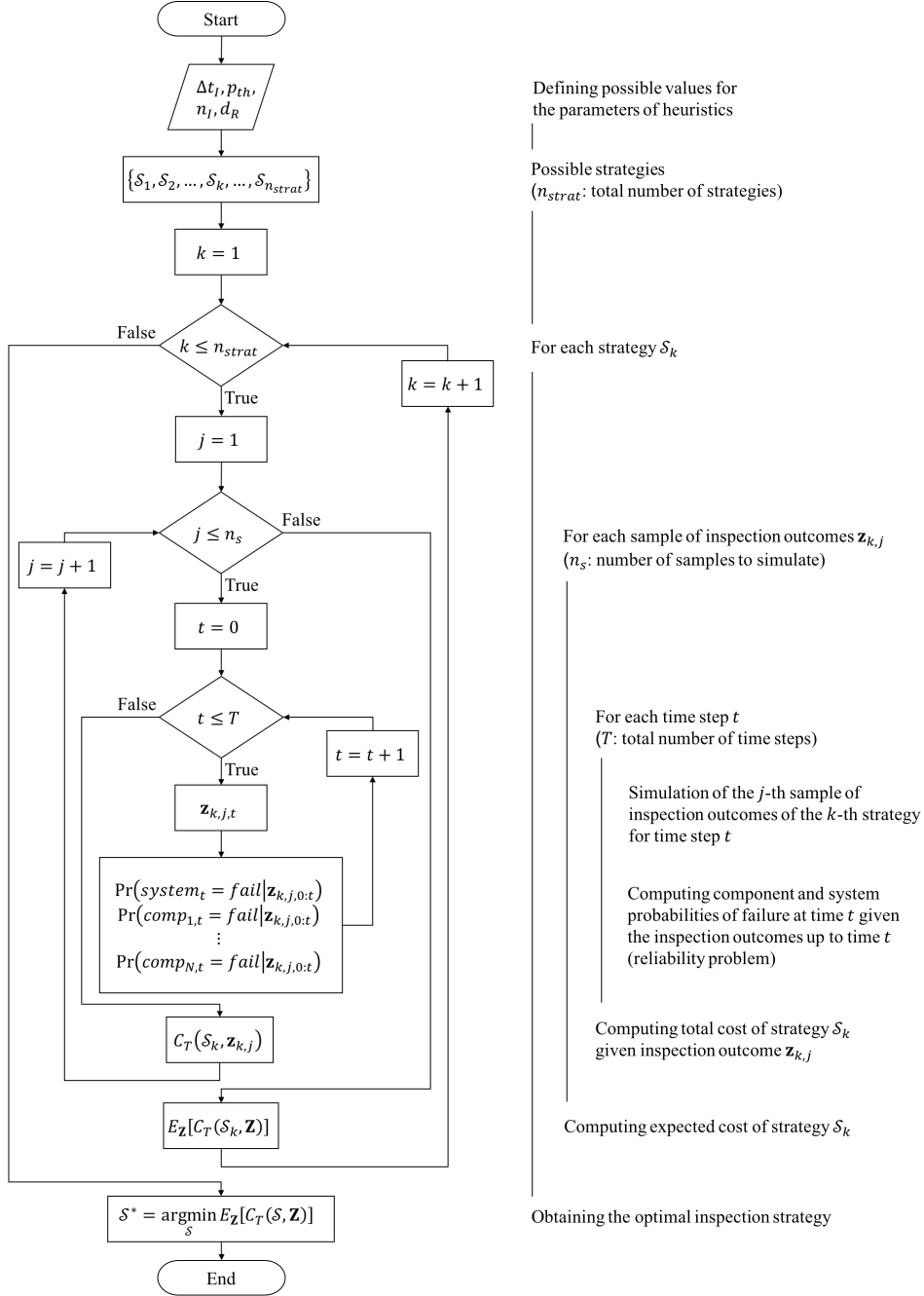


Figure 9. Flowchart of the optimization algorithm at the system level.

3.3.6 Additional extensions and improvements to the DBN model

Bismut et al. (submitted) generalize the proposed solution to the RBI problem using a cross-entropy-based method (De Boer et al. 2005) to reduce the noise that the Monte Carlo approach generates, and they also include adaptive planning in order to incorporate recent inspection and monitoring data to modify the current strategy. The details of such extensions and improvements to the framework are not discussed in this thesis.

4 Case studies / Results

This chapter summarizes the main case studies that support this thesis:

- Case 4.1 shows how a hierarchical DBN can be used to model uniform corrosion deterioration in ship vessels (Paper C). To obtain the updated estimations given inspection data, Markov Chain Monte Carlo (MCMC) is used.
- Cases 4.2 and 4.3 show how to apply the DBN framework from Paper B to model fatigue deterioration in two different types of structures: 1) the Daniels system (a theoretical structure), and b) the Zayas frame (a laboratory structure). In both cases the accuracy and robustness of the inference algorithm to solve the reliability problem is demonstrated and compared to other approaches like MCMC.
- Case 4.4 compares heuristic-based strategies against other approaches such as LIMIDs to approximate the optimal inspection strategy of a component (Paper A)
- Case 4.5 demonstrates how to combine the DBN framework from Paper B with heuristic rules and a simulation-based approach to solve the optimal inspection planning problem (Paper D).

4.1 Hierarchical model for uniform corrosion in ship vessels

Corrosion in ship structures is influenced by multiple factors that vary in time and space. Existing corrosion models used in practice only partially address the spatial variability of the corrosion process. Typical estimations of corrosion model parameters are based on averaging measurements for one ship type over structural elements from different ships and operational conditions. Most models do not explicitly predict the variability and dependency of the corrosion process among multiple locations in the structure. This correlation is of relevance when determining the necessary inspection coverage, and it can influence the reliability of the ship structure.

In this case study, Paper C develops a probabilistic spatio-temporal corrosion model using a hierarchical approach to represent the spatial variability and correlation of the deterioration process. It accounts for the dependences among corrosion states at different locations due to common influencing factors. The model is learned with data from thickness measurements obtained during in-service inspection campaigns and it estimates the current and future corrosion in the structure based on such measurements.

The hierarchical Bayesian model for corrosion in ship vessels has the following main aspects:

- *Hierarchical levels (from lower to higher)*: single plate, structural element, frame, compartment, vessel, fleet (Figure 10). The framework is flexible and the levels in the hierarchy can be arbitrarily increased, modified, or reduced. At the lowest level, which is the one of the plate element, the corrosion process can be modeled as a spatial random field.
- *Corrosion loss (as deterioration amount)*: The model considers plate thickness diminution (or corrosion loss) to quantify uniform corrosion deterioration. This is obtained as the difference between the as-built and current thickness of a plate.
- *Corrosion function*: The hierarchical BN uses a corrosion function to model the deterioration amount in a structural element. Table B1 shows a list of the most commonly used functions to represent uniform corrosion in single plates.
- *Thickness margin*: When building ship vessels, it is common that many plates are thicker than what construction plans indicate. This difference between the as-built and gross thickness (i.e. value given in plans) is defined here as thickness margin.
- *Coating life*: It is defined as the time it takes to break the protective coating of a plate allowing corrosion to start.
- *Measurement model*: It aggregates all sources of errors, of which human and measurement devices are the most common types.

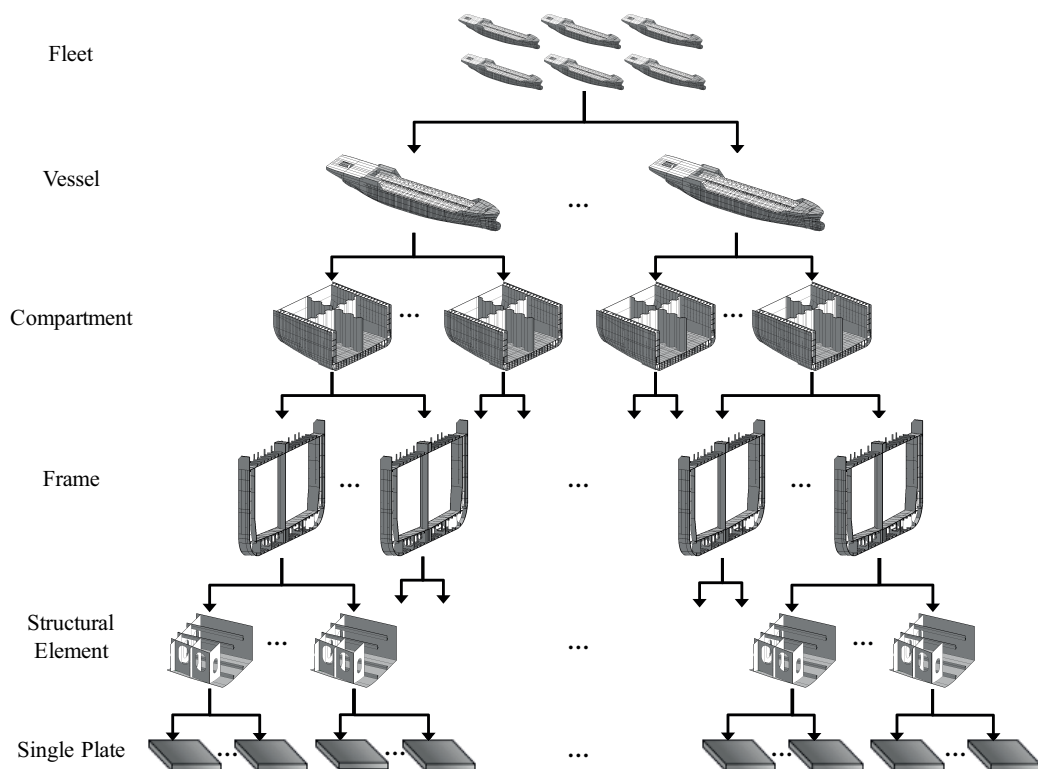


Figure 10. Hierarchical structure of the spatial corrosion model.

The graphical representation of the hierarchical corrosion model is depicted in Figure 11.

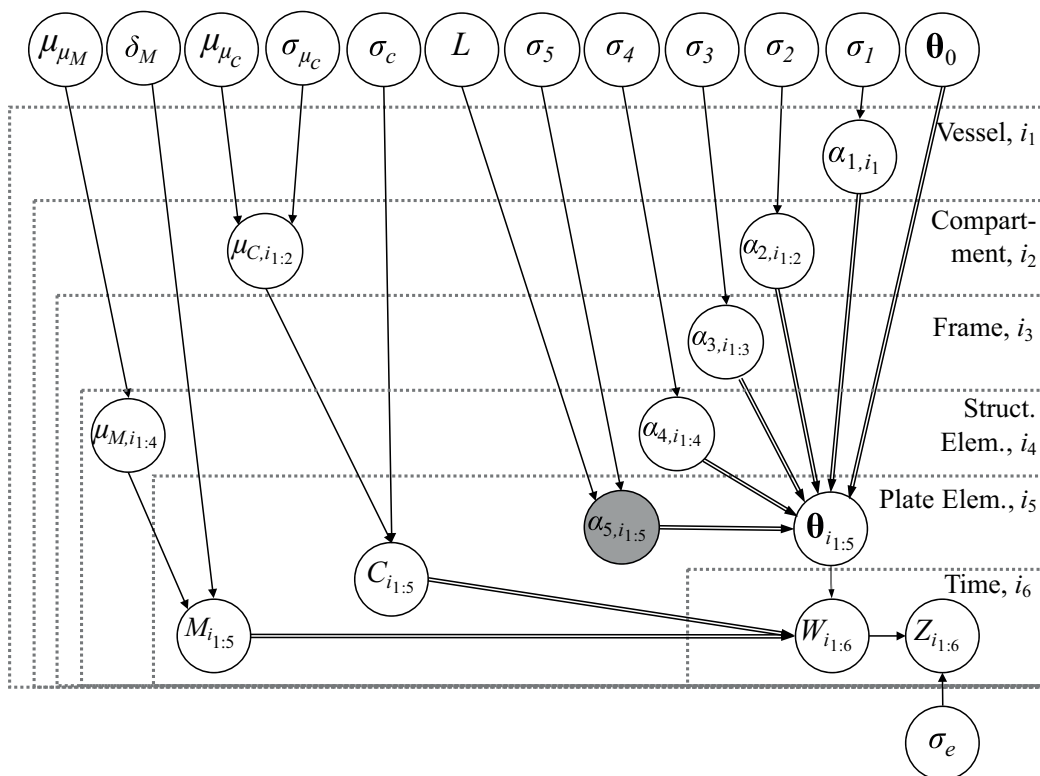


Figure 11. Hierarchical corrosion model for ship structures. Node W_i represent the current thickness of the plate and Z_i its observation; σ_e represents the variability of the measurement error; θ_i is the set of parameters of the corrosion function; μ_X and σ_X are the mean and standard deviation of the indicated random variable X ; M_i represents the thickness margin; C_i is the coating life; $\alpha_1, \alpha_2, \alpha_3, \alpha_4, \alpha_5$ are variability factors used to model the difference in corrosion processes at different locations; and L is the correlation length when α_5 is modeled as a random field.

The case study consists of two parts. The first part corresponds to a hypothetical study using simulated data to assess the performance of the model and the parameter learning against an assumed “true” model. The second part presents the learning of the model using thickness measurements from a set of sister ship tankers (i.e. vessels with virtually identical design). Then the model predicts the corrosion of a specific tanker out of the original training sample. For both parts, Bayesian estimation is carried out using Markov Chain Monte Carlo (MCMC). The details of the MCMC analysis are presented in Section C3.1.

The results from the first part show a good agreement between the original and the estimated values for most of the parameters that were learned from the simulated data (Table 1). Only for one parameter (variability factor α_5) the credible interval that the model obtained does not contain the “true” value. As more data is included in the model, the uncertainty in the estimations decreases (i.e., the estimated posterior distributions become narrower).

Table 1. Statistics of the stochastic parameters of the model.

	Original (true) value	Estimates		
		Mean	StDev	95% Credible Interval
<i>Margin</i>				
Mean μ_{μ_M} , [mm]	0.8	0.824	0.032	(0.76,0.89)
<i>Coating</i>				
Mean μ_{μ_C} , [years]	7	6.91	0.255	(6.4,7.4)
<i>Corrosion rate and variability factors</i>				
Vessel variability σ_1	0.3	0.389	0.118	(0.22,0.68)
Compartment variability σ_2	0.2	0.214	0.048	(0.14,0.32)
Struct. element variability σ_4	0.3	0.289	0.0149	(0.26,0.32)
Plate variability σ_5	0.1	0.129	0.0123	(0.11,0.16)
Base corrosion rate r_0 , [mm/yr]	0.3	0.249	0.034	(0.19,0.32)

The second part of the case study includes thickness measurements from real inspection campaigns to estimate the distribution of the model parameters. This analysis is focused on floor plates (Figure 12a) because they were inspected in all ship tankers. Figure 12b shows the spatial distribution of the thickness measurements of one inspection campaign as an example.

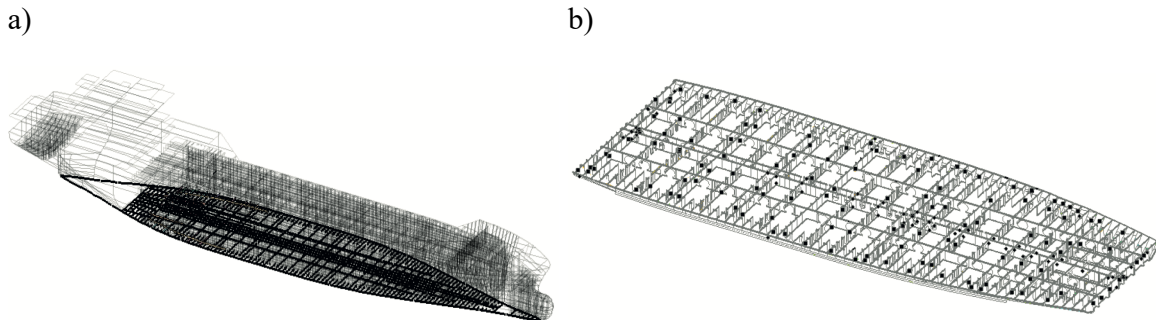


Figure 12. a) Location of the structural element Floor in tankers; b) locations of thickness measurements in one of the measurement campaigns.

Because of the small number of inspection campaigns and to avoid convergence problems in the MCMC analysis, some model parameters were neglected (i.e., set equal to zero) or assumed known and based on previous statistics from literature. The results obtained with the model showed a good agreement with those values reported in literature for this type of structural elements (Sone et al. 2003). It was also concluded that the variation of the corrosion rate among

compartments is larger than the variation within, which agrees with the fact that environmental conditions are more even among plates from the same compartment than from different ones.

Another important outcome of the model is its flexibility to include variables as the thickness margin. The model obtained an estimated mean margin of 0.315mm, which is not negligible compared to the average corrosion loss observed in floor plates for this type of ships (0.26 mm). Not considering this parameter in the model and simply using the gross thickness (i.e. thickness from plans) as the initial thickness would lead to estimations of negative corrosion, which would clearly be wrong and useless.

These results are then used as a prior probabilistic model for the analysis of a specific vessel. Figure 13 shows the estimated expected value of the thickness margin, coating life, and corrosion rate at different locations of the analyzed ship. As a remark, the model obtains not only the expected value but a complete distribution for each point shown in the previous figure, but for the sake of simplicity, only the mean value is plotted.

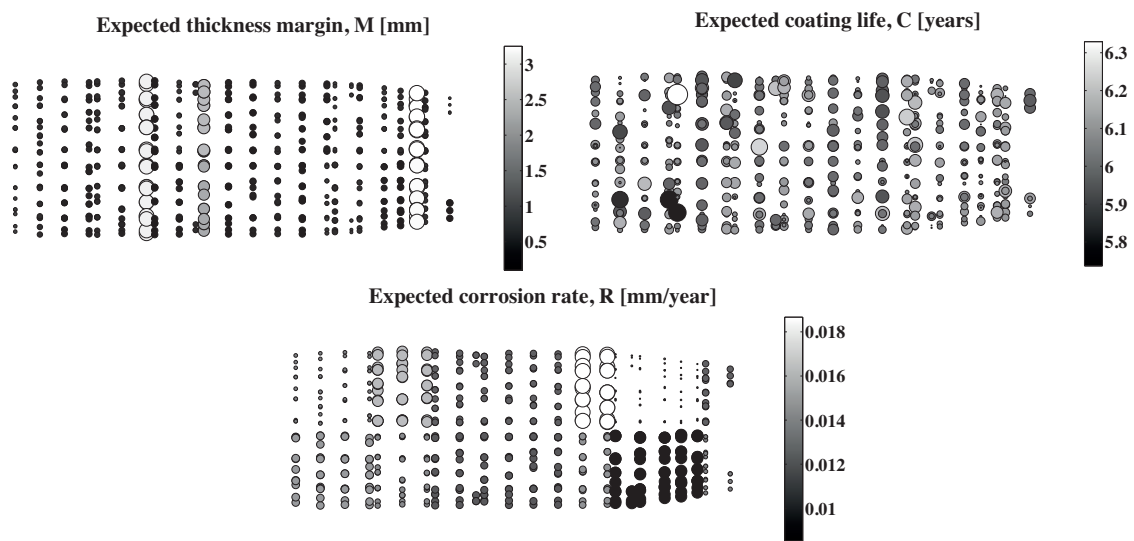


Figure 13. Spatial distribution of the expected value of thickness margin M , coating life C , and corrosion rate R per measured location. The darkness of a circle represents the mean estimate and the size of a circle reflects the deviation of the value at this location from the total mean value (i.e. from all measured points).

Finally, the model can also show the difference between the estimated corrosion rate in the original set of ship tankers and the additional ship (Figure 14).

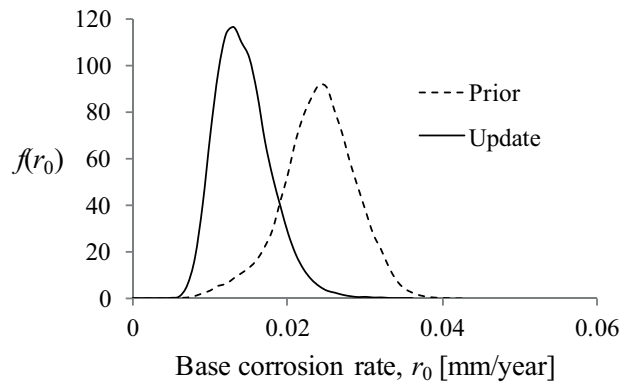


Figure 14. Comparison between the prior distribution of the corrosion rate obtained from a fleet of ship tankers and the updated (posterior) distribution of a specific ship.

This spatio-temporal corrosion framework allows to probabilistically quantify the dependence among the deterioration states at different locations in the structure. It also provides a systematic and effective way of using all available information from inspections and measurement campaigns. Using MCMC as inference algorithm, one can estimate the posterior distribution of the model parameters. With these results, one can predict the deterioration that might occur in the next years, and even estimate the condition at locations that were not inspected during some campaigns. If a failure criterion is defined, one can also estimate the probability of failure at different levels of the structure (e.g. a single plate failure or a complete cross section failure) using structural reliability methods. The deterioration process considered here is uniform corrosion in floor plates of tankers, but the model principles are applicable to any ship structural elements and to other corrosion process types, such as pitting corrosion, or other deterioration processes, such as fatigue.

The case study presented here also shows some of the limitations of this framework. A critical aspect of it is the amount of data. To accurately estimate the posterior distribution of the model parameters, one needs large amount of information in space (i.e. many different locations inside the structure) and time (i.e. multiple inspection campaigns at different times). Insufficient data in one of these aspects might compromise MCMC convergence, forcing to reduce the number of model parameters to obtain adequate results. For most applications of this framework, the computations can be performed offline in a reasonable time. Only when one requires near real-time estimations (e.g. deciding during inspection time where else to inspect or even stopping the inspection based on what has been already observed), the computation time of MCMC might be an issue. In this use case, this approach gives accurate results because it is only focused on estimating the posterior distribution of the parameters of the deterioration process, for which the number of required samples is still low (less than 10^5 samples).

Even though this framework could theoretically be used for solving the RBI problem, it presents several limitations due to the large number of samples that would be required to accurately estimate low probabilities of failure, and its computation time would considerably increase with the number of observations included in the model. The next case studies show the efficiency and accuracy of a different approach, the DBN framework from Paper B, which is compared to MCMC for solving a reliability problem of structures with low probabilities of failure.

4.2 Reliability analysis of a Daniels system

In this case study from Paper B, the accuracy and robustness of the deterioration DBN framework is evaluated using a theoretical structure, the Daniels system. This system facilitates studying characteristics of load sharing among the elements in redundant structural systems.

A Daniels system consists of a set of N load-sharing elements with independent and identically distributed random capacities $R_i, i = 1, \dots, N$, and an external random load L (Daniels 1945, Gollwitzer and Rackwitz 1990). The system is illustrated in Figure 15 and its parameters are summarized in Table D.1.

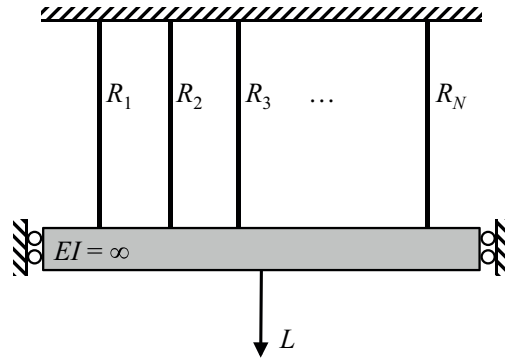


Figure 15. Daniels system with N elements, capacities $R_i, i = 1, \dots, N$, and external load L .

Here, the components of the Daniels system are affected by fatigue deterioration. The fatigue deterioration is described by a simple fracture mechanics model based on Paris' law:

$$\frac{dD_i(t)}{dt} = \nu C_i \left[\Delta S_{e,i} \sqrt{\pi D_i(t)} \right]^{M_i} \quad (9)$$

where ν is the stress cycle rate; $\Delta S_{e,i} = \left(\mathbb{E}[\Delta S_i^{M_i}] \right)^{\frac{1}{M_i}}$ is the equivalent constant stress range for all stress cycles used before, and ΔS_i the stress range per cycle; C_i, M_i are material parameters.

Failure of the i -th component occurs when the crack depth D_i exceeds a critical value d_c . Fatigue deterioration is represented by a binary model, in which the i -th component has either

its full capacity (prior to fatigue failure) or zero capacity (after fatigue failure). Any interaction between the extreme load L and the fatigue deterioration is neglected.

Because of the exchangeability of its components, the system reliability is a function only of the number of components that have failed. This property is used here to define an alternative representation of the convergent connection from the condition of the components $E_{C,1:N,t}$ to the condition of the system $E_{S,t}$ (see Figure 8) and consequently to reduce the complexity of the algorithm. The service life of the structure is discretized in $t = 0, 1, 2, \dots, T$ time steps.

Observations of the deterioration state are available through inspections. The observation Z is a binary random variable with possible states *no crack detection* ($z = 0$) and *crack detection* ($z = 1$). The inspection quality is described by an exponential probability of detection (POD) model as a function of the crack depth, i.e. the deeper a crack, the higher the probability of detecting it (see Equation B.17).

The hyperparameters $\alpha = (\alpha_M, \alpha_K, \alpha_D)$ represent the dependence of the deterioration process among components, linking material parameters, stress parameters, and initial crack depths. In this case, the hierarchy contains one single level represented by three (a-priori) independent hyperparameters. These hyperparameters represent the dependence coming from, e.g. a common manufacturer (i.e. similar material properties and initial crack conditions among structural elements) and common deterioration conditions (i.e. related stresses).

All the model parameters and the discretization scheme are presented in Tables B.1 and B.2. The Daniels system is defined with $N = 10$ components and $T = 100$ time steps. The resulting DBN of the Daniels system is presented in Figure 16.

The results of the proposed inference algorithm are compared to those obtained using Monte Carlo simulation (MCS) and MCMC. The computations are done for the unconditional (i.e. without observations) and conditional (i.e. with observations from inspections) cases. The estimations of the probability of failure at both component and system level using the different methods show a good agreement (Figure 17). At the system level, the difference between the probability estimates from the proposed DBN model and the Monte Carlo methods is due to the discretization scheme of the hyperparameters alpha. This issue can be mitigated by increasing the number of discrete states for each hyperparameter with an associated increase in computation time.

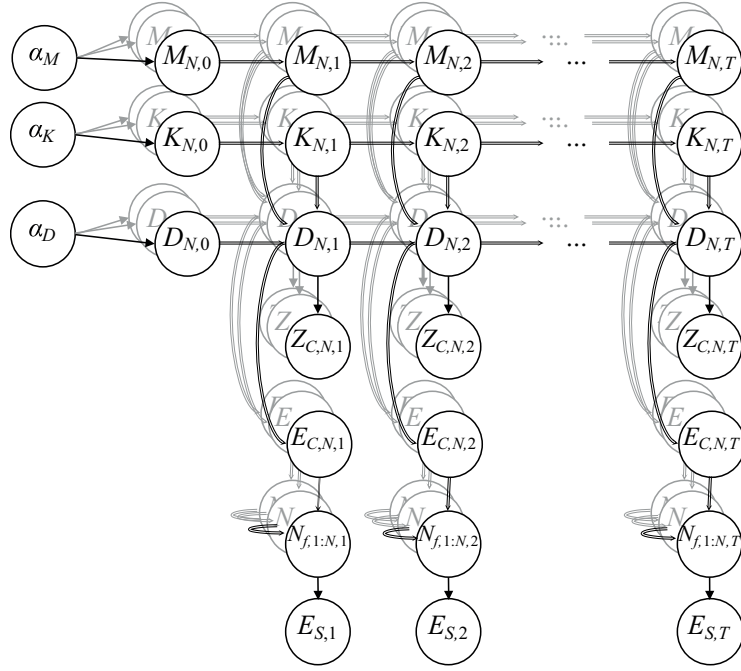


Figure 16. DBN of the Daniels system with N components; hyperparameters $\alpha_M, \alpha_K, \alpha_D$; material parameter M ; fatigue parameter K ; crack depth D ; observation Z ; component condition E_C ; number of failed components N_f ; and system condition E_S .

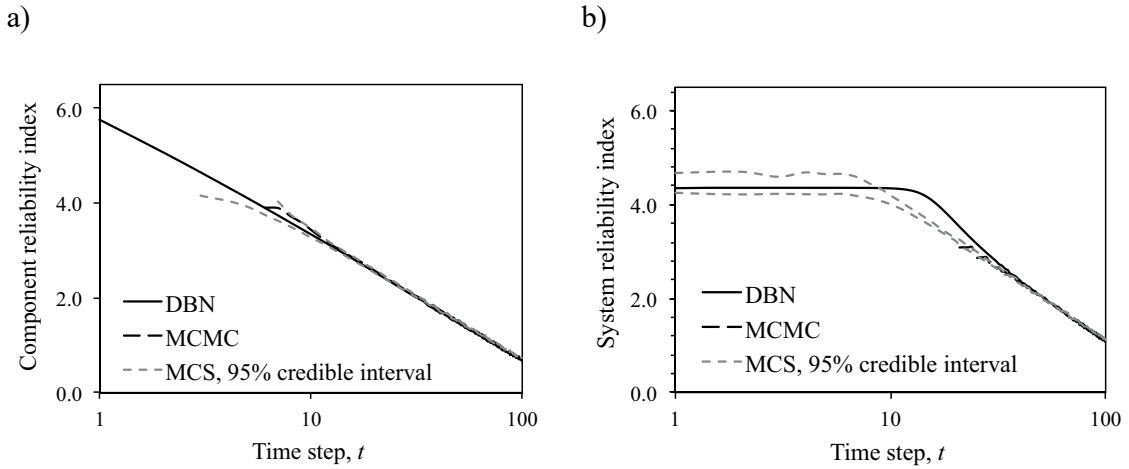


Figure 17. Reliability index for the unconditional case of a) a component, and b) the Daniels system.

For the conditional case (i.e. with inspection observations), the results of the DBN model and the MCMC match better than for the unconditional case (Figure 18). The necessary computation time for the solution of the DBN model using the exact inference algorithm is orders of magnitude lower than that for the applied standard MCMC algorithm. The complexity of both approaches with respect to the number of system components is linear, but the proposed

inference algorithm is not affected by the number of observations or the order of magnitude of the probability of failure.

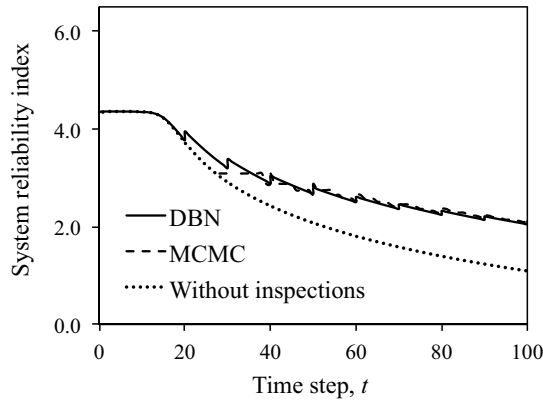


Figure 18. Reliability index of the system for the conditional case (here: no detection of cracks).

To demonstrate the efficiency of the DBN algorithm as the number of components and inspections is increased, this case study from Paper B also investigates a Daniels system with $N = 100$ components and inspection observations for some of its components, as described in Table B.3. The results of the computed system reliability for both with and without inspection cases are shown in Figure 19. Since the inspection resulted in detection of multiple cracks and no repairs are considered in this example, the system reliability is lower after including the inspections. MCMC results are not computed for this case due to the associated large computation times.

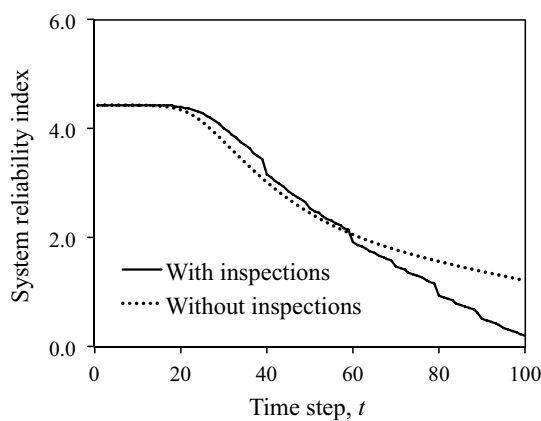


Figure 19. Reliability index of the Daniels system with 100 components with and without inspections.

As a conclusion, the deterioration DBN framework is able to represent the dependencies among system components. The accuracy and efficiency of the developed inference algorithm is

successfully demonstrated in this theoretical case study, showing good agreement with MCMC and MCS in the updated probabilities, but with computation times that are orders of magnitude lower. This difference in the computation time becomes more remarkable as the amount of inspection data increases.

4.3 Reliability analysis of a 2D tubular structure – the Zayas frame

In this case study from Paper B, the applicability of the deterioration DBN framework is evaluated by investigating a more realistic structure, the Zayas frame.

The Zayas steel frame is commonly used as a benchmark in structural analysis of steel offshore structures (Zayas et al. 1980). It consists of 23 tubular members with welded connections. The fatigue hotspots are located at the welded connections of the 13 horizontal and diagonal members. There are $N = 22$ fatigue hotspots, which represent the system components in the DBN model. The structure is loaded in horizontal direction by a concentrated force L at the upper left node of the structure and by gravity load. The details of the geometrical and material properties of the structure are described in Schneider et al. (2017).

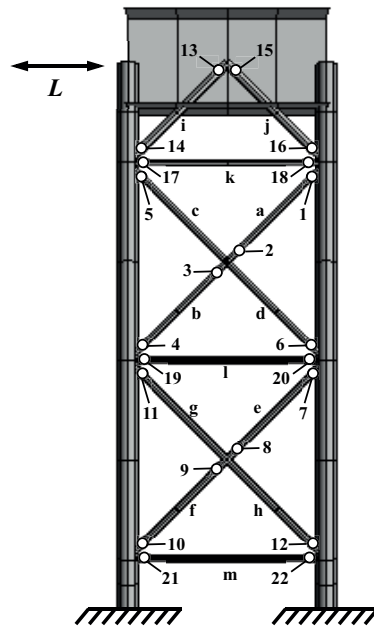


Figure 20. Zayas steel frame structure with 22 fatigue hot spots in 13 tubular members (a – m).

The model used in this case study considers fatigue deterioration in all hotspots of the Zayas frame according to Section B4.1.1 with parameters listed in Table B.1. As in the previous case study from Section 4.2, a redistribution of fatigue stresses when some system components fail is neglected, i.e. $K_{i,t}$ is modeled as a time-invariant parameter.

The inspection observations have the following characteristics: a) measurements of crack sizes at the hotspots are taken; b) observation $Z_{i,t}$ is equal to the true crack sizes plus a random measurement error; c) observation $Z_{i,t}$ is discretized with the same scheme as the crack depth $D_{i,t}$ with one additional state representing no detection. Note that the number of discrete states of $Z_{i,t}$ has no effect on the computational demand.

The relation between hotspots, structural elements and system condition has the following characteristics:

- Each structural element has either one or two fatigue hotspots associated to it
- Condition of hotspots and elements is modeled through random variables E_h and E_e , respectively
- It is assumed that an element fails if any of its hotspots fails

Given the number of structural members in the Zayas frame, the total number of possible system configurations (i.e. surviving elements after component failures) is $2^{13} = 8192$, which are explicitly managed in this case study. To estimate the probability of failure of the system, the ultimate capacity of the structure is obtained for each possible system configuration through a pushover analysis. The condition of the system $E_{S,t}$ is defined as a child node of the system configuration $\Psi_{S,t}$ and the extreme load L_t . The complete DBN model is shown in Figure 21.

In the unconditional case (i.e. without inspections), the estimations of the reliability index using the exact inference algorithm of the DBN approach, MCS, and MCMC give consistent results for a single hotspot and the system (Figure 22).

When including crack measurements (i.e. conditional case), the exact inference algorithm of the DBN framework is able to compute the reliability at the component and system level, but the MCMC algorithms implemented in OpenBUGS (Lunn et al. 2009) have convergence issues and no reliability estimates were obtained (Figure 23).

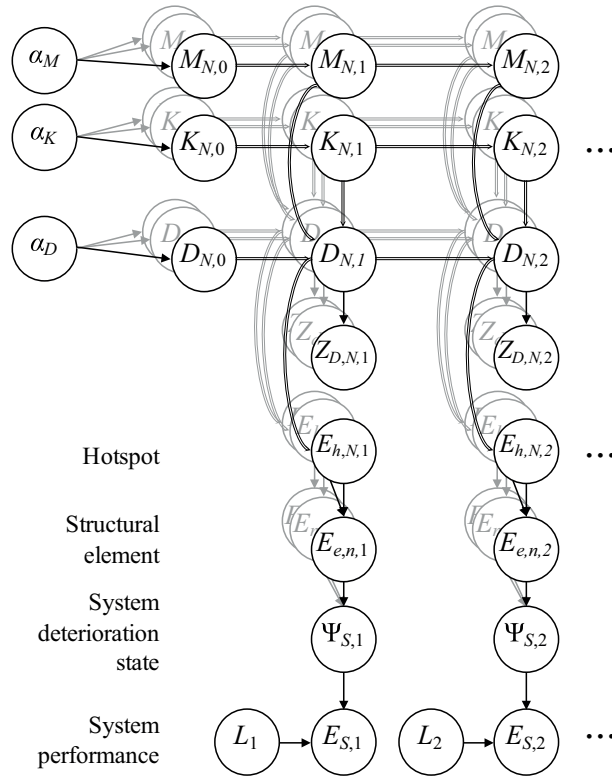


Figure 21. DBN of the Zayas frame with hyperparameters $\alpha_M, \alpha_K, \alpha_D$; material parameter M ; fatigue parameter K ; crack depth D ; observation Z ; hotspot condition E_h ; structural element condition E_e ; system configuration Ψ_S ; external load L ; and system condition E_S .

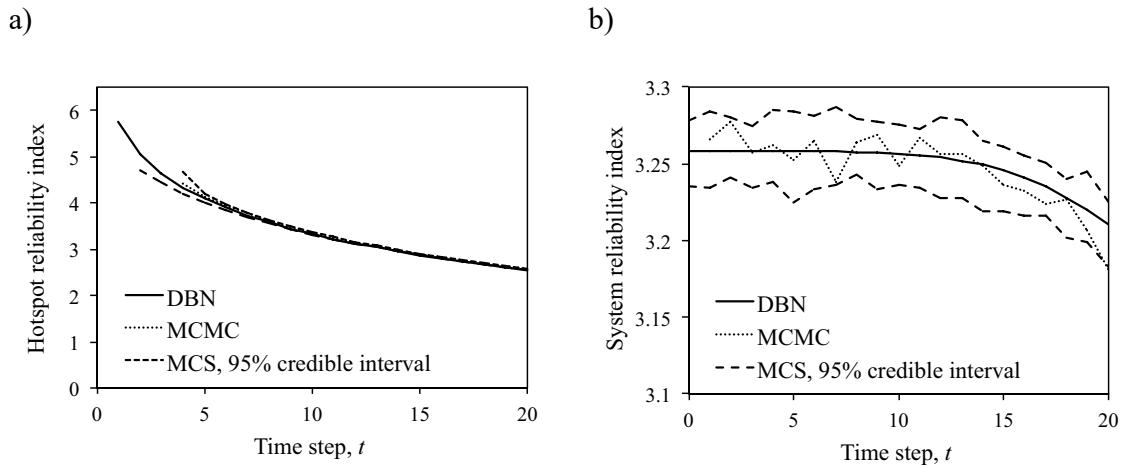


Figure 22. Reliability index for the unconditional case (i.e. without inspections) of a) a single hotspot, and b) the complete system (here Zayas frame).

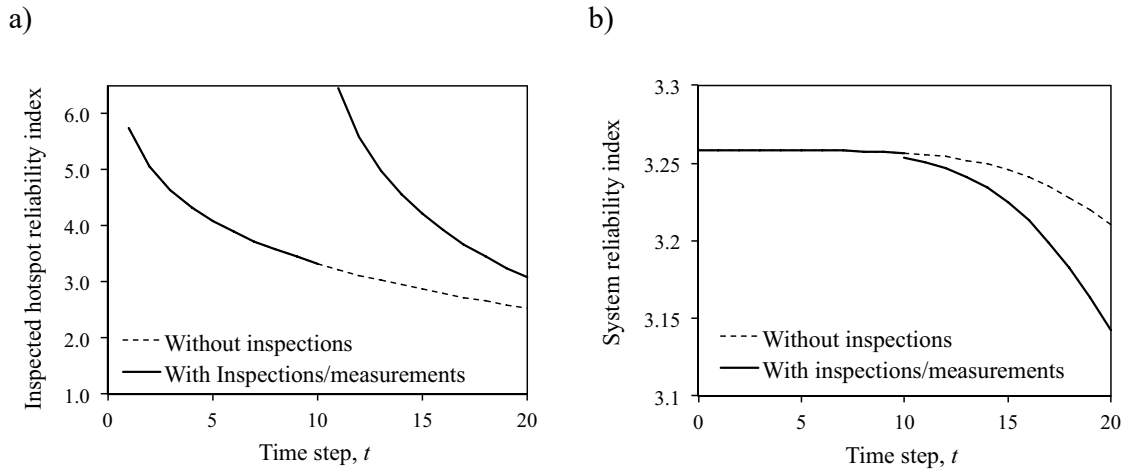


Figure 23. Reliability index for the conditional case (i.e. with inspections) of a) an inspected single hotspot, and b) the complete system (here Zayas frame).

To demonstrate the flexibility of the DBN framework, a case with more inspection measurements at different locations and multiple time steps on the Zayas frame is also analyzed. Figure 24 presents the reliability index of the system given multiple observations at hotspots 1 to 4 and time steps 10, 20, 30, and 40.

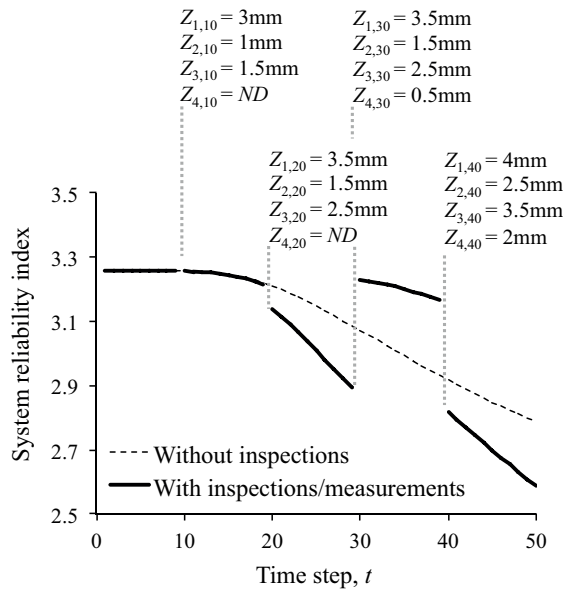


Figure 24. Reliability index of the system for the conditional case (i.e. with inspection) with observations from hotspots 1 to 4 at time steps 10, 20, 30 and 40. A measurement ND represents a no-detection case.

4.4 Full optimization vs heuristic rules

In this case study from Paper A, multiple approaches to compute the optimal inspection strategy based on influence diagrams are compared. For the numerical investigation, a structural element subject to fatigue deterioration is studied using a DBN model that incorporates information from previous inspection campaigns.

Figure 25 shows the influence diagram (ID) associated to the decision problem of this case study. In the LIMID, only those nodes with links to the decision nodes are assumed to be known at the time of making the decision. This assumption strongly reduces the computational effort when optimizing the decisions. With increasing memory, i.e. with increasing number of links to the decision nodes, the policy domain of the decision nodes increases, making the solution of the optimization problem intractable as discussed in Section 2.5. However, reducing the number of information links toward the decision node leads to suboptimal solutions, in particular if compared to the no-forgetting assumption.

The elements of this ID are summarized in the following (more details in Paper A):

- Deterioration state: Fatigue crack depth is represented with node a
- *Inspection decisions*: At every time step t , a decision node D_t is included that indicates if an inspection is carried or not
- *Observations*: In case an inspection is carried out at time t , the random variable Z_t will indicate if a crack was detected or not
- *Repairs*: Repair actions are included in the model as a function of the observed conditions of the component and the system. Node a' represents the deterioration state of the component after repair.
- *Component and system condition*: Nodes E_C and E_S represent the condition of the component and the system before inspection. System failure is defined based on the redundancy of the system (more details in Section A.3.2). This simple model does not account for multiple element failures.
- *Utilities*: Utilities from the system condition, inspection decision, and observation nodes are modeled by nodes $U_{S,t}$, $U_{I,t}$, and $U_{R,t}$
- *Memory*: It is assumed that no information is available when the inspection decision is made. We call this the *no-memory* ID. The advantage of the no-memory ID is that all inspections can be planned a-priori, since no observation during the service life will influence the inspection decisions.

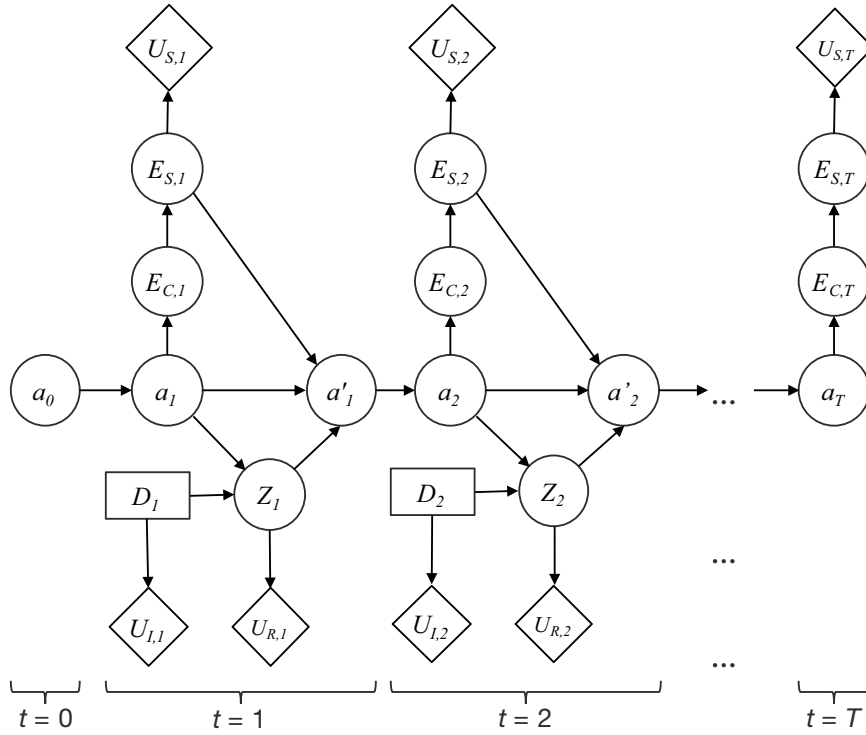


Figure 25. ID model of the fatigue inspection planning problem for the no-memory case with crack depth a before and a' after repair; inspection decision node D ; observation Z ; component and system conditions E_C and E_S ; and utility nodes U_I , U_R , and U_S .

The ID from Figure 26 represents an extension of the previous ID (Figure 25), where information from past observations and decisions is considered when planning the inspections. In this ID, it is assumed that the last inspection observation is known when deciding upon inspection. Two additional variables, Z_t^* and τ_t , are included in the model and contain the observation from the last inspection and the time when it was performed. We call this ID the *last-inspection ID*.

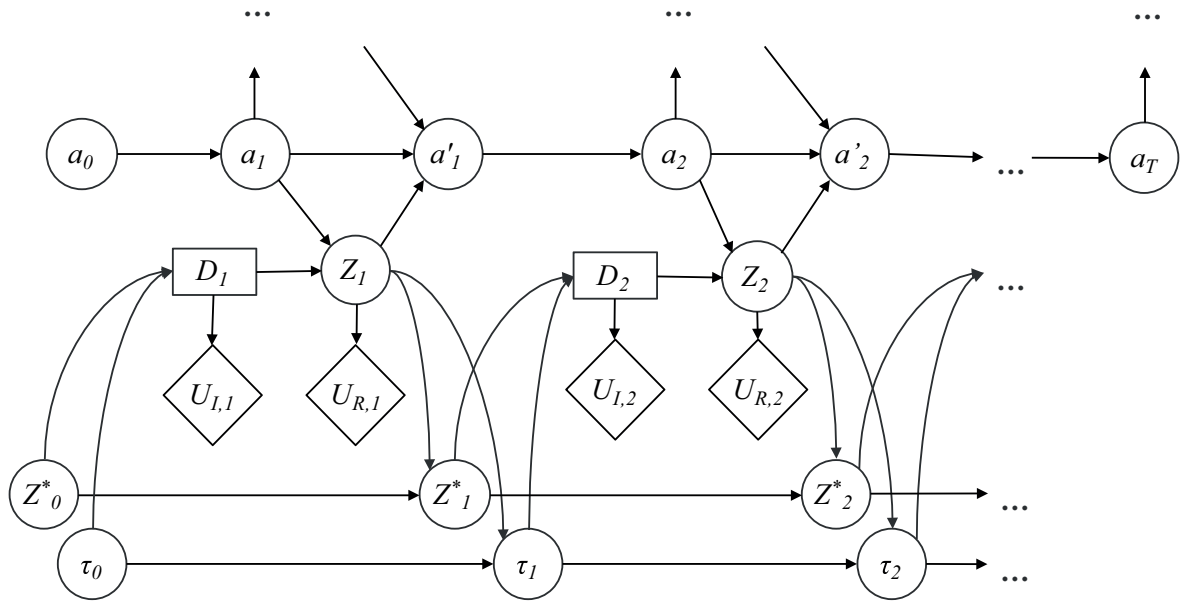


Figure 26. ID model of the fatigue inspection planning problem for the last-inspection case with the same original nodes as in Figure 25 and additional nodes Z_t^* and τ_t containing the observation from the last inspection and the time when it was performed.

The inspection planning problem is solved with the periodic inspections and the reliability threshold heuristics, with the SPU algorithm for the no-memory and last-inspection cases, and with a full search for the no-memory ID case for comparison. The full search approach covers all 2^{15} possible inspection schedules. Heuristics approximate the solution of the decision problem because their possible solution domains are considerably smaller subsets of the complete solution domain, thus reducing the computational effort (see Sections 3.2 and 3.3.1). Both heuristic approaches define a single parameter optimization problem. Their algorithms have a linear complexity order with respect to the number of time steps whereas SPU complexity depends on the maximum size of the variable domains considered in the decision problem.

The total expected costs for all five solution strategies are estimated using Monte Carlo simulation of the component deterioration and their inspection outcomes, and final results are summarized in Table 2. The difference in the total expected cost among the optimal solutions is relatively small despite the inspection times and disaggregated costs (i.e. failure, inspection and repair costs) being quite different among the solutions. The reason for the small differences in expected costs is probably that all optimal solutions of the no-memory ID have six inspections, and the minimum reliability obtained with these optimal solutions is similar. The

best strategy is obtained with the last-inspection case using the SPU algorithm. This is not surprising, since this is the only strategy that allows adapting the inspection times based on inspection results. The optimal policy obtained with this approach is a set of rules that indicate when to inspect or not given the information from the last inspection (e.g. inspect after two years if the last detected crack depth is larger than x mm). This implies that the exact inspection times will not be known in advance but are dependent on how the component deteriorates and if such deterioration is detected.

Table 2. Solutions of the optimal inspection problem using different approaches.

Approach	Expected cost	Inspection times	CPU time (sec)
Periodic inspections	14.91	2, 4, 6, 9, 11, 13	0.4
Reliability threshold	14.70	2, 4, 6, 8, 10, 13	4.3
SPU (no-memory ID)	14.05	1, 2, 4, 5, 7, 9	164
Exact solution (no memory ID)	13.97	1, 2, 3, 5, 7, 10	313
SPU (last-inspection ID)	13.75	Policies for each decision node	165

Comparing the SPU solutions, it is seen that the expected cost decreases from 14.05 to 13.75 when using the last-inspection case. In this case, the SPU algorithm provides an adaptive policy for each decision node. For example, the resulting policy of the decision node D_{12} indicates that an inspection is always carried out unless there was an inspection in the previous year (independent of what was observed) or there was an inspection two years ago without crack detection. While the SPU algorithm requires significantly more computation time than the heuristic approaches, it gives more flexibility adapting the inspections to the results of previous observations, as already exemplified. Figure 27 shows the computation time of each evaluated approaches for different service life periods T . For illustration purpose, the last two points of the exact solution for the no-memory case ($T = 25$ and $T = 50$) are estimated as proportional to the number of possible inspection schedules.

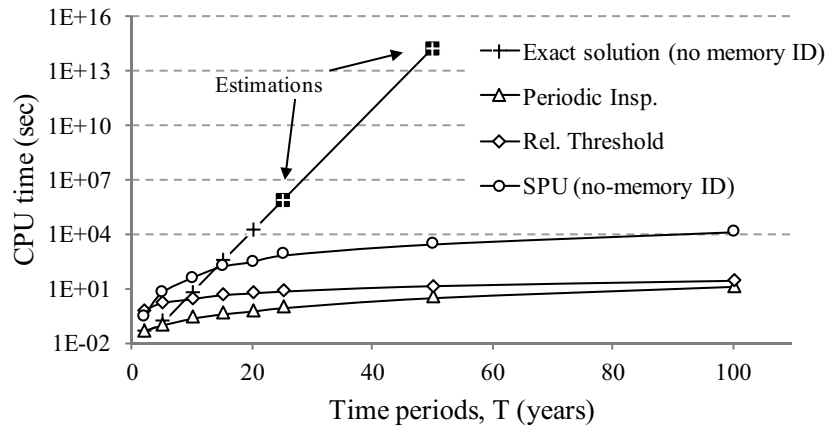


Figure 27. CPU time for finding the optimal solution.

In conclusion, SPU is found to give solutions that are slightly better than those obtained with simple heuristics, such as reliability threshold or periodic inspections, which is in agreement with Nielsen and Sørensen (2011). However, the much larger computation time of adaptive-policy-based approaches compared to simple heuristics is prohibitive for application to structural systems, even when only a reduced number of components is considered.

The results from this case study provide an argument in favor of using heuristic rules to reduce the solution space of the RBI problem at the system level (which is considerably more complex and computationally demanding than the one for single components) without much compromise in the accuracy of the solution. The following section shows a case study using such approach.

4.5 Integral risk-based inspection planning

This case study outlines a methodology for an integral risk-based optimization of inspections in structural systems. It extends the results from Section 4.2 for the Daniels system by nesting the DBN inside a Monte-Carlo simulation for computing the expected cost associated with a system-wide inspection strategy (Section 3.3.2). The solution space of inspection strategies is simplified using a heuristic approach (Section 3.3.1). The extension of the DBN model from Figure 16 into an ID is represented in Figure 28.

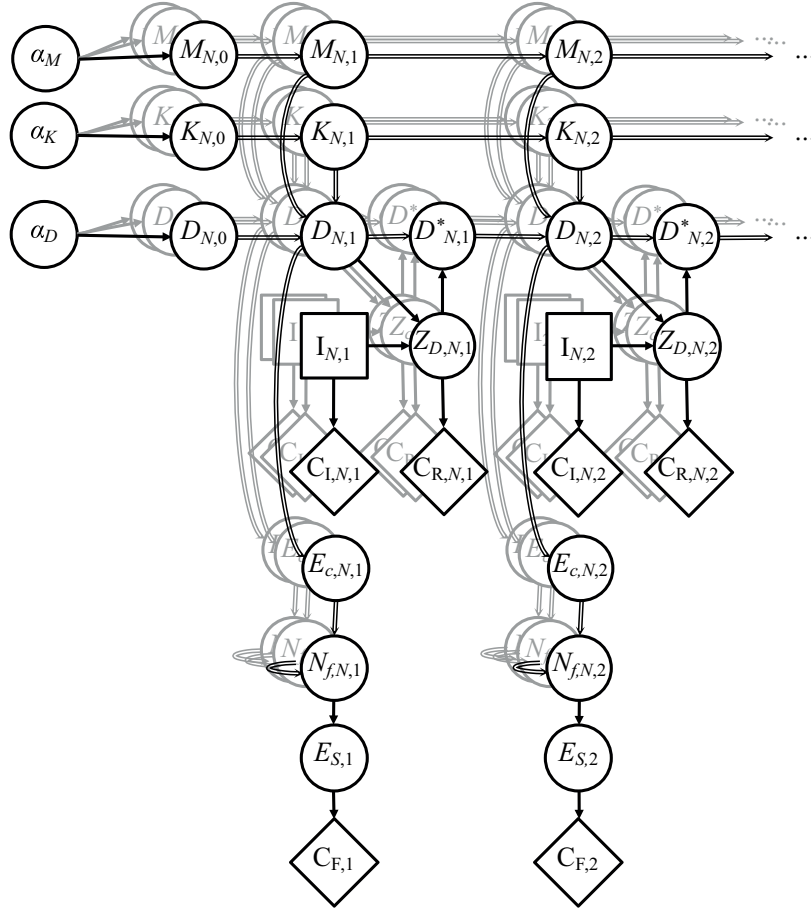


Figure 28. Influence diagram of the Daniels system with material parameter M ; scale parameter of the stress range distribution K ; fatigue crack depth D ; hyperparameters $\alpha = \{\alpha_M, \alpha_K, \alpha_D\}$; inspection decision I ; inspection outcome Z_D ; crack depth after repair D^* ; component condition E_C ; number of failed components N_f ; system condition E_S ; inspection, repair, and failure costs C_I , C_R , and C_F .

Inspection campaigns have a fixed cost c_C independent of the number of components to be inspected. This is the mobilization cost of personnel and equipment and the cost of interrupting operations. Individual inspections and repairs per component have costs c_I and c_R . The consequences of system failure are represented by the failure cost c_F . All costs are discounted to their present value through the following discounting factor based on the real interest rate r (i.e. the interest rate after allowing for inflation). Two cost cases are considered in this case study: (a) one case with high mobilization costs and potentially large consequences of failure (e.g. an offshore structure), and (b) another case with lower failure costs relative to the inspection campaign (e.g. metallic bridge structures subject to fatigue). The details of each cost case can be found in Table D.4.

As discussed in Section 3.3.1, an inspection strategy \mathcal{S}_k is defined through the parameters:

- Δt_I , the time between regular (i.e. fixed-interval) inspections;

- p_{th} , the failure probability threshold at which additional inspections are performed;
- n_I , the pre-defined number of components to inspect during a campaign;
- d_R , the repair criterion, which is here set to 0.

The condition of a repaired component is as new. If no crack is found after inspecting component i at time t , then $D_{i,t}^* = D_{i,t}$. The possible values of the parameters defining the heuristic strategies for this case study are given in Table D.5.

Following the heuristic defined in Section 3.3.1, in each campaign the components with the largest VoI are inspected first. Because of the exchangeability of the components in a Daniels system, and because the dependence among all components is the identical (at least a-priori), the VoI is a direct function of the probability of failure (PoF) of the component. A component with a higher PoF has a larger impact on the system reliability; it also has larger uncertainty, hence the learning effect is higher for such a component. Therefore, components are selected for inspection according to their PoF.

Finally, the optimal strategy is obtained through an exhaustive search among a discrete set of predefined set of parameters as described in Section 3.3. The expected costs of the strategies evaluated in this case study for both cost models are shown in Figure 29 and Figure 30.

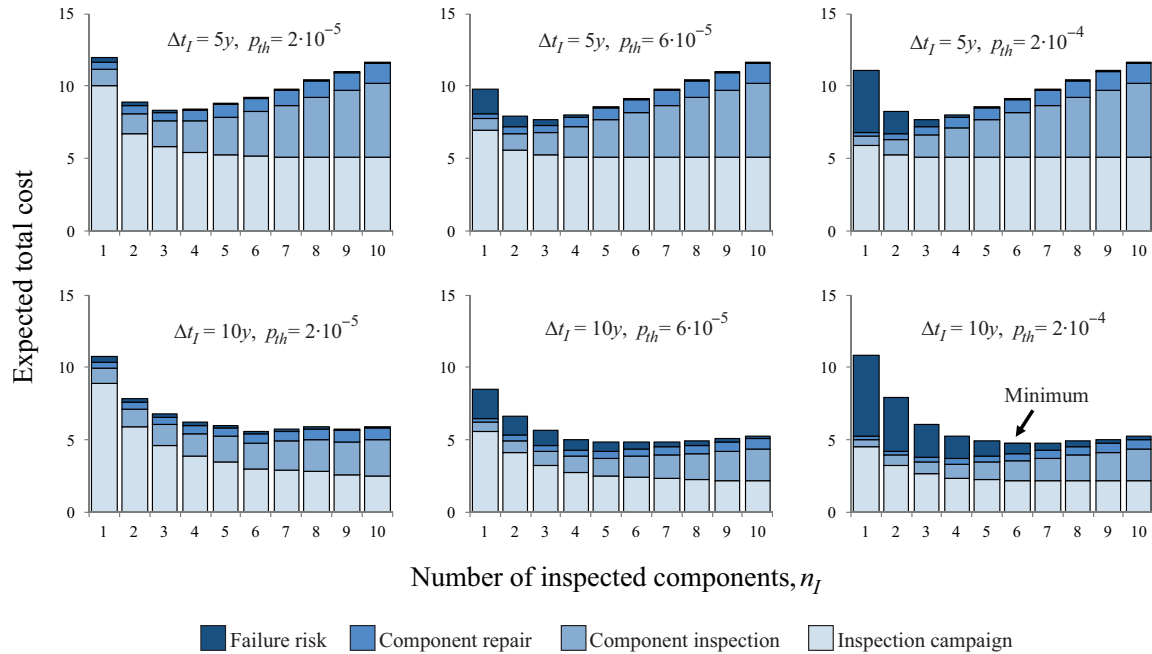


Figure 29. Comparison of the expected total cost (case 1) varying the number of inspected components n_I , the probability threshold p_{th} , and the regular inspections periodicity Δt_I . The first row corresponds to $\Delta t_I = 5y$ and the second row to $\Delta t_I = 10y$. Columns correspond to the probability thresholds $2 \cdot 10^{-5}$, $6 \cdot 10^{-5}$, and $2 \cdot 10^{-4}$.

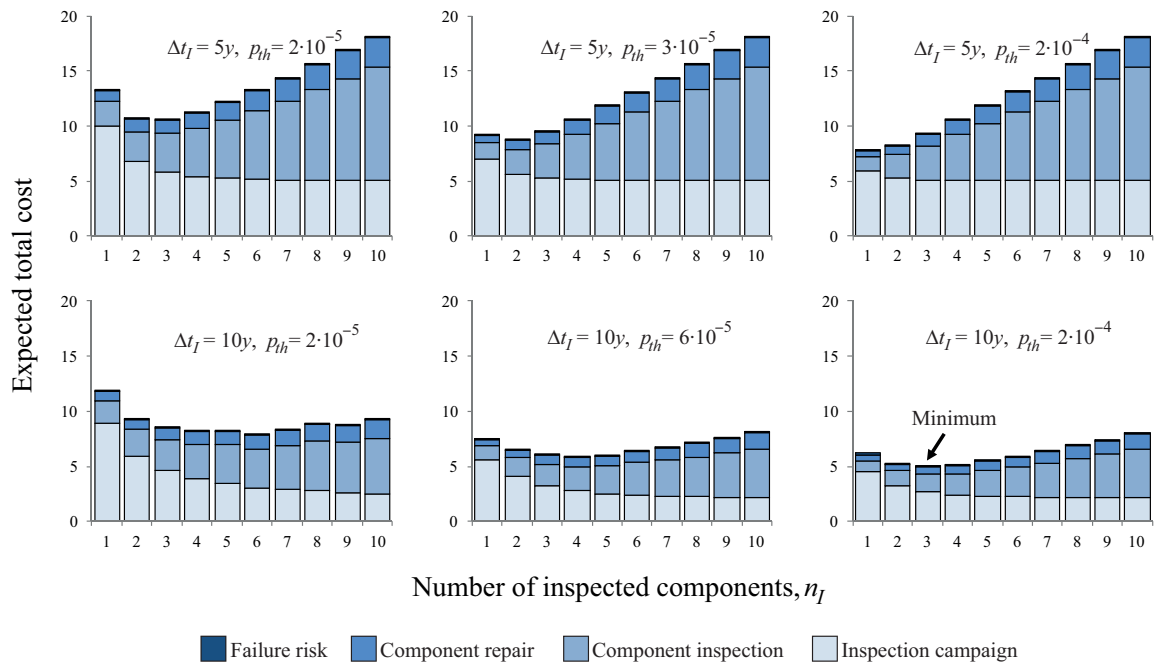


Figure 30. Comparison of the expected total cost (case 2) varying the number of inspected components n_i , the probability threshold p_{th} , and the regular inspections periodicity Δt_I . The first row corresponds to $\Delta t_I = 5y$ and the second row to $\Delta t_I = 10y$. The columns correspond to the probability thresholds $2 \cdot 10^{-5}$, $6 \cdot 10^{-5}$, and $2 \cdot 10^{-4}$.

The DBN framework combined with the heuristic rules shown in this section have also been applied to obtain the optimal inspection strategy of the Zayas frame (Bismut et al. 2017) leading to similar conclusions than those for the Daniels system in terms of efficiency of the algorithm and effectiveness of the approach.

As a conclusion, the proposed framework determines optimal inspection-repair strategies for structural systems in an integral manner considering interdependences among component deterioration states and using the information from inspections. It also explicitly includes the interaction between the reliability of components and the structural system. By applying the DBN framework to computing the conditional reliability given inspection results, the method has a computational cost that is suitable for applications in practice.

5 Paper A

Algorithms for optimal risk-based planning of inspections using influence diagrams

Jesus Luque & Daniel Straub

Engineering Risk Analysis Group, Technische Universität München, Germany (jesus.luque@tum.de, straub@tum.de)

Abstract

Risk-based optimization of inspection using influence diagrams is investigated. To this end, a fatigue deterioration model using a Dynamic Bayesian Network (DBN) approach is presented. The DBN incorporates information from previous inspection campaigns. Decision and utility nodes are de-fined inside the network to represent inspection and repair activities. The optimal inspection strategy (subject to safety or utility constraints) is approximated using the Limited Memory Influence Diagram (LIMID) approach, and is solved using the single policy updating, a local optimization strategy. In a numerical investigation, this method is found to give solutions that are slightly better than those obtained with simple heuristics that were previously applied, such the reliability threshold or periodic inspection heuristic. Finally, the numerical example demonstrates the superiority of adaptive inspection strategies, whereby inspections are planned based on the results of previous inspections.

Keywords

optimal inspections, Bayesian network, decision models, fatigue, influence diagrams.

A.1 Introduction

Deterioration processes, in particular fatigue and corrosion, lead to a reduction of the reliability of structural systems. Because deterioration processes are commonly associated with significant uncertainty, inspection and monitoring are often an effective means to increase the reliability. Based on the results of inspections, repair and replacement actions can be planned. This is known as condition-based maintenance (Swanson 2001).

The uncertainty in deterioration processes is commonly represented through probabilistic models, comprising of deterministic deterioration models whose parameters are represented by random variables. In order to assess the effect of different inspection and/or monitoring strategies, their expected costs, including the risk associated with potential failures, can be computed and compared. This is commonly known as risk-based planning of inspection and monitoring (Straub and Faber 2006) and is a special case of the pre-posterior analysis of the Bayesian decision theory (Jordaan 2005, Raiffa and Schlaifer 1961). The computation of the expected costs for a given inspection strategy requires integration over the entire outcome space of all random variables in the deterioration model as well as over all possible inspection outcomes. This is a computationally demanding problem. In addition, to compute the expected cost it is also necessary to include (and optimize) the maintenance and repair actions into the analysis. Since the number of potential alternative inspection and monitoring strategies is very large, solving the complete optimization problem is thus computationally intractable for realistic applications. For this reason, different heuristics (e.g. Straub and Faber 2006, Nielsen and Sørensen 2011) have been developed in order to approximate the optimal solution, including periodic inspections (PI) and reliability threshold (RT). More recently, the use of the limited memory influence diagram (LIMID) was suggested by Nielsen and Sørensen (2011).

In this paper, we present and compare different algorithms for the optimal planning of inspections in a structural element subject to fatigue deterioration. The fatigue crack growth process is represented through a dynamic Bayesian network (DBN). The optimization parameters are the times of inspections and times of repair actions. This decision problem is modelled as an influence diagram. Besides the classical PI and RT heuristics, we investigate two alternative formulations of the problem as a LIMID. We find that the LIMID outperforms the classical approaches, but also has increased computational demands. However, the complexity of the LIMID algorithm is shown to be of similar order than PI and RT. It is thus a viable alternative, which is particularly promising for planning inspections in systems, where the number of decision alternatives is much larger and simple heuristics such as PI and RT are not available.

A.2 Dynamic Bayesian networks and influence diagrams

A.2.1 Bayesian networks

A Bayesian network (BN) is a probabilistic model. It consists of a set of random variables (nodes) and directed links which form a directed acyclic graph (DAG), i.e. there is no directed path from any variable to itself. A discrete BN furthermore fulfils the following requisites Jensen and Nielsen (2007):

- Each variable has a finite domain
- To each variable X with parents Y_1, Y_2, \dots, Y_N is attached a conditional probability table $p(x|y_1, y_2, \dots, y_N) = \Pr(X = x|Y_1 = y_1 \cap \dots \cap Y_N = y_N)$. Y_i is called a parent of X if it has a link towards X . If a variable has no parents, the table corresponds to its unconditional probability mass function (PMF).

In Fig. A.1, exemplarily a simple BN representing the condition of a structural element before and after applying a load is shown. The condition of the element is represented by a_0 and a_1 , the damage size (crack depth) before and after the application of load L_1 , respectively. Variable Z_1 represents a possible inspection outcome of the condition a_1 in case an inspection is carried out. Nodes a_0 and L_1 are described by unconditional PMFs. The probability table of a_1 contains the PMFs of the damage size conditional on the previous damage size a_0 and the load L_1 . The probability table attached to Z_1 describes the likelihood of the inspection outcome, i.e. the probability of an observation (e.g. detect damage) given the condition a_1 .

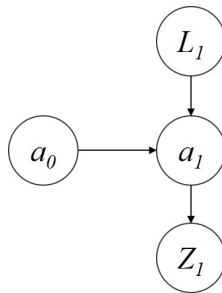


Fig. A.1. Example of a Bayesian network.

If the states of some variables are known (i.e. instantiated) in the BN, the PMFs of the remaining nodes can be updated to their posterior. For example, in the BN of Fig. A.1, an inspection outcome Z_1 can be included by instantiating the corresponding node with the observed state z_1 , e.g. no detection of a defect. The PMFs of the remaining nodes a_0 , a_1 , and L_1 are then updated to their conditional PMF given z_1 . This ability to efficiently perform Bayesian updating makes

BNs suitable for modeling deterioration processes when partial observations from inspections and monitoring are to be included (Straub 2009).

A.2.2 Dynamic Bayesian networks

In some cases, BNs contain a repetitive sequence of nodes which are associated with multiple times or spatial locations. Such a BN is called dynamic Bayesian network (DBN) and is useful for modeling time-dependent processes, including structural deterioration (Straub 2009). Extending the BN of Fig. A.1 to multiple loads L_t , conditions a_t , and observations Z_t at times $t = 1, \dots, T$ the DBN shown in Fig. A.2 is obtained.

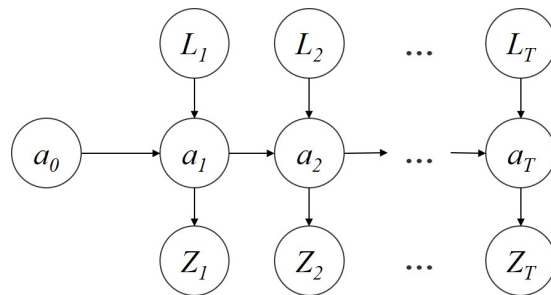


Fig. A.2. Example of a dynamic Bayesian network.

A.2.3 Influence diagrams

BNs can be extended to influence diagrams (ID), which additionally include decisions and utility (cost). In the ID, decisions are shown as squared nodes and utilities as diamond-shaped nodes. In the latter, a utility value is assigned to each combination of states of the parent nodes, which can be either random variables or decision nodes, but not utility nodes. In case there are several utility nodes, the total utility is the sum of the individual utilities. In the ID, the optimal decision is the one that maximizes the total expected utility, in agreement with classical decision analysis (Raiffa and Schlaifer 1961).

The decision nodes describe different decision options, which influence the random variables that are children of the decision node. This influence is quantified through the conditional PMF of these child nodes. Links pointing towards the decision nodes represent the available information at the time of making the decision. All parents of the decision nodes are known when making the decision. However, there exist different versions of IDs, which differ in the way information is handled. Often, the ID is based on the no-forgetting assumption: When making a decision, all previous decisions as well as previous observations are known. This requires that there is a temporal ordering of the decisions. The no-forgetting assumption leads

to significant computational demands. For this reason, the limited memory ID (LIMID) was introduced, which makes an explicit link between the nodes that are known before taking the decision and the decision node (Lauritzen and Nilsson 2001). In the LIMID, only the direct parents of a decision node are known at the time of making the decision. This reduces (or limits) the number of nodes that will be considered for the decision, decreases the size of the policy domain and facilitates the obtaining of the optimal strategy that gives the maximum expected utility. In this paper, we use LIMIDs to represent the inspection and repair decision processes.

Fig. A.3 shows an example ID for the deterioration example presented earlier as a DBN in Fig. A.2. Here, the decisions R_t are included on whether or not to repair the structural element at times $t = 1, \dots, T$. These decisions are made based on the result of the inspections Z_t , hence the links $Z_t \rightarrow R_t$. To differentiate the condition of the element before and after the repair, the nodes a'_t are introduced. The conditional PMF of these nodes are identical to that of a_t in case no repair is carried out, and they differ if a repair is carried out. The utilities $U_{R,t}$ are the (negative) cost of repairs and the utilities $U_{F,t}$ are the cost associated with failure at time t . The last slice does not include a repair decision, since such an action would be pointless at the end of the service life.

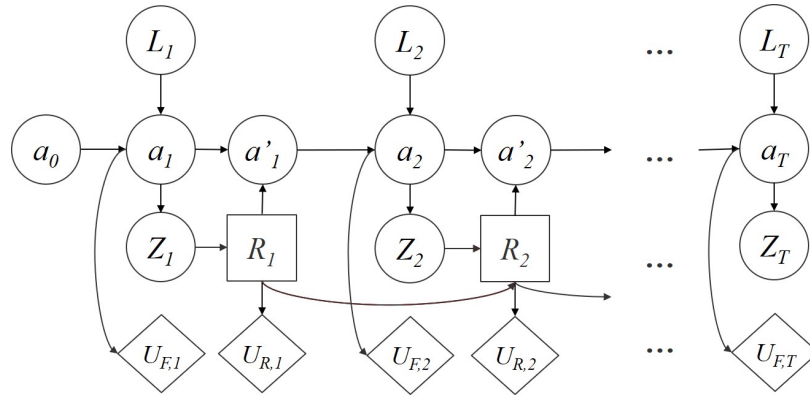


Fig. A.3. ID of the multi-decision structure condition example.

A.2.4 Policies and strategies

In the ID, decisions are taken based on information available when making that decision. In the LIMID, these are the nodes with links pointing to the decision node. A policy consists of a set of rules defining which decision to take as a function of the available information. The more information is used for making a decision, the larger the policy domain and consequently the computational demand. A set of policies of all decision nodes in the ID is called a strategy.

A.3 Risk-based planning of inspections using influence diagrams for a structural element subject to fatigue

In condition-based maintenance of structures, it has to be decided when, where and how to inspect. Here we restrict ourselves to finding optimal decisions on when to inspect, and we present IDs to solve this problem. The optimal inspection strategy is defined as the one that minimizes the expected cost, defined as the sum of inspection, repair and failure cost. Note that the expected cost of failure is the risk.

For the numerical investigation, a structural element subject to fatigue deterioration is considered. Inspections are possible in each year of the service life, potentially followed by repair actions in case of adverse inspection outcomes.

A.3.1 Fatigue crack growth model

To model the fatigue crack growth, we consider a simplified case corresponding to crack growth in an infinite plate, described by Paris' law (e.g. Ditlevsen and Madsen 1996):

$$\frac{da(n)}{dn} = C \left[\Delta S \sqrt{\pi a(n)} \right]^m \quad (\text{A.1})$$

where a is the crack depth; n is the number of stress cycles; ΔS is the stress range per cycle with constant stress amplitudes; and C and m are empirically determined model parameters. Parameters ΔS , C , and m are modeled as time invariant random variables. Using the boundary condition $a(n = 0) = a_0$, the previous equation leads to

$$a(n) = \left[\left(1 - \frac{m}{2}\right) C \Delta S^m \pi^{m/2} n + a_0^{(1-m/2)} \right]^{(1-m/2)^{-1}} \quad (\text{A.2})$$

In order to use a DBN for the fatigue model, the time is discretized in intervals of 1 year. If $n_t = n(t)$ is the number of cycles at time step t , then the crack depth at the end of each year can be expressed recursively as a function of the crack depth in the previous year as

$$a_t = \left[q \pi^{m/2} + a_{t-1}^{(1-m/2)} \right]^{(1-m/2)^{-1}} \quad (\text{A.3})$$

where $q = \left(1 - \frac{m}{2}\right) C \Delta S^m \Delta n$. Here, $\Delta n = n_t - n_{t-1}$ is the number of stress cycles per year. Variable q is defined in order to reduce the dimension of the variable space.

The failure event of the component is defined by the limit state function

$$g = a_c - a(n) \quad (\text{A.4})$$

where a_c represents the critical crack depth. The condition of the component is indicated by the binary variable E_t , which takes value 1 when $g > 0$ (i.e. safe event) and 0 when $g \leq 0$ (i.e. failure event).

In Straub (2009), a DBN model and algorithm was developed for this simple crack growth law, as presented in Fig. A.4a. For the purpose of the present study, the model is simplified by eliminating the variables q_t and m_t , leading to a simple homogeneous Markovian deterioration model for a_t as shown in Fig. A.4b. The resulting discrete Markov process for the crack depth a_t follows the recursive relation

$$\mathbf{p}_a(t) = \mathbf{A} \mathbf{p}_a(t - 1) \quad (\text{A.5})$$

where $t = 1, 2, \dots, T$, \mathbf{A} is the transition probability matrix and $\mathbf{p}_a(t)$ is the vector describing the discretized probability distribution of a_t . $\mathbf{p}_a(0)$ is given by the probability distribution of a_0 . The Markov model is homogenous if all random variables in the model are time-invariant. Note that the unconditional marginal distribution of the crack depth and the unconditional probability of failure of the two models in Fig. A.4 are identical. However, as soon as observations are made, the conditional distributions computed with the two models will differ.

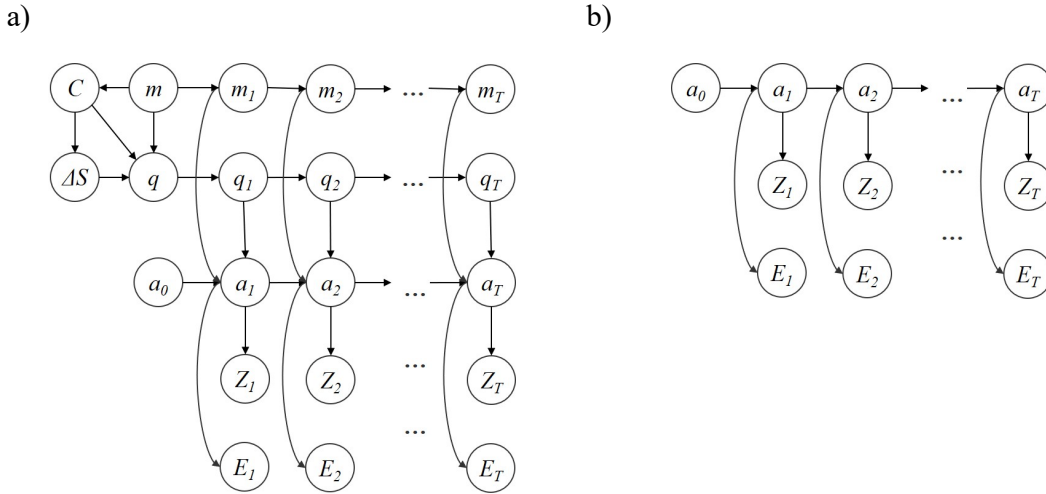


Fig. A.4. DBN of the original (a) and simplified (b) fatigue crack growth model.

A.3.2 Influence diagram for modeling inspections

To assess the effect of inspections and to determine optimal inspection times, the fatigue DBN of Fig. A.4 is extended to an influence diagram (ID). The ID is presented in Fig. A.5. The elements of this ID are introduced in the following.

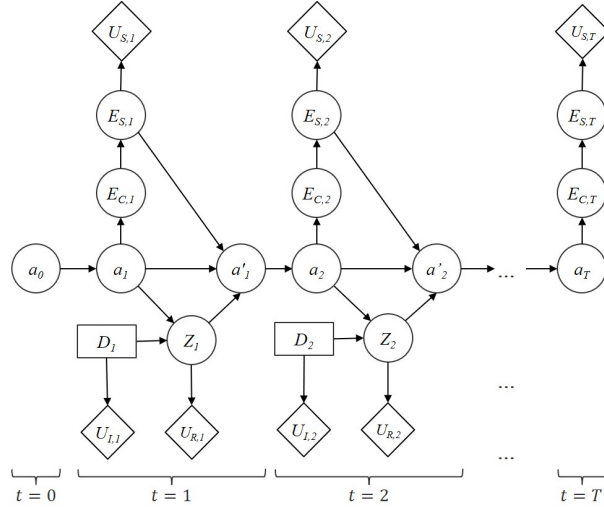


Fig. A.5. ID modeling the fatigue inspection planning (no-memory ID).

Inspection decisions. At every time step t , a decision node D_t is included in the BN. Each decision has two possibilities: no inspection ($D_t = 0$) or inspection ($D_t = 1$). In the ID shown in Fig. A.5, this decision node has no parents. Because we follow the LIMID convention described above, this implies that the inspection is planned without any previous knowledge. This assumption will later be relaxed.

Observations. In case an inspection is carried out at time t , the random variable Z_t will indicate if a crack was detected ($Z_t = 1$) or not detected ($Z_t = 2$). If no inspection was carried out (i.e. $D_t = 0$), then the corresponding state of the variable will be no measurement ($Z_t = 3$). In case an inspection is performed, the probability of detection (PoD) describes the probability of detecting the crack. It is a non-decreasing function of the crack depth (i.e. larger cracks have larger probabilities to be detected) and is here represented by the following relation (Straub 2009):

$$\Pr(Z_t = 1|a_t) = PoD(a_t) = 1 - \exp(-a_t/10\text{mm}) \quad (\text{A.6})$$

Repairs. Repair actions are included in the model as a function of the observed conditions of the component and the system. Whether or not to repair at time t is in principle also a decision that may be optimized jointly with the inspection decision. However, it has been found that simple decision rules are sufficient for the repair action in the considered case, and no optimization is needed (Straub and Faber 2006). The rule is that if the system fails or a crack is detected during an inspection, the component will be repaired. This is included in the ID through the variable a'_t . If no repair is carried out, the state of a'_t will be identical to a_t ; if a

repair is carried out, its conditional distribution is equal to the distribution of the initial crack depth a_0 , assuming that the new condition is probabilistically identical to the original one.

Component and system condition. Structural systems are often redundant, so that failure of an element does not necessarily imply a system failure. Here, the redundancy of the system with respect to component failure is defined in a simplifying manner as the probability that the system does not fail when the component does. $E_{S,t}$ and $E_{C,t}$ denote the condition (i.e. failure or safe) of the system and the component, respectively, at time t . We define the redundancy r as:

$$\Pr(E_{S,t} = \text{safe} | E_{C,t} = \text{failure}) = r \quad (\text{A.7})$$

In the extreme case with no redundancy $r = 0$, element failure will directly lead to system failure. Similarly, if the system is fully redundant with respect to element failure, $r = 1$, then the system will not fail if only this element fails. This simple model does not account accurately for multiple element failures, which must be addressed by an advanced model (Straub and der Kiureghian 2011).

Utilities. The variables $E_{S,t}$ (system condition), D_t (inspection decision), and Z_t (observation) are associated with costs. These are modeled by the utility nodes $U_{S,t}$, $U_{I,t}$, and $U_{R,t}$. The utility of an inspection, repair and system failure events are $-C_I$, $-C_R$, and $-C_S$.

A.3.3 Memory assumptions in the ID model

In the LIMID, only those nodes with links to the decision nodes are assumed to be known at the time of making the decision. This assumption can strongly reduce the computational effort when optimizing the decisions. With increasing memory, i.e. with increasing number of links to the decision nodes, the policy domain of the decision nodes increases, making the solution of the optimization problem intractable. On the other hand, reducing the number of information links toward the decision node leads to suboptimal solutions, in particular if compared to the no-forgetting assumption.

In the first ID presented in Fig. A.5, it is assumed that no information is available when the inspection decision is made. We call this the no-memory ID. The advantage of the no-memory ID is that all inspections can be planned a-priori, since no observation during the service life will influence the inspection decisions.

Alternatively, we consider the ID presented in Fig. A.6, where information from previous observations and decisions is taken into account when planning the inspections. In this ID, it is

assumed that the observation made at the previous inspection is known when deciding upon inspection. Two additional variables, Z_t^* and τ_t , are included in the model and contain the observation from the last inspection and the time when it was performed. We call this ID the last-inspection ID.

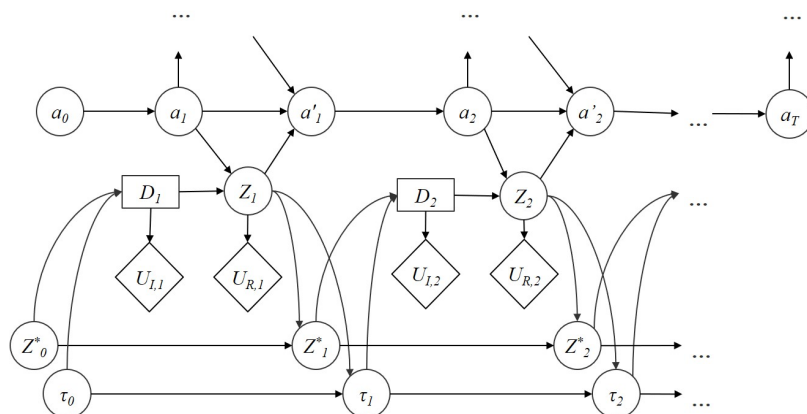


Fig. A.6. ID modeling the fatigue inspection planning (last-inspection ID).

A.3.4 Finding optimal inspection times with the ID

When solving decision problems, the size of the solution domain can quickly become intractable as the number of decision nodes increases. Depending on the type of application, some characteristics (e.g. symmetry) can be used to reduce the computational demands of the decision problem (Jensen and Nielsen 2007). Alternatively, approximate solutions can be obtained. In particular, single policy updating (SPU) is an iterative algorithm for solving LIMIDs that runs over each decision node, obtaining its locally optimum policy that maximizes the expected utility of the decision problem by keeping the remaining policies fixed. An iteration is completed when all decision nodes are locally maximized, and the algorithm stops when the next iteration does not further reduce the expected utility. Due to its local nature, the solution obtained with SPU is likely to be suboptimal.

For the inspection planning problem, simple heuristics were defined in the past to reduce the solution space (see e.g. Straub and Faber 2006). The two most common heuristics are summarized in the following.

Periodic inspections (PI), also known as equidistant inspections: The number of possible inspection times of the decision problem increases exponentially with the number of time steps T (i.e. 2^T combinations). However, if it is required that the inspection intervals are fixed, then the number of possible combinations is reduced to T . The optimization problem can be

formulated in terms of a single variable, the number of inspections n_p . If n_p periodic inspections are performed in T time steps, then the inspection times are

$$\left\lfloor \frac{T}{n_p + 1} \right\rfloor, \left\lfloor \frac{2T}{n_p + 1} \right\rfloor, \dots, \left\lfloor \frac{n_p T}{n_p + 1} \right\rfloor \quad (\text{A.8})$$

where $\lfloor \cdot \rfloor$ is the smaller integer function. The goal is to find the optimal number of equally spaced inspections that gives the maximum expected utility.

Reliability threshold (RT). The reliability of the component at time step t is its probability of being in a safe condition $\Pr(\bar{F}_t) = \Pr(a_c - a_t > 0)$. Often, it is expressed through the reliability index $\beta_t = \Phi^{-1}(\Pr(\bar{F}_t))$, with Φ^{-1} being the standard normal cumulative distribution function. A reliability threshold β_m defines a lower bound of the reliability index. For a given threshold, an inspection is planned at time t if it would hold that $\beta_{t+1} < \beta_m$ without this inspection. In this way, the inspection times follow directly from β_m . Note that the implementation of the RT heuristic with the ID differs slightly from the original version, because the computation of $\Pr(\bar{F}_t)$ and β_t is based on the averaged performance, i.e. it is not computed based on the actual repair history as in Straub and Faber (2006).

The PI and RT heuristics approximate the solution of the no-memory decision problem. Their possible solutions domains are considerably smaller subsets of the complete solution domain, thus reducing the computational effort. Both PI and RT approaches define a single parameter optimization problem. Their algorithms have a linear complexity order with respect to the number of time steps whereas SPU complexity depends on the maximum size of the variable domains considered in the decision problem.

A.4 Numerical investigations

To investigate the different algorithms for optimizing the inspection planning with respect to the minimal life cycle cost, the simple DBN crack growth model presented in Sec. A.3.1 is implemented. The parameters of the model are summarized in Tab. A.1. These parameters as well as the discretization scheme are taken from Straub (2009). In Tab. A.2, the variables of the IDs are summarized. The cost of repair, C_R , and system failure, C_S , are expressed relative to the cost of inspection, C_I . The transition matrix \mathbf{A} of Eq. (A.5) is estimated by Monte Carlo simulation with 10^6 samples of parameters C , ΔS and m according to the prior distributions of Tab. A.1.

In this analysis, the following parameter values were assumed for the life cycle model: total time period $T = 15$ years; system failure cost $C_S = 5000$; inspection cost $C_I = 1$; repair cost $C_R = 0.1$; and redundancy $r = 0.2$. Discounting was neglected for the purpose of this example.

The inspection planning problem was solved for the no-memory ID (Fig. A.5) with the PI and RT heuristics, with the SPU algorithm and – for comparison – with a full search (i.e. covering all 2^{15} possible inspection schedules). Furthermore, it was solved for the last-inspection ID (Fig. A.6) with the SPU algorithm.

Tab. A.1. Parameters of the decision problem.

Variable	Distribution	Mean	Standard deviation and correlation
a_0 [mm]	Exponential	1	1
a_c [mm]	Deterministic	50	–
ΔS [N mm ⁻²]	Normal	60	10
$\ln(C), m^a$	Bi-Normal	(-33; 3.5)	(0.47; 0.3), $\rho = -0.9$
Δn [yr ⁻¹]	Deterministic	10^5	–

^a Dimensions corresponding to Newton and millimeter

The total expected cost of the inspection planning solutions obtained with the PI and the RT heuristics are shown in Fig. A.7. For the PI approach, the optimal number of inspections is found to be 6, with the RT approach the optimal reliability threshold is found to be $\beta_m = 3.34$.

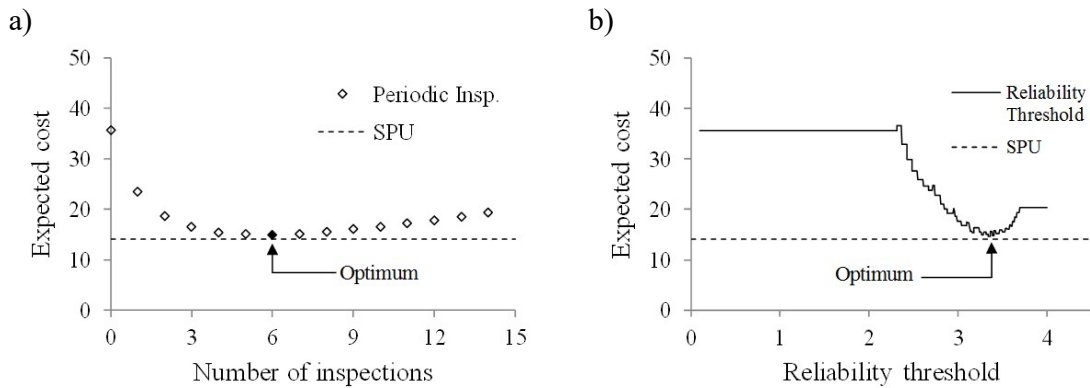


Fig. A.7. Expected cost of inspection schedules with (a) periodic inspections and (b) reliability thresholds.

The total expected costs for all five solution strategies are summarized in Tab. A.3. The difference in the total expected cost among the optimal solutions is relatively small despite the inspection times and disaggregated costs (i.e. failure, inspection and repair costs) being quite

different among the solutions. As an example, Fig. A.8 shows the disaggregated expected costs for the PI and the SPU (no-memory ID) solution. The reason for the small differences in expected costs is likely the fact that all optimal solutions of the no-memory ID have six inspections, and the minimum reliability obtained with these optimal solutions is also fairly similar, as evident from Fig. A.9.

Tab. A.2. Domains and variable discretization.

Variable	Number of states	Discretization / states	Conditional Probability Distribution
a_t (mm)	80	$0, \exp\{\ln(0.01): [\ln(50) - \ln(0.01)]/78: \ln(50)\}, \infty$	$\Pr(a_t \in I_j a_{t-1} \in I_k) = A_{j,k}$ where I_j is the j -th interval of the discretization of a_t or a'_{t-1} .
$E_{C,t}$	2	1: Safe 0: Fail	$\Pr(E_{C,t} = e a_t) = \begin{cases} 0 & \text{if } e = 1, a_t \geq a_c \\ 1 & \text{if } e = 0, a_t \geq a_c \\ 1 & \text{if } e = 1, a_t < a_c \\ 0 & \text{if } e = 0, a_t < a_c \end{cases}$
$E_{S,t}$	2	1: Safe 0: Fail	$\Pr(E_{S,t} = e E_{C,t}) = \begin{cases} r_i & \text{if } e = 1, E_{C,t} = 0 \\ 1 - r_i & \text{if } e = 0, E_{C,t} = 0 \\ 1 & \text{if } e = 1, E_{C,t} = 1 \\ 0 & \text{if } e = 0, E_{C,t} = 1 \end{cases}$
$U_{S,t}$	1	—	$U_{S,t} = \begin{cases} 0 & \text{if } E_t^S = 0 \\ -C_S & \text{if } E_t^S = 1 \end{cases}$
D_t	2	0: No inspection 1: Inspection	
$U_{I,t}$	1	—	$U_{I,t} = \begin{cases} 0 & \text{if } D_t = 0 \\ -C_I & \text{if } D_t = 1 \end{cases}$
Z_t	3	1: Insp. with detection 2: Insp. with no detection 3: No measurement	$\Pr(Z_t = z a_t, D_t) = \begin{cases} 1 & \text{if } D_t = 0, z = 3 \\ PoD(a_t) & \text{if } D_t = 1, z = 1 \\ 1 - PoD(a_t) & \text{if } D_t = 1, z = 2 \\ 0 & \text{otherwise} \end{cases}$
$U_{R,t}$	1	—	$U_{R,t} = \begin{cases} 0 & \text{if } Z_t = 2,3 \\ -C_R & \text{if } Z_t = 1 \end{cases}$
a'_t (mm)	80	$0, \exp\{\ln(0.01): [\ln(50) - \ln(0.01)]/78: \ln(50)\}, \infty$	$\Pr(a'_t \in I_j a_t, Z_t, E_{S,t}) = \begin{cases} \Pr(a_0 \in I_j) & \text{if } E_{S,t} = 0 \\ \Pr(a_0 \in I_j) & \text{if } E_{S,t} = 1, Z_t = 1 \\ 1 & \text{if } E_{S,t} = 1, a_t \in I_j, Z_t = 2,3 \\ 0 & \text{otherwise} \end{cases}$ where I_j is the j -th interval of the discretization of a_t or a'_{t-1} .

Tab. A.3. Optimal solutions obtained with different algorithms.

Approach	Expected cost	Inspection times	CPU time (sec)
PI	14.91	2, 4, 6, 9, 11, 13	0.4
RT	14.70	2, 4, 6, 8, 10, 13	4.3
SPU (no-memory ID)	14.05	1, 2, 4, 5, 7, 9	164
Exact solution (no memory)	13.97	1, 2, 3, 5, 7, 10	313
SPU (last-inspection ID)	13.75	Policies for each decision node	165

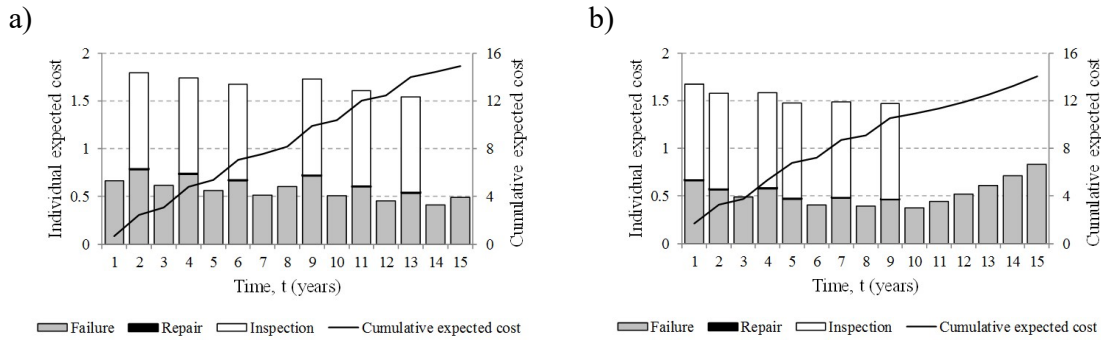


Fig. A.8. Expected cost of optimal solution for: a) PI, and b) SPU (no-memory ID).

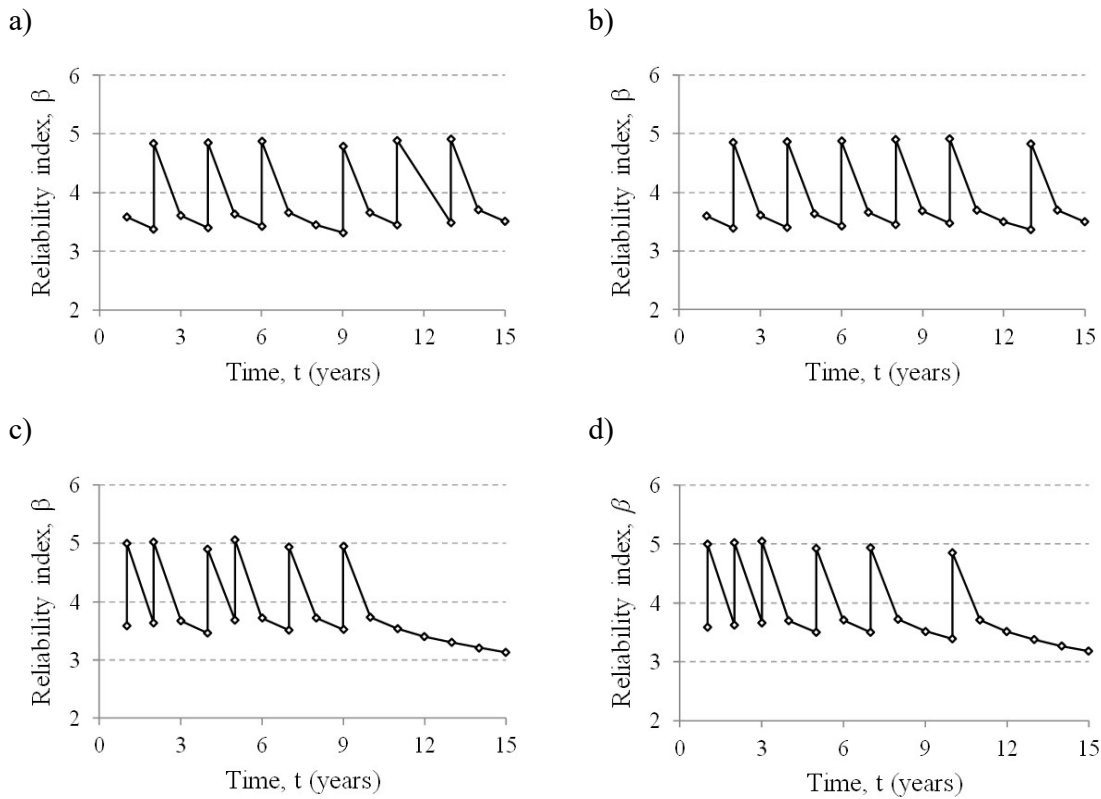


Fig. A.9. Reliability index of the optimal solutions for (a) periodic inspections; (b) reliability threshold; (c) SPU (no-memory ID); and (d) the exact solution (no-memory ID).

The optimal solution is obtained with the last-inspection ID, solved using the SPU algorithm. This is not surprising, since this is the only strategy that allows adapting the inspection times based on inspection results. The disadvantage of this strategy is that inspections cannot already be planned at the beginning of service life.

Comparing the SPU solutions obtained for the two different IDs, it is seen that the minimum expected cost decreases from 14.05 to 13.75 when the observation from the last performed inspection is taken into account for deciding on the next inspection (the last-inspection ID). In this case, the SPU algorithm provides an adaptive policy for each decision node. For example, the resulting policy of the decision node D_{12} indicates that an inspection is to be carried out unless there was an inspection in the previous year (independent of what was observed) or two years ago without crack detection.

The computation time for the SPU solution is considerably larger than for PI and RT. The same is observed when increasing the considered service life period T , and hence the number of steps in the DBN (see Fig. A.10). However, all these algorithms show a similar complexity order (a linear increase with the number of time steps). In contrast, the exact solution of the no-memory ID was obtained by a complete search among all possible combinations of inspection times. This procedure has an exponential complexity order with respect to the number of time steps. For illustration purpose, the last two points of the exact solution (no-memory) curve in Fig. A.10 ($T = 25$ and $T = 50$) were estimated by extrapolation.

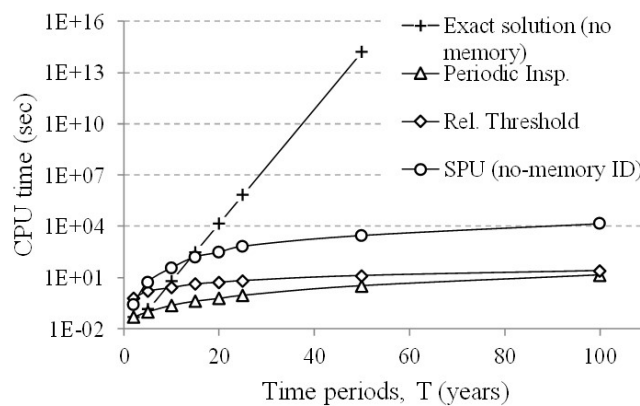


Fig. A.10. CPU time for finding the optimal solution.

While the SPU algorithm requires significantly more computation time than the PI and RT heuristics, it is more flexible because it allows to adapt the inspections to the results of previous observations, as shown for the case of the last-observation ID. If the observations from the previous inspections are considered before deciding to inspect, an adaptive policy is followed.

Since any information can only increase the expected utility of optimal decisions (Jordaan 2005, Straub 2014), it follows that the maximum expected utility of the last-observation ID (or any other adaptive policy implemented through an ID with memory) must be larger or equal than that of a fixed inspection schedule based on the no-memory ID.

A.5 Conclusions and outlook

In this paper, the optimal inspection times for a structural element subject to fatigue are identified through a set of algorithms. The optimization problem is formulated through influence diagrams, whereby varying assumptions regarding the adaptivity of the inspection schedule were made. As expected, the adaptive inspection scheduling leads to lower expected costs. Among the algorithms for optimizing a non-adaptive inspection plan, the one obtained with the single policy updating (SPU) algorithm performs the best. However, the examined heuristics, which allow to significantly reduce the computational effort in the optimization, also perform well.

These results of this paper are useful in the investigation of inspection planning problems in systems with multiple elements, whose deterioration characteristics are correlated. The proposed DBN/ID framework can be extended to solve such problems, but the associated computational complexity will increase with increasing system size, and simple heuristics are no longer readily available. Therefore, it is essential to have efficient algorithms for solving these problems, and the SPU algorithm seems promising for this purpose.

6 Paper B

Reliability Analysis and Updating of Deteriorating Systems with Dynamic Bayesian Networks

Jesus Luque & Daniel Straub

Engineering Risk Analysis Group, Technische Universität München (jesus.luque@tum.de, straub@tum.de, www.era.bgu.tum.de)

Abstract

To estimate and update the reliability of deteriorating structural systems with inspection and monitoring results, we develop a modeling and computational framework based on dynamic Bayesian networks (DBNs). The framework accounts for dependence among deterioration at different system components and for the complex structural system behavior. It includes the effect of inspection and monitoring results, by computing the updated reliability of the system and its components based on information from the entire system. To efficiently model dependence among component deterioration states, a hierarchical structure is defined. This structure facilitates Bayesian model updating of the components in parallel. The performance of the updating algorithm is independent of the amount of included information, which is convenient for large structural systems with detailed inspection campaigns or extensive monitoring. The proposed model and algorithms are applicable to a wide variety of structures subject to deterioration processes such as corrosion and fatigue, including offshore platforms, bridges, ships, and aircraft structures. For illustration, a Daniels system and an offshore steel frame structure subjected to fatigue are investigated. For these applications, the computational efficiency of the proposed algorithm is compared with that of a standard Markov Chain Monte Carlo algorithm and found to be orders of magnitude higher.

Keywords

Bayesian analysis; System reliability analysis; Deterioration; Inspection; Fatigue.

B.1 Introduction

Engineering structures are commonly subjected to deterioration processes, which can reduce their service life and affect the safety of the environment, people and the structure itself. For this reason, significant resources are invested to identify, model, quantify, mitigate and prevent deterioration processes in structures (Swanson 2001, Brownjohn 2007, Farrar and Worden 2007). Structural deterioration, such as metal corrosion and fatigue, is mathematically represented using mostly empirical or semi-empirical models (e.g. Stephens 2001, Gardiner and Melchers 2003, Qin and Cui 2003, Wells and Melchers 2014). Because of their empirical nature, predictive deterioration models are typically associated with significant uncertainty. Hence deterioration is ideally modeled probabilistically (e.g. Madsen et al. 1985, Lin and Yang 1985, Melchers 1999, Frangopol et al. 2004).

Probabilistic deterioration models are developed mainly at the structural component level. However, deterioration at different locations in a structural system is typically correlated, and system considerations should be made (Moan and Song 2000, Vrouwenvelder 2004, Straub and Faber 2005). Probabilistic models of deterioration in large structural systems have been proposed and applied to different types of structures and deterioration processes (e.g. Guedes Soares and Garbatov 1997, Kang and Song 2010, Straub 2011b, Luque et al. 2014, Schneider et al. 2015).

Bayesian methods have been used to combine probabilistic deterioration models with inspection and monitoring outcomes (e.g., Tang 1973, Madsen et al. 1985, Maes et al. 2008, Straub 2009). They allow quantifying the impact of inspections and monitoring on the reliability of the structure, and so facilitate maintenance decisions and the planning of future inspections (e.g. Thoft-Christensen and Sørensen 1987, Faber et al. 2000, Moan 2005, Straub and Faber 2005). Bayesian analysis is mainly performed at the component level, where the probability of failure of a structural component due to deterioration is updated with the inspection and monitoring outcomes. Only a few publications consider the updating of the reliability at the structural system level. Therein, the dependence among component deterioration states is modeled either through the correlation among the deterioration limit states (Moan and Song 2000, Lee and Song 2014, Maljaars and Vrouwenvelder 2014) or through a hierarchical model (Mahadevan 2001, Faber et al. 2006, Maes and Dann 2007, Straub et al. 2009, Schneider et al. 2017). More recently, a number of researchers have considered the planning and optimization of inspection and maintenance actions in structural systems with dependent component deterioration (Straub and Faber 2005, Qin and Faber 2012, Nielsen and Sørensen 2014, Memarzadeh et al. 2014).

A challenge in Bayesian system reliability analysis is to keep the computation time at a feasible level. Methods belonging to classical structural reliability methods are efficient for estimating the probability of system failure, but do not facilitate Bayesian analysis or have computation times that increase exponentially with the number of observations. Recently, a class of methods has been proposed that efficiently combine structural reliability methods with Bayesian updating (Straub 2011a, Straub and Papaioannou 2015). Nevertheless, also this approach has the drawback that its performance is a function of the number of inspection and monitoring data, which can be considerable in structural systems.

Bayesian Networks (BNs) have become popular in engineering risk analysis due to their intuitive nature and their ability to handle many dependent random variables in a Bayesian analysis (Jensen and Nielsen 2007, Straub and Der Kiureghian 2010, Weber et al. 2010). The graphical structure of the BN is formed by nodes and directed links. The nodes represent random variables or deterministic parameters, and the links the dependence among nodes. Ideally, the link between two nodes is based on a causal relation, but this is not necessary. As an example, if deterioration D is modeled as a function of an external random load S and a material parameter M , then a corresponding BN may look like the one in Figure B.1. Here, an additional node Z is included, representing an outcome of an inspection. Since each random variable in the BN is specified by its conditional probability distribution given its parents, the inspection outcome is defined by $p(z|d)$, i.e. the probability of the inspection outcome $Z = z$ given the damage state $D = d$. This is known as the likelihood function, and corresponds to classical models used for describing inspection or monitoring performance, such as Probability of Detection (POD). Generally, the BN is established using commonly available probabilistic models; it allows combining these in a consistent and (in most cases) intuitive manner.

Using BNs it is possible to obtain the posterior distribution of a set of random variables given a set of observations. This task is called inference. For instance, if an inspection result is included in the previously presented example, i.e. if Z is given, then the (joint) probability distribution of the random variables S , M and D conditional on the observed value of Z is calculated using inference algorithms. There are many algorithms available for inference in BNs (e.g. Hanea et al. 2006, Langseth 2009, Shenoy and West 2011). In this paper, the focus is on BN with discrete random variables, for which exact inference algorithms exist (e.g. Murphy 2002, Jensen and Nielsen 2007).

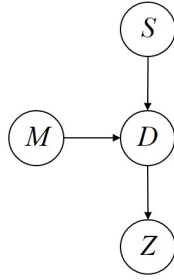


Figure B.1. BN deterioration model example.

The links in the BN provide information on the dependence between random variables in the model. For example, in the BN of Figure B.1, M and S are assumed to be independent a-priori, and hence no direct link between them is present. The link from D to Z indicates that the inspection provides information on the damage state. It provides no direct information on S and M . However, it does so indirectly, because the information obtained on D also updates the probability distribution of S and M , as long as D is not known with certainty. In this way, by observing one random variable, potentially all others are updated. However, for efficient computation, all BN inference algorithms make use of the graphical structure by performing computations locally, exploiting the conditional independence assumptions encoded in the graph.

Modeling of deterioration often involves random processes, which can be represented in a discrete-time manner by dynamic Bayesian networks (DBN), as proposed in Straub (2009). For illustration, we extend the BN of Figure B.1 to include a time-variant load S_t and inspection results at multiple points in time $t = 1, \dots, T$. The resulting DBN is shown in Figure B.2. Each “slice” of the DBN represents a time step in the analysis. The random process $\{S_1, S_2, \dots, S_T\}$ is a Markov chain where each random variable is defined conditionally on the random variables of the previous time step. The deterioration D_t at time t is a stochastic function of the previous deterioration state D_{t-1} and the current load S_t . The probability distributions of the material parameter M , the loads $\{S_1, S_2, \dots, S_T\}$, and the deterioration states $\{D_1, D_2, \dots, D_T\}$ are all updated once inspection outcomes Z_1, \dots, Z_T , or a subset thereof, are observed.

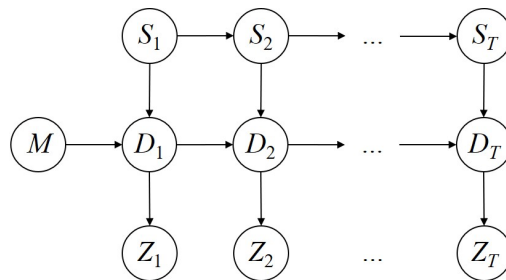


Figure B.2. DBN deterioration model example.

In this paper, the DBN model for structural deterioration from Straub (2009) is extended from the component to the system level, based on work presented by the authors in Luque and Straub (2015). An efficient algorithm is developed, which assesses the reliability of a deteriorating system when partial observations of its condition are available. The deterioration factors of the system components are interrelated using a hierarchical structure and a set of hyperparameters, which model the correlation structure among components. In the following section, the concept of dynamic Bayesian networks and its application to efficiently model component deterioration are presented. Thereafter, in Section B.3, the model is extended to represent the complete structural system. Sections B.4.1 and B.4.2 present two case studies where the model and algorithm are applied and compared to other methods for estimating the system probability of failure. To demonstrate the advantages of the proposed algorithm, the number of system components is increased to a point where classical MCMC algorithms are no longer efficient for estimating the system reliability.

B.2 Dynamic Bayesian network for assessing component deterioration

B.2.1 DBN model of a single component

The DBN model framework developed in Straub (2009) is used to represent the deterioration of components. This model includes the following elements:

- Time-invariant model parameters $\boldsymbol{\theta}$, which are constant in time.
- Time-variant model parameters $\boldsymbol{\omega}_t$, which vary with time steps $t = 0, \dots, T$.
- Deterioration model: A parametric function h for describing the deterioration D as a function of t , $\boldsymbol{\theta}$, $\boldsymbol{\omega}_0, \dots, \boldsymbol{\omega}_t$ and the deterioration level at the previous time step D_{t-1} , i.e.

$$D_t = D(t) = h(t, D_{t-1}, \boldsymbol{\theta}, \boldsymbol{\omega}_1, \dots, \boldsymbol{\omega}_t), \quad t = 1, \dots, T \quad (\text{B.1})$$

- Observations: At any time step t , information on the condition of a model parameter or the deterioration D_t may be available from inspections, monitoring systems, recordings of environmental parameters or other measurements, which are related to the model parameters. These observations are denoted by $Z_{\boldsymbol{\theta},t}$, $Z_{\boldsymbol{\omega},t}$, and $Z_{D,t}$, depending on the random variables to which they relate.

Figure B.3 depicts the generic DBN deterioration model for a single component, where vectors $\boldsymbol{\theta}_1, \dots, \boldsymbol{\theta}_T$ are added in order to have a repetitive sub-BN for each time step. These vectors are

deterministically defined as $\theta_t = \theta_{t-1} = \theta_0$ for all $t = 1, \dots, T$. The DBN model illustrates how the parameters and the deterioration of a single component are related in time. Each set $\{\theta_t, \omega_t, D_t, Z_{\theta,t}, Z_{\omega,t}, Z_{D,t}\}$ represents a time step t in the DBN.

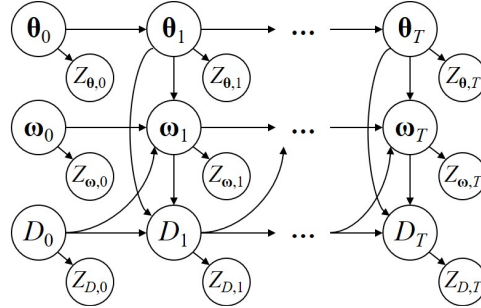


Figure B.3. Generic DBN of the deterioration model at the component level (following Straub 2009).

B.2.2 Computation of the posterior distribution

DBN models can be evaluated using exact or approximate inference algorithms. Most approximate methods are sampling-based; the most popular among these belong to the family of Markov Chain Monte Carlo (MCMC) methods. MCMC using Gibb's sampler is particularly effective, as it exploits the conditional independence properties of the BN (Gamerman and Lopes 2006). Nevertheless, the computational cost of MCMC increases considerably as the number of observations included in the model increases and/or the probability of failure of interest decreases. This motivates the use of exact inference algorithms with discretized random variables, whose performance does not deteriorate with increasing amount of observation and is independent of the magnitude of the probabilities of interest.

For DBN models consisting exclusively of discrete random variables, exact inference algorithms exist. In particular the forward-backward algorithm (Murphy 2002, Russell and Norvig 2003) is effective for DBN. In Straub (2009), a variant of the forward-backward algorithm is proposed, which is tailored towards evaluating the generic DBN for deterioration modeling shown in Figure B.3.

B.2.3 Discretization of continuous random variables

With the exception of some special cases, exact inference algorithms can be applied only to DBNs with exclusively discrete random variables. However, most deterioration models include continuous random variables. To apply the exact inference algorithms, these must be discretized. To this end, the original continuous domain of each random variable is partitioned into discrete

intervals and the probability of each interval is computed from the conditional or the marginal PDF of the random variable. Even though these algorithms are exact for a given discretization, the discretization itself does introduce an error. The number and location of the discrete intervals have an impact on the computation time and accuracy of the approximation. Several algorithms have been developed to obtain optimal intervals based on a specific estimation, typically the probability of failure (Chang and Chen 2005, Neil et al. 2007, Marquez et al. 2010, Zwirgmaier and Straub 2016).

Here the heuristic principles presented in Straub (2009) to define the discretization scheme are used. To keep the model simple, the discretization scheme, and hence the conditional probabilities, are the same in all time steps, resulting in a homogenous DBN. The discretization scheme of the random variables θ and ω_t is chosen so that after applying the deterioration model h , they result in approximately equally spaced intervals in D . This method is simple to implement and has proven to be effective. For more details on discretization approach, the reader is referred to Straub (2009).

B.3 Bayesian network model of system deterioration

One challenging aspect of modeling deteriorating structural systems is the representation of the interrelation among the system components and the common factors that affect their condition. Only a limited number of investigations of the dependence among component deterioration states can be found in the literature (e.g. Hergenröder and Rackwitz 1992, Vrouwenvelder 2004, Maes et al. 2008, Malioka 2009, Luque et al. 2014). The two most common mathematical representations of such dependence are hierarchical models and random field models. The latter are suitable for systems where dependence among component deterioration is a function of the geometrical location (Maes 2003, Stewart and Mullard 2006). Hierarchical models are suitable where the dependence among component deterioration depends on common features and common influencing factors (Maes and Dann 2007, Maes et al. 2008, Banerjee et al. 2015). They have computational advantages over random fields, in particular in the context of DBN modeling.

In the DBN model, care is required to correctly represent the statistical dependence among the random variables without increasing the complexity and computational cost of the inference. For general statistical dependence among components, most DBN models of systems rapidly become computationally intractable when the number of components in the system or the number of random variables increases. Strategies for reducing the computational efforts when

representing random fields in the BN have been proposed (Bensi et al. 2011), but their applicability is still limited. In the proposed approach, the dependence structure is modeled by hierarchical models. Hierarchical models can capture the dependence structure of deterioration in most structural systems quite adequately, because the dependence is typically caused mainly by common influencing factors rather than geometrical proximity.

B.3.1 Hierarchical models

Hierarchical models are an effective way of representing systems whose characteristics can be grouped using multiple levels (Raudenbush and Bryk 2008). The random variables within a level are interrelated through common influencing parameters, which are modeled at a higher level in the hierarchy. The random variables at the highest level are called hyperparameters. As a simple example, Figure B.4 shows a BN representing a set of random variables $\{V_1, V_2, \dots, V_n\}$ with common mean value α . As long as the value of α is uncertain, the random variables $\{V_1, V_2, \dots, V_n\}$ are statistically dependent. The correlation between V_i and V_j will depend on the distribution parameters. If the random variables V_i conditional on α all have standard deviation σ_V , and α has standard deviation σ_0 , then the linear correlation between any pair V_i and V_j , $i \neq j$, is

$$\rho(V_i, V_j) = \frac{\sigma_0^2}{\sigma_0^2 + \sigma_V^2} \quad (\text{B.2})$$

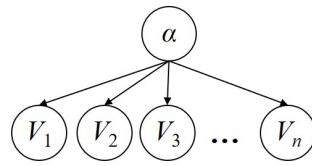


Figure B.4. Hierarchical BN with a hyperparameter α .

B.3.2 Hierarchical model based on correlation models

In many instances, influencing parameters are not modeled explicitly, as in the example above, but instead models of the correlation among components are available. In this section, we describe how such correlation models are translated into a BN. To simplify the presentation, we consider an equi-correlated set of random variables $\mathbf{V} = [V_1, \dots, V_n]^T$, for which the correlation between any two components is ρ_V . All V_i 's have identical marginal distribution, described by the cumulative distribution function (CDF), F_V . The extension to more general

cases is outlined afterwards. The presentation is limited to the (commonly implied) case that the joint distribution of \mathbf{V} follows a Gaussian copula, i.e. the Nataf transformation can be used for transforming the \mathbf{V} to equivalent standard normal random variables (Liu and Der Kiureghian 1986).

Following the principle of the Nataf transformation, the V_i are related to corresponding standard normal distributed Y_i through the following marginal transformation:

$$V_i = F_V^{-1}[\Phi(Y_i)] \quad (\text{B.3})$$

where F_V^{-1} is the inverse CDF of V_i and Φ is the standard normal CDF.

The Y_i are jointly normal distributed with correlation coefficient ρ_Y , which is the equivalent correlation in standard normal space and is a function of ρ_V and F_V . Its value is such that, after applying the transformation $F_V^{-1}[\Phi(\cdot)]$, the resulting random variables V_1, \dots, V_n have correlation ρ_V . ρ_Y can be found numerically or from the approximate expressions provided in (Liu and Der Kiureghian 1986).

The dependence among the equi-correlated standard normal random variables Y_1, \dots, Y_n can be defined through a hierarchical structure. To this end, a standard normal hyperparameter α is introduced, as shown in Figure B.5. The Y_i are defined as normal random variables conditional on α with mean $\sqrt{\rho_Y} \cdot \alpha$ and standard deviation $\sqrt{1 - \rho_Y}$. The unconditional Y_1, \dots, Y_n are then standard normal random variables with mutual correlation coefficient ρ_Y .

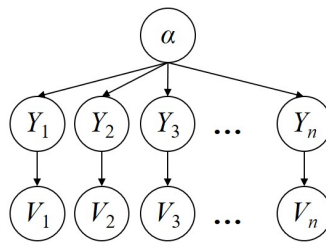


Figure B.5. Hierarchical BN of equally correlated random variables.

To reduce the number of random variables in the BN, the auxiliary random variables Y_i can be eliminated and replaced by a direct link between α and the V_i . The resulting BN is the one in Figure B.4. The corresponding conditional distribution of V_i given α is:

$$F_{V|\alpha}(v) = \Phi \left(\frac{\Phi^{-1}(F_V(v)) - \sqrt{\rho_Y} \cdot \alpha}{\sqrt{1 - \rho_Y}} \right) \quad (\text{B.4})$$

The conditional CDF of the random variables V_i of Eq. (B.4) is used to generate the conditional probability table (CPT) of V_i in the DBN system deterioration model.

The above model approach can be extended to random variables V_1, \dots, V_n with different marginal distributions and varying mutual correlation coefficients. As long as the pairwise correlation coefficients $\rho_{Y,ij}$ of the underlying standard normal Y_i 's are of the Dunnett-Sobel class (see e.g. Thoft-Christensen and Murotsu 1986, Kang and Song 2009), the BN structures of Figure B.4 and Figure B.5 still hold. No additional computational efforts are necessary in these cases.

B.3.3 DBN model of the system

The hierarchical DBN modeling approach is applied to model dependence among component deterioration in structures. To extend the component DBN model of Section B.2.1 to a model of the structural system, a set of hyperparameters $\alpha = [\alpha_\theta, \alpha_\omega, \alpha_{D_0}]^T$ are defined. In the system model, all components are connected through these hyperparameters α (Figure B.6). All random variables in the DBN are now indexed by the component number $i = 1, \dots, N$ and the time step $t = 0, \dots, T$, i.e. $D_{3,10}$ is the damage of component 3 at time step 10.

The α parameters may be determined from known correlation among components, following Section B.3.2, or derived from common influencing factors. In many cases, they will represent model uncertainties, which are typically shared among similar components within a system. In this case, the corresponding α parameters can be obtained by first estimating the magnitude of common model uncertainties relative to component-specific uncertainties, then determining the corresponding correlations through Eq. (B.2) and from those the α parameters following Section B.3.2.

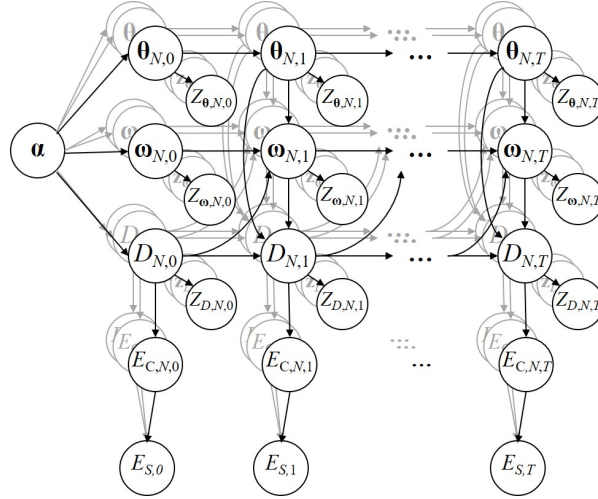


Figure B.6. DBN model of the structural system deterioration.

In the full system model DBN of Figure B.6, the binary random variable $E_{C,i,t}$ represents the condition (i.e. $E_{C,i,t} = 0$: not failed, $E_{C,i,t} = 1$: failed) of component i at time step t . $E_{C,i,t}$ is a (possibly probabilistic) function of the deterioration state $D_{i,t}$. The binary random variable $E_{S,t}$ represents the system condition (i.e. $E_{S,t} = 0$: not failed, $E_{S,t} = 1$: failed) as a function of all component conditions. $E_{C,i,t}$ and $E_{S,t}$ can be extended to multi-state random variables, if a more detailed description of the components and system condition is desirable. The relation between the system condition $E_{S,t}$ and the condition of its components $E_{C,i,t}$, $i = 1, \dots, N$, is quantified by the probability of system failure given the conditions of its components. To obtain these conditional probabilities, a probabilistic model of the structural system is necessary and structural reliability computations must be performed in a pre-processing step.

For many real structural systems, the number of system components subject to deterioration is large, and hence there is a prohibitively large number of combinations of component deterioration states in the system, as discussed in Straub and Der Kiureghian (2011). In the DBN model of Figure B.6, this is reflected by the number of links pointing from the component condition nodes $E_{C,i,t}$, $i = 1, \dots, N$ to the system condition node $E_{S,t}$. For each combination of possible element conditions, a system configuration Ψ_t is defined. A total of 2^N different system configurations must be examined, which rapidly becomes intractable as the number of components increases, because a system reliability analysis must be carried out for each configuration to determine $\Pr(E_{S,t} = 1 | \Psi_t = \Psi_t)$. In specific applications of the framework, it is therefore necessary to use a more efficient representation of structural system behavior. For this purpose, the convergent connection from the $E_{C,i,t}$ to $E_{S,t}$ may be replaced by an alternative dependence structure. Different techniques can be used to this end, in function of the considered system. One possible alternative is to reduce the number of system configurations to consider

based on their contribution to the probability of failure (Kim et al. 2013). Alternatively, in many systems one can exploit the fact that some components are (approximately) exchangeable with respect to their static function. In this case, it is sufficient to consider the number of component failures in the group (Straub and Der Kiureghian 2011). In the numerical investigations presented later, we consider a Daniels system to demonstrate the DBN modeling in such cases. Furthermore, in some systems it is possible to pursue a hierarchical modeling approach also for the static functions. Such a strategy is utilized in the second numerical example presented later.

B.3.4 Inference algorithm

To perform inference with the system DBN, i.e. to compute the probability of component and system failure given inspection and monitoring results, the forward-backward algorithm presented in Straub (2009) for exact inference is extended to the system level. The algorithm presented here is limited to the forward operation, which is used to solve the filtering problem, i.e. to compute the posterior distribution of the random variables α , θ_i , $\omega_{i,t}$, $D_{i,t}$, $E_{C,i,t}$ and $E_{S,t}$ for all $i = 1, \dots, N$ given the observations up to time t . The algorithm is formulated in a recursive manner for each time step and exploits the property of the hierarchical model that all components are statistically independent for given hyperparameters.

B.3.4.1 Component partial updating (forward operation)

This first part of the algorithm is applied to each component separately. The conditional joint probability mass function (PMF) of deterioration state $D_{i,t}$, the time-variant parameters $\omega_{i,t}$, and the time-invariant parameters θ_i are computed conditionally on the hyperparameters α and on all observations of the component up to time step t . The latter are denoted by $\mathbf{Z}_{i,0:t}$, and include all observations of the damage state $Z_{D,i,0:t}$, time-variant $Z_{\omega,i,0:t}$ and time-invariant parameters $Z_{\theta,i,0:t}$, i.e. $\mathbf{Z}_{i,0:t} = [Z_{D,i,0:t}, Z_{\omega,i,0:t}, Z_{\theta,i,0:t}]^T$. From application of Bayes' rule, and accounting for the independence properties encoded in the DBN structure, it follows:

$$\begin{aligned}
 & p(d_{i,t}, \omega_{i,t}, \theta_{i,t} | \alpha, \mathbf{z}_{i,0:t}) \\
 & \propto p(d_{i,t}, \omega_{i,t}, \theta_{i,t} | \alpha, \mathbf{z}_{i,0:t-1}) p(z_{D,i,t} | d_{i,t}) p(z_{\omega,i,t} | \omega_{i,t}) p(z_{\theta,i,t} | \theta_{i,t})
 \end{aligned} \tag{B.5}$$

where $i = 1, \dots, N$, $t = 1, \dots, T$. The proportionality constant is found by normalization: $\sum_{d_{i,t}} \sum_{\omega_{i,t}} \sum_{\theta_{i,t}} p(d_{i,t}, \omega_{i,t}, \theta_{i,t} | \alpha, \mathbf{z}_{i,0:t}) = 1$. The first term on the right-hand side of Eq. (B.5)

is calculated from the joint probability at the previous time step $p(d_{i,t-1}, \boldsymbol{\omega}_{i,t-1}, \boldsymbol{\theta}_{i,t-1} | \boldsymbol{\alpha}, \mathbf{z}_{i,0:t-1})$ through:

$$\begin{aligned}
& p(d_{i,t}, \boldsymbol{\omega}_{i,t}, \boldsymbol{\theta}_{i,t} | \boldsymbol{\alpha}, \mathbf{z}_{i,0:t-1}) \\
&= \sum_{d_{i,t-1}} p(d_{i,t} | d_{i,t-1}, \boldsymbol{\omega}_{i,t}, \boldsymbol{\theta}_{i,t}) \sum_{\boldsymbol{\omega}_{i,t-1}} p(\boldsymbol{\omega}_{i,t} | d_{i,t-1}, \boldsymbol{\omega}_{i,t-1}, \boldsymbol{\theta}_{i,t}) \\
&\times \sum_{\boldsymbol{\theta}_{i,t-1}} p(\boldsymbol{\theta}_{i,t} | \boldsymbol{\theta}_{i,t-1}) p(d_{i,t-1}, \boldsymbol{\omega}_{i,t-1}, \boldsymbol{\theta}_{i,t-1} | \boldsymbol{\alpha}, \mathbf{z}_{i,0:t-1})
\end{aligned} \tag{B.6}$$

The algorithm is applied recursively, starting at $t = 0$, for which the joint probability is

$$\begin{aligned}
& p(d_{i,0}, \boldsymbol{\omega}_{i,0}, \boldsymbol{\theta}_{i,0} | \boldsymbol{\alpha}, \mathbf{z}_{i,0}) \\
&\propto p(z_{D,i,0} | d_{i,0}) p(z_{\boldsymbol{\omega},i,0} | \boldsymbol{\omega}_{i,0}) p(z_{\boldsymbol{\theta},i,0} | \boldsymbol{\theta}_{i,0}) p(d_{i,0} | \boldsymbol{\alpha}) p(\boldsymbol{\omega}_{i,0} | \boldsymbol{\alpha}) p(\boldsymbol{\theta}_{i,0} | \boldsymbol{\alpha})
\end{aligned} \tag{B.7}$$

Note that all conditional probabilities required in Eqs. (B.5-B.7) are available from the definition of the BN.

B.3.4.2 Hyperparameter updating

Observations of each component have an indirect effect on the posterior distribution of the remaining components. These distributions are updated through the hyperparameters. For this reason, the second step is updating the hyperparameters given the observations from all random variables up to time t , i.e. $p(\boldsymbol{\alpha} | \mathbf{z}_{1:N,0:t})$. This is calculated recursively with respect to i (i.e. component by component) as:

$$p(\boldsymbol{\alpha} | \mathbf{z}_{1:i,0:t}) \propto p(\boldsymbol{\alpha} | \mathbf{z}_{1:i-1,0:t}) \prod_{j=0}^t p(\mathbf{z}_{i,j} | \boldsymbol{\alpha}) \tag{B.8}$$

for $i = 2, \dots, N$, and

$$p(\boldsymbol{\alpha}|\mathbf{z}_{1,0:t}) \propto p(\boldsymbol{\alpha}) \prod_{j=0}^t p(\mathbf{z}_{1,j}|\boldsymbol{\alpha}) \quad (\text{B.9})$$

where $p(\boldsymbol{\alpha}|\mathbf{z}_{1:i,0:t})$ is the conditional probability of the hyperparameters given all observations in components $1, \dots, i$ up to time t and $p(\boldsymbol{\alpha})$ is the prior probability of the hyperparameters (i.e. before observations). $p(\mathbf{z}_{i,t}|\boldsymbol{\alpha})$ is the inverse of the normalizing constant of Eq. (B.5), for component i and time step t . Equation (B.8) can also be expressed as a product over the index i , but it is expressed in recursive form here to indicate that the conditional probability of the hyperparameters given the observations can be partially calculated after each component is updated.

B.3.4.3 Posterior distributions

The next step in the algorithm is the computation of the joint posterior probability $p(d_{i,t}, \boldsymbol{\omega}_{i,t}, \boldsymbol{\theta}_{i,t}, \boldsymbol{\alpha}|\mathbf{z}_{1:N,0:t})$, the updated component state probability given the observations from all components up to time t :

$$p(d_{i,t}, \boldsymbol{\omega}_{i,t}, \boldsymbol{\theta}_{i,t}, \boldsymbol{\alpha}|\mathbf{z}_{1:N,0:t}) = p(d_{i,t}, \boldsymbol{\omega}_{i,t}, \boldsymbol{\theta}_{i,t}|\boldsymbol{\alpha}, \mathbf{z}_{i,0:t})p(\boldsymbol{\alpha}|\mathbf{z}_{\{1:N\}\setminus\{i\},0:t}) \quad (\text{B.10})$$

where $\mathbf{z}_{\{1:N\}\setminus\{i\},0:t}$ are the observations of all components excluding those of component i . Any marginal posterior distribution can be computed from these results. As an example, the posterior distribution of the damage in component i at time t is:

$$p(d_{i,t}|\mathbf{z}_{1:N,0:t}) = \sum_{\boldsymbol{\omega}_{i,t}} \sum_{\boldsymbol{\theta}_{i,t}} \sum_{\boldsymbol{\alpha}} p(d_{i,t}, \boldsymbol{\omega}_{i,t}, \boldsymbol{\theta}_{i,t}, \boldsymbol{\alpha}|\mathbf{z}_{1:N,0:t}) \quad (\text{B.11})$$

B.3.4.4 Posterior reliability of components and system

Finally, the updated probability of the component condition $E_{C,i,t}$ is obtained by simple application of the total probability theorem:

$$p(e_{C,i,t}|\mathbf{z}_{1:N,0:t}) = \sum_{d_{i,t}} p(e_{C,i,t}|d_{i,t})p(d_{i,t}|\mathbf{z}_{1:N,0:t}) \quad (\text{B.12})$$

where $e_{C,i,t}$ is a realization of the random variable $E_{C,i,t}$. The updated probability distribution of the system condition is:

$$\begin{aligned}
& p(e_{S,t} | \mathbf{z}_{1:N,0:t}) \\
&= \sum_{e_{C,1,t}, \dots, e_{C,N,t}} p(e_{S,t} | \mathbf{e}_{C,1:N,t}) \sum_{\alpha} p(\mathbf{e}_{C,1:N,t} | \alpha, \mathbf{z}_{1:N,0:t}) p(\alpha | \mathbf{z}_{1:N,0:t}) \\
&= \sum_{e_{C,1,t}, \dots, e_{C,N,t}} p(e_{S,t} | \mathbf{e}_{C,1:N,t}) \sum_{\alpha} p(\alpha | \mathbf{z}_{1:N,0:t}) \prod_i p(e_{C,i,t} | \alpha, \mathbf{z}_{1:N,0:t})
\end{aligned} \tag{B.13}$$

where $\mathbf{e}_{C,1:N,t} = [e_{C,1,t}, \dots, e_{C,N,t}]^T$ is a realization of $\mathbf{E}_{C,1:N,t} = [E_{C,1,t}, \dots, E_{C,N,t}]^T$.

B.3.5 Computational complexity of the algorithm

The computational complexity of the forward operation for a single component is $O[m_{\theta}(t+1)(m_D^2 m_{\omega} + m_D m_{\omega}^2)]$, where m_D , m_{ω} , m_{θ} are the number of states of the discretized random variables $D_{i,t}$, $\theta_{i,t}$, $\omega_{i,t}$ (see Straub 2009). In analogy, the complexity of the algorithm described in Section B.3.4.1 for updating all components with their respective observations is $O[m_{\theta} m_{\alpha} N(t+1)(m_D^2 m_{\omega} + m_D m_{\omega}^2)]$, where m_{α} is the number of states of the hyperparameters. The complexity of the hyperparameter updating step of Section B.3.4.2 is $O[m_D m_{\omega} m_{\theta} m_{\alpha} N]$. The complexity of updating the condition of all components is $O[m_C m_D N]$ and that of updating the system reliability is $O[(N+1)m_{\alpha} + 1]m_{E_S} m_{E_C}^N$ in the general case (Section B.3.4.3).

With the exception of the updating of the system condition E_S , the complexity of the algorithm is proportional to the number of components and time steps and it is independent of the number of observations included in the analysis. However, updating of E_S can quickly become intractable as the number of components increases, unless a more efficient system representation than the convergent connection (Figure B.6) can be found. Such strategies were already discussed in Section B.3.3. Alternatively, if such alternative system representations are not possible or not convenient, the conditional system reliability may be evaluated using sampling-based structural reliability methods. This could be achieved by employing the conditional probability distributions computed with the DBN algorithm to generate samples from the posterior.

A second important aspect of computational performance is the necessary memory allocation. This is strongly influenced by the size of the largest joint PMF used in the procedure, which

can be either $p(D_{i,t}, \omega_{i,t}, \theta_{i,t} | \alpha)$ or $p(\omega_{i,t} | D_{i,t-1}, \omega_{i,t-1}, \theta_{i,t})$. Memory allocation as well as computational complexity are therefore a direct function of the discretization scheme, which must be defined carefully to find an optimal trade-off between accuracy and computational cost.

B.4 Numerical investigation

The following numerical examples serve to investigate and illustrate the workings of the proposed model and inference algorithm. For validation purposes, the results obtained with the exact inference algorithm are compared to those obtained with two alternative methods: 1) Monte Carlo simulation (MCS) for the case without observations, and 2) MCMC for cases with and without observations. The MCMC computations are implemented with OpenBUGS (Lunn et al. 2009).

B.4.1 Daniels system

For illustration purposes, we consider a Daniels system (Daniels 1945, Gollwitzer and Rackwitz 1990), which consists of a set of N elements with independent and identically distributed capacities R_i for $i = 1, \dots, N$. The elements have ideally brittle material behavior. The system is subject to a load L (Figure B.7).

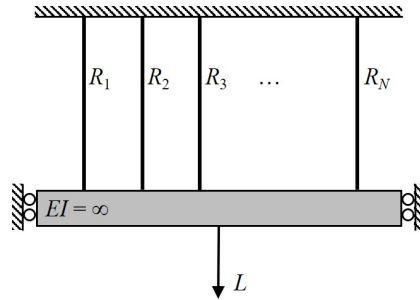


Figure B.7. Daniels system.

Prior to the application of the load, each component in the system is in one of two possible states: a) full capacity, or b) zero capacity due to a fatigue failure. For a discussion of this model see Straub and Der Kiureghian (2011).

B.4.1.1 Deterioration model

The system components are subject to fatigue deterioration, which - for illustration purposes - is modeled by simple fracture-mechanics-based crack growth model (e.g. Ditlevsen and Madsen 1996). It uses Paris' law to describe the growth of the crack depth D_i at component i :

$$\frac{dD_i(n)}{dn} = C_i \left[\Delta S_{e,i} \sqrt{\pi D_i(n)} \right]^{M_i} \quad (\text{B.14})$$

where n = number of stress cycles; $\Delta S_{e,i} = (E[\Delta S_i^M])^{\frac{1}{M}}$ = equivalent stress range per cycle with $E[\cdot]$ being the expectation operator; ΔS_i = stress range per cycle; C_i, M_i = empirically determined material parameters.

The long-term distribution of the fatigue stress range ΔS_i is described by a Weibull distribution with scale and shape parameters K_i and λ_i . $\Delta S_{e,i}$ is then given by (Madsen 1997):

$$\Delta S_{e,i} = K_i \Gamma \left(1 + \frac{M_i}{\lambda_i} \right)^{\frac{1}{M_i}} \quad (\text{B.15})$$

where $\Gamma(\cdot)$ is the Gamma function. Using the initial condition $D_i(n=0) = D_{i,0}$, the following analytical solution for the crack depth after n stress cycles can be obtained from Eq. (B.14):

$$D_i(n) = \left[\left(1 - \frac{M_i}{2} \right) C_i \Delta S_{e,i}^{M_i} \pi^{M_i/2} n + D_{i,0}^{1-M_i/2} \right]^{(1-M_i/2)^{-1}} \quad (\text{B.16})$$

B.4.1.2 Observations and probability of detection

In this example, we only consider observations of the deterioration state through inspections, e.g. visual inspections or non-destructive evaluation of the fatigue hot spots. The observation $Z_{D,i,t}$ is a binary random variable with possible states “no crack detection” (i.e. $Z_{D,i,t} = 0$), and “crack detection” (i.e. $Z_{D,i,t} = 1$). The inspection quality is described by an exponential probability of detection (POD) model with parameter ξ , in function of the crack depth d :

$$\Pr(Z = 1 | D = d) = \text{POD}(d) = 1 - \exp \left(-\frac{d}{\xi} \right) \quad (\text{B.17})$$

B.4.1.3 Relation between component and system conditions

Failure of the i -th component after t time steps (equivalent to $n = n(t)$ stress cycles) occurs when the crack depth exceeds the critical value d_c , i.e. $\{E_{C,i,t} = 1\} = \{D_{i,t} \geq d_c\}$. If the component has not failed, it is assumed to have its full capacity.

In a Daniels system, due to the exchangeability of the components, the probability of having a system failure at time step t is a function only of the total number of component failures. Following Section B.3.3, to avoid a convergent connection between the $E_{C,i,t}$ and $E_{S,t}$, the cumulative number of component failures up to component i , $N_{f,1:i,t}$, is defined as follows:

$$N_{f,1:i,t} = \sum_{j=1}^i E_{C,j,t} = E_{C,i,t} + N_{f,1:i-1,t} \quad (\text{B.18})$$

The relation between the component conditions $E_{C,i,t}$, $i = 1, \dots, N$ and the system condition $E_{S,t}$ defined in the general model of Figure B.6 can be replaced by the network depicted in Figure B.8. The complete DBN of the Daniels system is presented in Figure B.9.

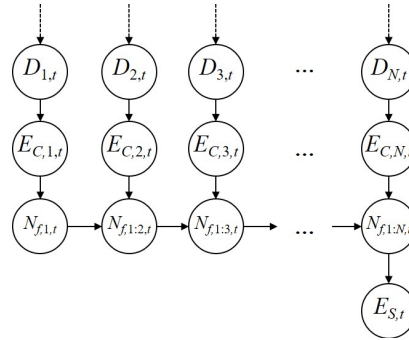


Figure B.8. DBN model of the Daniels system condition. $N_{f,1:i,t}$ is the total number of component failures among the first i components at time t .

A Daniels system with $N = 10$ components and $T = 100$ time steps is investigated. The parameters of the fatigue deterioration model are summarized in Table B.1 and the corresponding discretization scheme is presented in

Table B.2. Each time step corresponds to $\Delta n = 5 \cdot 10^6$ fatigue stress cycles. The correlation of fatigue parameters among components are $\rho_{D_0} = 0.5$, $\rho_M = 0.6$, and $\rho_K = 0.8$.

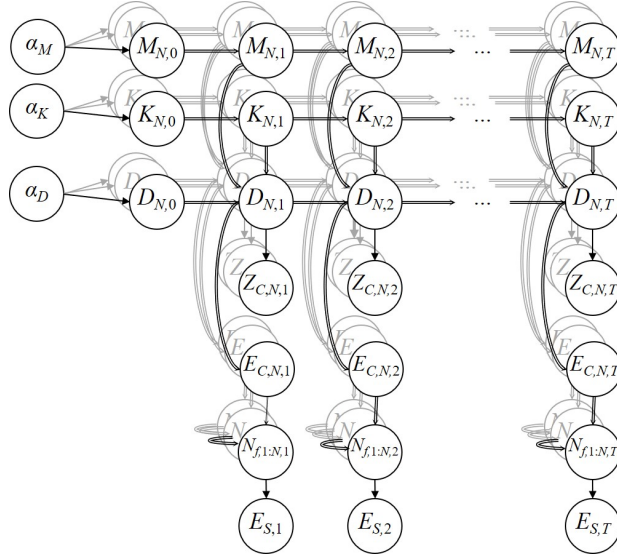


Figure B.9. DBN of the Daniels system.

Table B.1. Parameters of the fatigue deterioration model.

Random variable	Distribution	Mean	Std. deviation
α_{D_0}	Normal	0	1
α_K	Normal	0	1
α_M	Normal	0	1
$D_{0,i}$ (mm)	Exponential	1	1
$M_{0,i}$	Normal	3.5	0.3
$M_{t,i}$	$M_{t,i} = M_{t-1,i}$		
$\ln C_{t,i}$	$\ln C_{t,i} = -3.34M_{t,i} - 15.84$		
$K_{0,i}$	Lognormal	1.6	0.22
$K_{t,i}$	$K_{t,i} = K_{t-1,i}$		
λ_i	Deterministic	0.8	
d_c (mm)	Deterministic	50	
ξ (mm)	Deterministic	10	

Table B.2. Discretization scheme.

Random variable	Number of states	Final interval boundaries
$\alpha_{D_0}, \alpha_M, \alpha_K$	5	$\Phi^{-1}(0:0.2:1)$
D (mm)	80	$0, \exp\{\ln(0.01) : [\ln(50) - \ln(0.01)]/78 : \ln(50)\}, \infty$
M	20	$0, \ln\{\exp(2.2) : [\exp(4.8) - \exp(2.2)]/18 : \exp(4.8)\}, \infty$
K	20	$0, \{0.86 : (2.83 - 0.86)/18 : 2.83\}, \infty$

The load L is lognormal distributed with coefficient of variation $\delta_L = 0.25$, the capacities R_i , $i = 1, \dots, 10$, are independent and normal distributed with $\delta_R = 0.15$ and the mean safety factor is $n\mu_{R_i}/\mu_L = 2.9$. The conditional probability of failure of the system given j failed components is computed according to Eq. (B.19) and is presented in Figure B.10.

$$\Pr(E_{S,t} = 1 | N_{f,1:N,t} = j) = \Pr\left(\sum_{i=1}^{n-j} R_i - L \leq 0\right) \quad (\text{B.19})$$

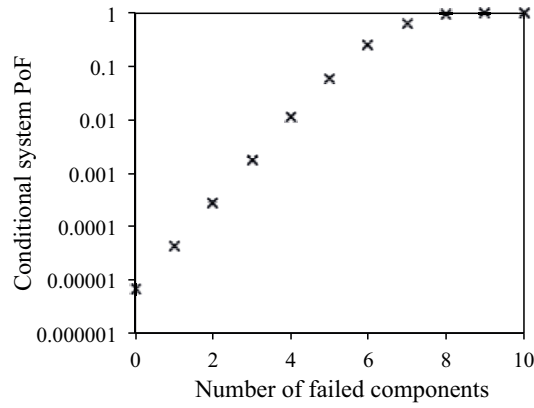


Figure B.10. Probability of failure of the Daniels system conditional on the number of components with fatigue failures.

B.4.1.4 Results

For the unconditional case (i.e. without observations), the reliability index β calculated with the proposed inference algorithm is compared to the results obtained using MCS and MCMC for a single component (Figure B.11) and the system (Figure B.12). The reliability index is defined as $\beta = -\Phi^{-1}[\Pr(E = fail)]$, with Φ^{-1} being the inverse standard normal CDF.

A good agreement among the three methods is observed at the component level. At the system level, the difference between the probability estimates from the proposed DBN model and the Monte Carlo methods is due to the discretization of the hyperparameters α in the DBN. The relatively coarse discretization of α_{D_0} , α_M , and α_K using $m_{\alpha_{D_0}} = m_{\alpha_M} = m_{\alpha_K} = 5$ discrete states each (

Table B.2) leads to an underestimation of the correlation in the fatigue performance among components. This in turn leads to an overestimation of the system reliability in a redundant system, such as the Daniels system. The effect can be mitigated by increasing the number of

discrete states for each hyperparameter, with an associated increase in computation time. Following Section B.3.5, the computation time is linear with respect to m_α , the total number of states of the hyperparameters. Here it is $m_\alpha = m_{\alpha_{D_0}} \cdot m_{\alpha_M} \cdot m_{\alpha_K}$, and doubling the number of states of all hyperparameters would lead to an 8-fold increase in computation time. As shown later, the performance of the present discretization scheme in the case with observation is much better, and the accuracy is thus deemed acceptable.

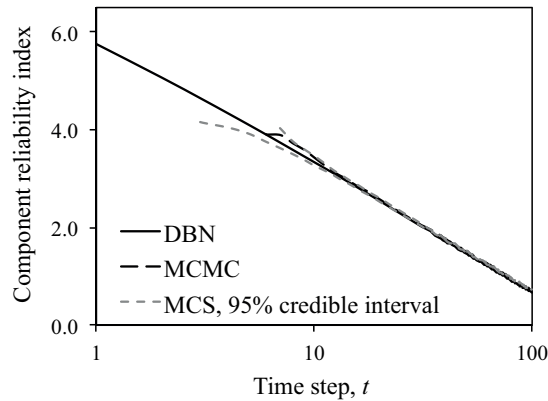


Figure B.11. Reliability index of a single component.

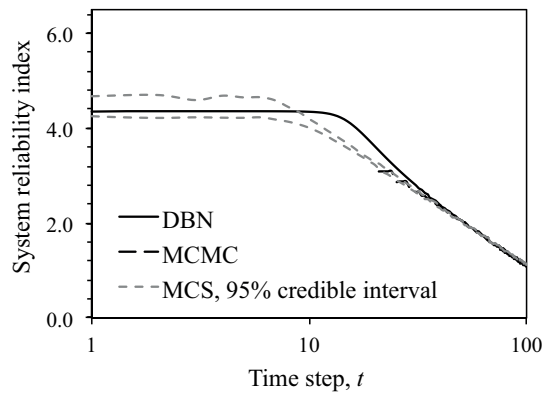


Figure B.12. Reliability index of the Daniels system

To better understand the dependence among component deterioration, the correlation among crack depths D_i and D_j and among component failure events $E_{C,i} = 1$ and $E_{C,j} = 1$ is computed. These are obtained directly from the DBN or the Monte Carlo samples. Figure B.13 shows the correlation between the crack depth of two components $D_{i,t}$ and $D_{j,t}$ using the proposed algorithm for DBNs, MCS and MCMC. As expected, the correlation is slightly underestimated by the DBN algorithm.

The dependence in fatigue performance among components is here due to inter-correlation of three parameters: a) the material parameter M , b) the stress parameter K , and c) the initial crack depth D_0 . The correlation between the crack depths in two components at the beginning of the service life is dominated by the correlation in the initial crack depth D_0 . The effect of the correlation in the material and stress parameters, M and K , increases with time.

The correlation between component failure events is shown in Figure B.14. The correlation is low at the beginning of the service life, due to overall low probabilities of failure. In agreement with the above results, the DBN slightly underestimates the correlation.

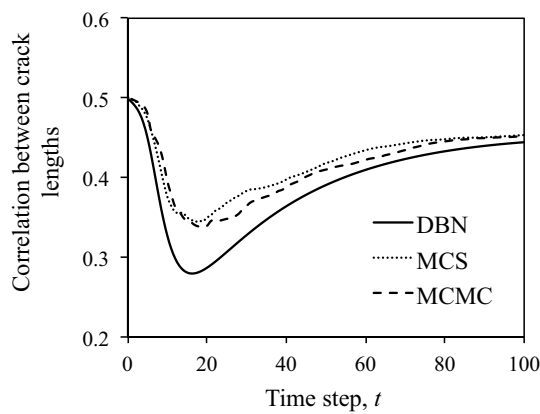


Figure B.13 Correlation between the crack depths of two system components as a function of time, estimated using the DBN algorithm, MCS and MCMC.

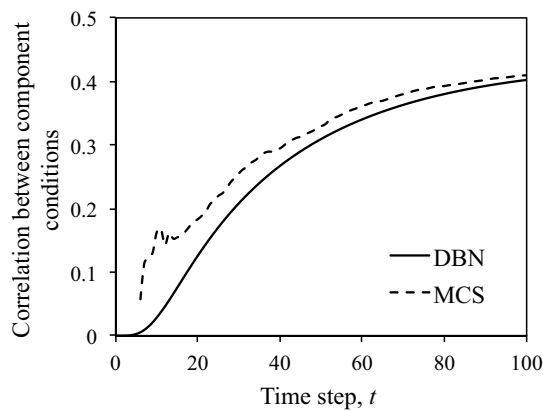


Figure B.14. Correlation between the condition states E_C (i.e. failed/not failed) of two system components as a function of time, estimated using the DBN algorithm and MCS.

The relevant case for the DBN model is the conditional case, i.e. with the inclusion of inspections results. It is assumed that one component is inspected every $5 \cdot 10^7$ cycles, i.e. after every 10 time steps, without detecting any crack. The updated reliability index of the inspected

component is considerably larger than in the unconditional case, due to the no-detection observation (Figure B.15). This observation also affects the non-inspected components, due to the correlation defined by the hyperparameters (Figure B.16). The reliability of the system is affected by the reliability of both the inspected and the non-inspected components (Figure B.17). By inspection only one component every 10 time steps, and assuming that the inspections always result in a no-detection, the system reliability index at the end of the service life increases from 1.1 to 2.1.

In Figures B.15-B.17, the results of the DBN model are compared with results obtained by MCMC for verification. The results from the two algorithms match very well, and the slight differences observed in the unconditional case (Figure B.12) are not seen here.

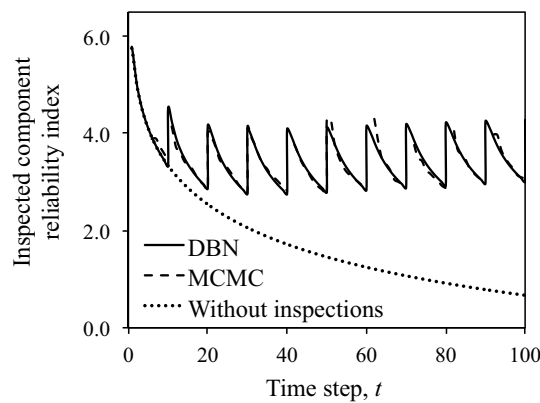


Figure B.15. Reliability index of the inspected component after no detection of a crack at inspections every 10 time steps.

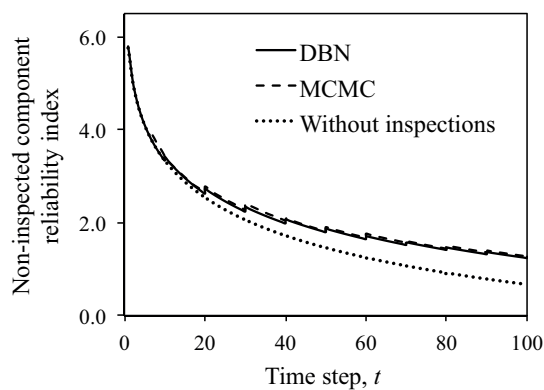


Figure B.16. Reliability index of a non-inspected component given the no-detection outcome of the inspected component.

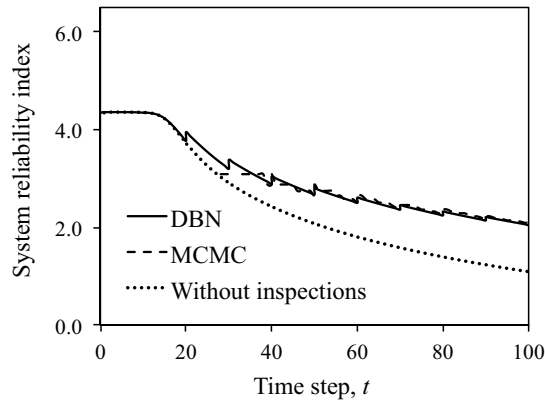


Figure B.17. Reliability index of the system after no detection of a crack in all inspection times.

It is pointed out that the necessary computation time for the solution of the system DBN is orders of magnitudes lower than that for the applied standard MCMC algorithm. Additionally, the computation time of the forward-backward algorithm is not affected by the number of observations or the order of magnitude of the probability of failure, which is not the case of MCMC. If the number of system components increases, the computation time in both the forward-backward algorithm and MCMC increases linearly with number of components.

To demonstrate the efficiency of the DBN algorithm as the number of components and inspections is increased, we analyze a Daniels system with $N = 100$ components, in which 5 components are inspected every 10 time steps. The assumed inspection outcomes of the five components are specified in Table B.3. The probability of failure of the system using the forward-backward algorithm is shown in Figure B.18. Since the inspection resulted in detection of multiple cracks, and no repairs are considered, the system reliability is lower after including the inspections. MCMC results are not computed for this case, due to the associated large computation times.

Table B.3. Inspection outcomes of the Daniels system with 100 components.

Component	Inspection time step								
	10	20	30	40	50	60	70	80	90
1	x	✓	✓	✓	✓	✓	✓	✓	✓
2	x	x	x	✓	✓	✓	✓	✓	✓
3	x	x	x	x	x	✓	✓	✓	✓
4	x	x	x	x	x	x	x	✓	✓
5	x	x	x	x	x	x	x	x	x

✓: Detection; x: No detection

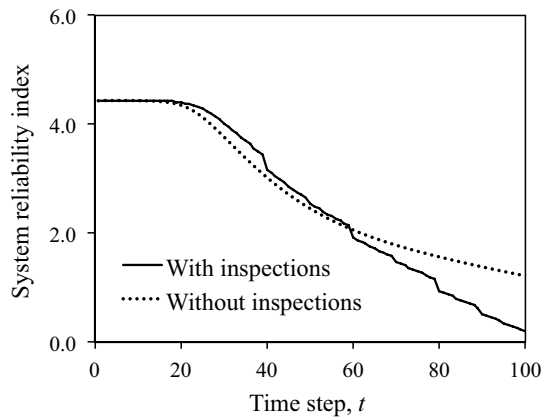


Figure B.18. Reliability index of the Daniels system with 100 components for cases with and without inspections.

B.4.2 Steel frame

The Zayas steel frame shown in Figure B.19 is commonly used as a benchmark in structural analysis of steel offshore structures (Zayas et al. 1980). It consists of 23 tubular members with welded connections. The fatigue hotspots are located at the welded connections of the 13 horizontal and diagonal members. There are $N = 22$ fatigue hotspots, which represent the system components in the DBN model. The structure is loaded in horizontal direction by a concentrated force L at the upper left node of the structure and by gravity load. The details of the geometrical and material properties of the structure are described in (Schneider et al. 2017).

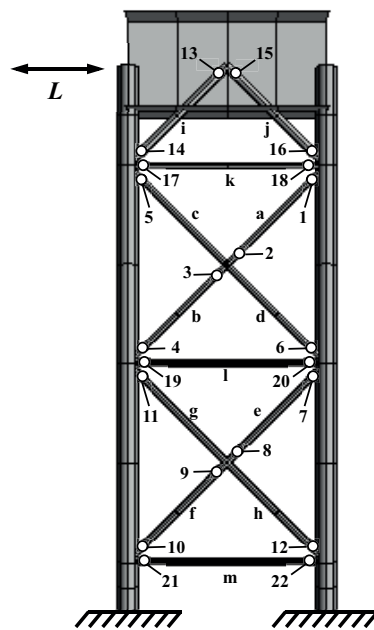


Figure B.19. Zayas steel frame structure with 22 fatigue hotspots in 13 tubular members (a – m).

B.4.2.1 Deterioration model

For ease of presentation, fatigue deterioration in all hotspots of the Zayas frame structure is represented by the same model as used in Section B.4.1.1 with the parameters listed in Table B.1. In a real structure, fatigue stresses will vary among hotspots. However, this has no impact on the computational demand and the accuracy of the reliability computations and the updating. As in example 1, a redistribution of fatigue stresses when some system components fail is neglected, i.e. $K_{i,t}$ is modeled as a time-invariant parameter.

B.4.2.2 Crack measurements as observations

In this example, measurements of crack sizes at the hot spots are included. To this end, the observation $Z_{i,t}$ conditional on $D_{i,t}$ is defined as

$$\Pr(Z_{i,t} = z | D_{i,t} = d) = f_{\epsilon}(z - d)$$

where f_{ϵ} is the normal probability distribution of the measurement error with zero mean and standard deviation $\sigma_{\epsilon} = 0.1\text{mm}$. The observation $Z_{i,t}$ is discretized with the same scheme as the crack depth $D_{i,t}$, with one additional state representing no detection. Note that the discretization of $Z_{i,t}$ has no effect on the computational demand.

B.4.2.3 Relation between hotspots, structural elements and system condition

To each of the structural elements, one or two fatigue hotspots are associated (Figure B.19). The condition of hotspots and elements is modeled through the random variables E_h and E_e , respectively. It is assumed that an element fails if any of its hotspots fails, where a hotspot failure is defined according to Section B.4.1.3. Considering the number of structural members included in the Zayas frame, the total number of possible system configurations is $2^{13} = 8192$, which is still manageable. To estimate the probability of failure of the system, the ultimate capacity of the structure is obtained for each possible system configuration through a pushover analysis. The ultimate capacity of the structure when all components are intact is $2.8 \cdot 10^5\text{N}$. The condition of the system $E_{S,t}$ is defined as a child node of the system configuration and the extreme load L_t observed during time step t . The load L affecting the structure is assumed lognormal distributed with mean $4 \cdot 10^3\text{N}$ and standard deviation $2 \cdot 10^4\text{N}$. The complete DBN model is shown in Figure B.20.

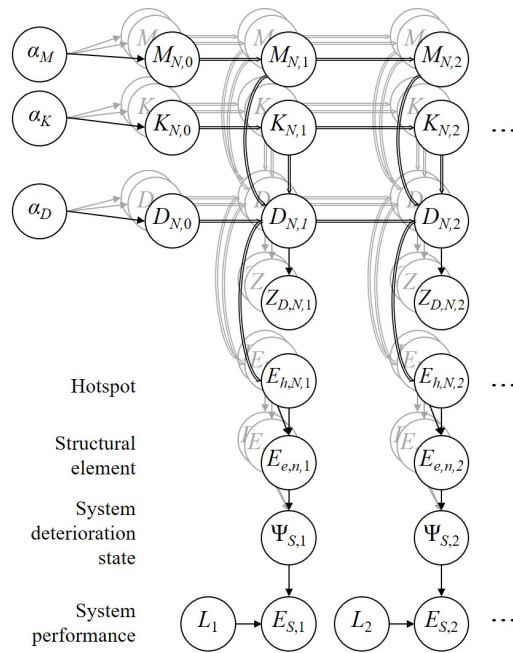


Figure B.20. DBN of the Zayas frame.

B.4.2.4 Results

The accuracy of the proposed algorithm is compared to MCMC and MCS results. In the unconditional case, the three methods give consistent results for a single hotspot (Figure B.21) and the system (Figure B.22).

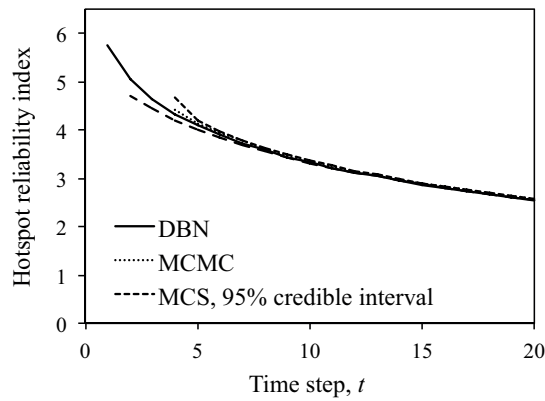


Figure B.21. Reliability index of a single hotspot for the unconditional case (i.e. without inspection).

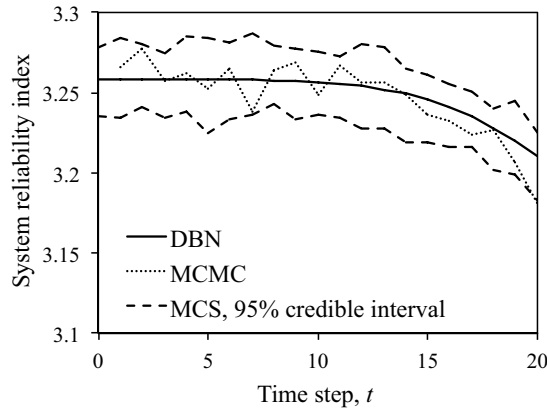


Figure B.22. Reliability index of the system for the unconditional case (i.e. without inspection).

For the conditional case, it is assumed that hotspot 1 (in structural element 1) is inspected at time step $t = 10$. A crack of depth $Z_{D,1,10} = 3\text{mm}$ is measured, which should be compared to the expected crack depth before the observation of $E[D_{1,10}] = 1.2\text{mm}$. Results are obtained using the algorithm described in Section B.3.4 for the inspected hotspot (Figure B.23), a non-inspected hotspot (Figure B.24), and the system (Figure B.25). When including crack measurements, MCMC using OpenBUGS has convergence issues and no reliability estimates are obtained.

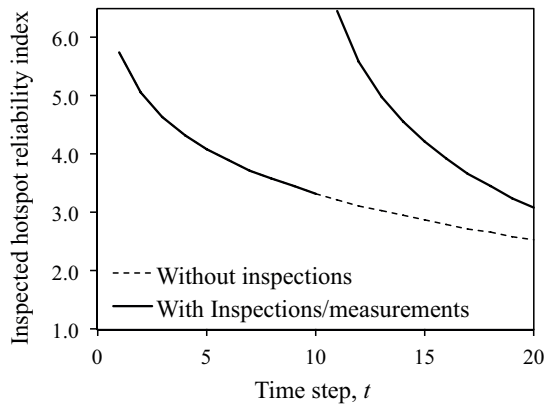


Figure B.23. Reliability index of the inspected hotspot.

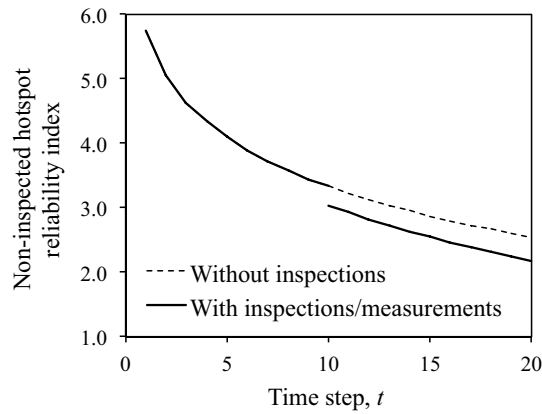


Figure B.24. Reliability index of a non-inspected hotspot for the conditional case (i.e. with inspection).

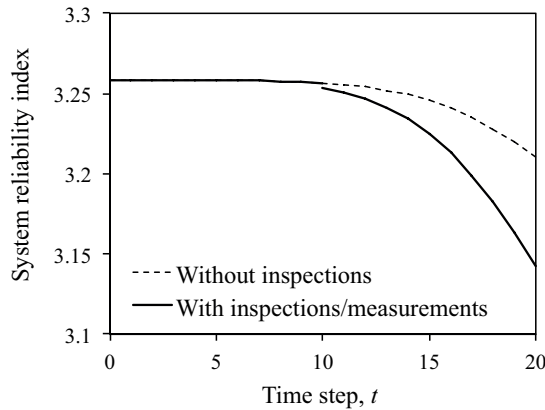


Figure B.25. Reliability index of the system for the conditional case (i.e. with inspection).

Although the measured crack is larger than the expected crack depth for that hotspot, the reliability of the inspected hotspot increases after the inspection due to the combination of two factors: 1) the measurement of 3mm is considerably smaller than the critical crack length 50mm, 2) the measurement error is small, and the overall uncertainty on the crack length is reduced. However, because the measured crack is larger than the expected, the reliability indexes of the other components are reduced, and this leads to a reduction in the estimate of system reliability.

As stated earlier, increasing the number of observations does not affect the computation time of the proposed algorithm. To include an example with more inspection results, Figure B.26 presents the reliability index of the system given multiple observations at hotspots 1 to 4 and time steps 10, 20, 30, and 40.

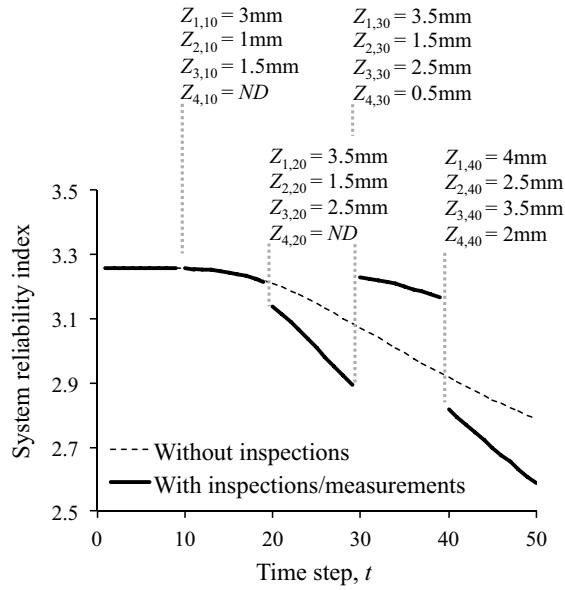


Figure B.26. Reliability index of the system for the conditional case (i.e. with inspection) with observations from hotspots 1 to 4 at time steps 10, 20, 30 and 40. A measurement *ND* represents a no-detection case.

B.5 Discussion

We propose the use of a hierarchical DBN model for probabilistically representing deterioration in structural systems and for updating the probabilities and reliability when inspection and monitoring results are available. We also introduce an efficient algorithm for evaluating the hierarchical DBN. A major motivation for the use of the DBN in conjunction with the exact inference algorithm is its fast and robust computational performance. With the exception of the last step, the system deterioration model presented in Figure B.6 can be solved with almost linear computational complexity with respect to the number of time steps and the number of components. Importantly, the computation time is not affected by the number of inspection and monitoring outcomes included in the model. In addition, due to the hierarchical definition of the model, the proposed inference algorithm can be run in parallel for each component before and after the hyperparameters are updated. This part of the algorithm represents a considerable percentage of the total computation time, e.g. more than 90% for the Daniels system and 80% for the Zayas frame examples investigated in this paper.

For the last step, the updating of the system condition, a direct modeling of the structural system is in most cases prohibitively expensive for realistic structural systems, as this entails considering 2^N system configurations, with N being the number of affected components. Different application-specific modeling strategies for dealing with this issue are available. In

some cases, as demonstrated in the numerical investigations, components can be grouped and it is sufficient to consider their cumulative effect on the system reliability. The DBN model of the system behavior can accommodate such a modeling. Alternatively, approximate models of system behavior may be applied, such as the model proposed in Straub and Der Kiureghian (2011), which requires only the marginal effect of component failure on the system reliability as an input. Finally, one might combine the proposed exact algorithm with sampling-based methods to be used in the last step. Samples of the correlated component behavior can be generated from the posterior distribution of the component states obtained with the DBN algorithm. This has not been investigated in this paper and further work is needed on finding efficient representation of structural system behavior with component deterioration failures. However, it is important to realize that the challenges associated with the system representation are independent of the algorithm used for performing the Bayesian updating of the system reliability.

The investigated examples demonstrate the advantages of the proposed inference algorithm over a standard MCMC algorithm. The former leads to computation times that are orders of magnitude lower. Although a direct comparison of computation time has only a limited value due to the difference in software used for their implementation, the difference in computational complexity is noticeable. In particular, the performance of MCMC deteriorates when increasing the amount and accuracy of inspection and monitoring results. With tailor-made MCMC algorithms, its performance could be significantly increased, but it will always vary with the data. In addition, current simulation-based methods (e.g. MCMC) are not well suited to estimate small probabilities of failure, even if recent developments are improving this (e.g. Straub and Papaioannou 2015, Schneider et al.2017).

The limitations of the proposed approach are related to the discretization of the continuous random variables. More specifically, the computational complexity is a linear or quadratic function of the number of states used for discretizing the random variables (Section B.3.5). Therefore, the number of random variables that can be included explicitly in the DBN model is limited. While the deterioration model considered in this paper includes only four random variables, published state of the art models often include more random variables. Nevertheless, the problem is less critical as it may seem at first glance. The number of random variables can often be reduced by combining multiple random variables to a single random variable, as exemplarily shown in Straub (2009). In addition, in models with many random variables it is often possible to consider some as deterministic with limited loss of accuracy. Besides the need to limit the number of random variables, the second drawback of the proposed algorithm is the

increased effort in pre-processing. The choice of the discretization scheme and its implementation lead to an increased effort by the analyst. For this reason, the DBN framework is mainly of use when computations have to be performed repetitively (e.g. multiple function evaluations to solve an optimization problem) and/or included in software. This is e.g., the case when analyzing portfolios of structures, or in the operational planning of inspections, monitoring, maintenance activities, and in near-real-time situations.

B.6 Conclusions

A hierarchical dynamic Bayesian to model the deterioration process in structural systems is proposed. The model includes the dependence among system components when assessing the effect of (partial) observations of system components on the probability of system failure. An efficient algorithm for performing Bayesian updating at the system level is provided, which operates recursively among components and time steps. The hierarchical definition of the components facilitates parallelizing the code to further reduce computation time. The accuracy and performance of the model is tested through two case studies. A comparison with Markov Chain Monte Carlo (MCMC) shows good agreement in the updated probabilities, with computation times that are orders of magnitude lower. A particular advantage is that the computational cost of the proposed algorithm is independent of the number of included inspection and monitoring results and of the magnitude of the probability of failure. This efficiency and robustness make the proposed algorithm suitable for integral planning and optimization of monitoring, inspection and maintenance activities in structural systems.

Spatial probabilistic modeling of corrosion in ship structures

Jesus Luque ^a, Rainer Hamann ^b & Daniel Straub ^a

^a Engineering Risk Analysis Group, Technische Universität München, Theresienstr. 90, 80333 Munich

Germany (jesus.luque@tum.de, straub@tum.de)

^b DNV GL, Brooktorkai 18, 20457 Hamburg, Germany (rainer.hamann@dnvgl.com)

Abstract

Corrosion in ship structures is influenced by a variety of factors that are varying in time and space. Existing corrosion models used in practice only partially address the spatial variability of the corrosion process. Typical estimations of corrosion model parameters are based on averaging measurements for one ship type over structural elements from different ships and operational conditions. Most models do not explicitly predict the variability and correlation of the corrosion process among multiple locations in the structure. This correlation is of relevance when determining the necessary inspection coverage, and it can influence the reliability of the ship structure. In this paper, we develop a probabilistic spatio-temporal corrosion model based on a hierarchical approach, which represents the spatial variability and correlation of the corrosion process. The model includes as hierarchical levels vessel – compartment – frame – structural element – plate element. At all levels, variables representing common influencing factors (e.g. coating life) are introduced. Moreover, at the lowest level, which is the one of the plate element, the corrosion process can be modeled as a spatial random field. For illustrative purposes, the model is trained through Bayesian analysis with measurement data from a group of tankers. In this application, the spatial dependence among corrosion processes in different parts of the ships is identified and quantified using the proposed hierarchical model. Finally, it is demonstrated how this spatial dependence can be exploited when making inference on the future condition of the ships.

Keywords: Bayesian analysis; Hierarchical modeling; Probability; Deterioration, Corrosion; Inspection.

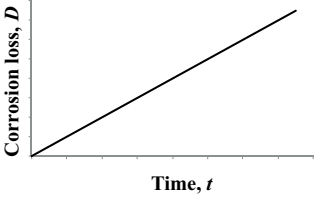
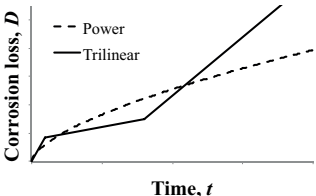
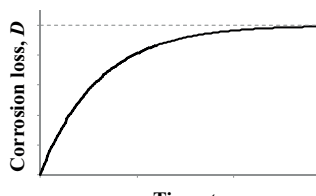
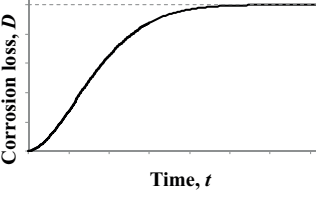
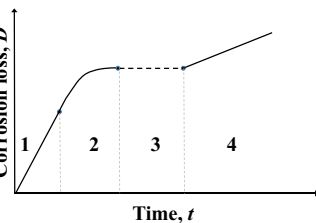
C.1 Introduction

Time-dependent structural degradation (including corrosion, fatigue cracking, mechanical damage) influences the safety of ships. The effect of structural degradation on safety increases with increasing age and often becomes critical when aging vessels with poor maintenance continue operating beyond their design service life (typically after 25 to 30 years). One of the most common causes of structural degradation in vessels is metal corrosion (Gardiner and Melchers 2003). It can occur as uniform (general) corrosion or as localized (pitting) corrosion. Both types can decrease the load bearing capacity of the structure and can lead to leakage or water ingress.

Significant resources are spent to delay or slow down the deterioration processes (Herzberg et al. 2010). Inspection, repair and renewal of corroded plates are crucial elements of structural strength maintenance strategies, in order to prevent structural failure and related consequences to person on board and environment. The challenge for inspection and maintenance schemes is to put the focus on the critical areas relevant for ship condition in order to comply with the safety expectations and minimize the effort.

Previous research on corrosion initiation and development has led to a set of deterministic relations that predict the amount of corrosion as a function of time. The resulting models range from simple linear models to more complex functions based on an understanding of the chemical and physical processes. An overview on models describing the corrosion process as a function of time is provided in Table C.1. Other models have been proposed for describing the direct effect of the influencing factors (e.g. temperature, salinity, pressure) on the corrosion amount (Paik et al. 2004, Melchers and Jeffrey 2007). However, all existing corrosion models are only a simplified representation of reality and cannot include all relevant influencing factors simultaneously. Additionally, most of those factors are not usually known and may vary during the deterioration process. For this reason, probabilistic approaches have been used to complement deterministic models. The uncertainty of the influencing factors is typically included by modeling them as random variables, described through their probability density function (PDF). By combining those PDFs with the deterministic mathematical functions for the corrosion loss, a probabilistic corrosion model is obtained (Southwell et al. 1979, Guedes Soares and Garbatov 1999, Melchers 1999, Qin and Cui 2003, Ayyub et al. 2015). Alternatively, stochastic process models have been proposed (e.g. Straub and Faber 2007), but these are not commonly applied in practice.

Table C.1. General corrosion models (without initiation time).

Model		
Linear model (Guedes Soares 1988, Shi 1993)	$D = R t$	<p>D: corrosion loss t: time R: constant corrosion rate</p> 
Trilinear and power models (Shreir 1976, Shi 1993, Melchers 1998)	$D = \begin{cases} c_1 t & 0 \leq t < T_1 \\ b_2 + c_2 t & T_1 \leq t < T_2 \\ b_3 + c_3 t & T_2 \leq t \leq T_3 \end{cases}$ $D = c t^a$	<p>b_2, b_3, c_1, c_2, c_3: empirical model parameters</p> <p>a, c: empirical model parameters</p> 
Guedes Soares and Garbatov's model (Guedes Soares and Garbatov 1999)	$D = d_\infty \left(1 - e^{-\frac{t}{\tau_T}}\right)$	<p>τ_T: scale parameter d_∞: long-term loss</p> 
Qin and Cui's model (Qin and Cui 2003)	$D = d_\infty \left(1 - e^{-\left(\frac{t}{\tau_T}\right)^\beta}\right)$	<p>τ_T: scale parameter d_∞: long-term loss β: shape parameter</p> 
Melchers' Physically-based model for steel immersed in sea water (Melchers 2003) with corrosion stages:	<ol style="list-style-type: none"> 1: Initial corrosion 2: Diffusion controlled 3: Aerobic activity 4: Anaerobic activity 	

Past investigations have shown how the corrosion process in ship structural elements is affected by their spatial location (Gardiner and Melchers 2003). To account for this dependence, corrosion rate and coating life have been estimated based on thickness measurements separately for different structural element types (Sone et al. 2003, Wang et al. 2003a, Wang et al. 2003b). Such approaches represent the state of the art in the marine industry.

Corrosion among different spatial locations in a ship structure is correlated, due to spatial proximity, but mainly due to common influencing factors, such as environment (temperature, humidity), cargo or maintenance. This correlation has an effect on what one can learn from

individual inspections. Intuitively, this is well understood: If multiple measurements in a particular section of the ship indicate a good condition, one implicitly assumes that the remainder of this section is also in a good condition. However, such correlation has not been modeled and analyzed quantitatively based on empirical data for ship structures.

Probabilistic models for representing spatial dependence among deteriorated elements in ship structures using random fields can be found in the literature (Guedes Soares and Garbatov 1997). For other types of structures, hierarchical models are commonly applied to represent spatial dependence (Maes 2002, Straub et al. 2009, Qin and Faber 2012, Andrade and Teixeira 2015, Schneider et al. 2015). These hierarchical models can be used to perform Bayesian analysis and reliability updating.

In this contribution, we present a hierarchical Bayesian model for representing the spatial variability of uniform corrosion in ship structures, based on work reported in Luque et al. 2014. The model accounts for the dependences among corrosion at different locations due to common influencing factors, and is able to estimate the current and future corrosion in the structure based on measurements from actual data. The model is defined with multiple spatial hierarchical levels and includes a random field at the lowest level. The model is learned with data from thickness measurements obtained during in-service inspection campaigns using Markov Chain Monte Carlo (MCMC).

Two case studies are presented to investigate the correlation of the corrosion process and to exemplify the implementation of the hierarchical Bayesian model in real structures. The deterioration process considered here is general corrosion in floor plates of tankers, but the model principles are applicable to any ship structural elements and to other corrosion process types, such as pitting corrosion, or other deterioration processes, such as fatigue. The first case study is based on simulated measurement campaigns and the second one on inspection data from a group of vessels with identical design and similar operational conditions. It is shown that the main spatial factors affecting corrosion progress can be clearly identified. The second case study also demonstrates how the proposed model can be used in an operational setting, when the model is updated during the service life with results from inspection campaigns.

C.2 Spatio-temporal corrosion models for ship structures

C.2.1 Hierarchical Bayesian models

Due to their simplicity and computational ease, hierarchical models are commonly used in spatio-temporal system models for representing dependencies among system elements. Their application to deterioration modeling is reported for deterioration in pipelines (e.g. Zhang et al. 2014, Qin et al. 2015) and in concrete structures (e.g. Qin and Faber 2012, Schneider et al. 2015). Hierarchical models can provide efficient probabilistic representations of large systems with correlated elements (Raudenbush and Bryk 2008). The observed correlation among system elements is incorporated in the model through the definition of multiple levels, which group elements with similar properties. In vessel structures, plate elements might be grouped according to their structural element type (e.g. main deck, bulkhead). These groups can be subdivided again into lower-level groups, which are based on the spatial location in the vessel (e.g. compartment), and so on. At each level in the hierarchy, a group must contain elements with similar characteristics among them but different from other groups.

In a Bayesian hierarchical model, the probability distributions of the random variables at each level are defined conditional on the random variables of the next higher level. The parameters of these conditional probability distributions, which are themselves random variables, are typically located at the highest level and are called hyperparameters (Gelman et al. 2004). In the Bayesian framework, these hyperparameters are learned jointly with the other random variables from available observations. The hyperparameters define the local and global correlation among the elements of the system. Such Bayesian hierarchical models can represent spatio-temporal processes (Maes et al. 2008, Ntzoufras 2009).

Probabilistic hierarchical models can be conveniently represented as Bayesian Networks (BN). A BN is a probabilistic model that consists of a set of random variables (nodes) and directed links, which represent conditional dependencies (Jensen and Nielsen 2007). As their name suggests, BNs facilitate Bayesian analysis, which makes them suitable for probabilistically modeling deterioration processes when partial observations from inspections and monitoring systems are to be included (Straub 2009). They allow to decomposing problems involving many random variables into multiple local problems. This facilitates Bayesian analysis through MCMC with Gibb's sampler (Gamerman and Lopes 2006).

For illustration purposes, two distinct graphical representations of the same simple hierarchical Bayesian model with two levels are shown in Figure C.1. Figure C.1a depicts an explicit representation of the problem, where all random variables and their dependencies are indicated. The number of random variables, however, soon becomes prohibitive for such an illustration. In contrast, Figure C.1b shows a hierarchical representation, where each hierarchical level is indicated by a corresponding box. In Figure C.1, D_{ij} is the deterioration of the j -th plate inside the i -th compartment, which is modeled by the corrosion rate R_{ij} . μ_{μ_R} and σ_{μ_R} are hyperparameters, and are the mean and standard deviation of the mean corrosion rate $\mu_{R,i}$ in compartments $i = 1, \dots, N_C$. The parameter σ_R , the standard deviation of the corrosion rate, is here a deterministic constant. In this illustration, and throughout this paper, the following notational convention is used:

- Stochastic nodes are represented by circles and deterministic nodes by double circles.
- Single arrows define stochastic conditional dependencies and double arrows deterministic dependencies (i.e. mathematical functions or logical relations) between the child node and its parents.
- Dashed lined squares represent the different levels in the hierarchy and they group the corresponding nodes that belong to each level.
- Indices are used to distinguish among the different elements in a group.
- Grey circles depict a random field.

The hierarchical structure of the example is defined through the hyperparameters μ_{μ_R} and σ_{μ_R} at the top level in the hierarchy, the mean corrosion rate per compartment $\mu_{R,i}$ at the second level, the corrosion rate R_{ij} and deterioration D_{ij} for the j -th plate in the i -th compartment at the third level, and the variability of the corrosion rate per plate, σ_R , as a deterministic parameter. Each hyperparameter has a prior probability distribution F_μ and F_σ , respectively, which are based on previous knowledge (in case there is no available information, a weakly informative distribution can be used as prior distribution).

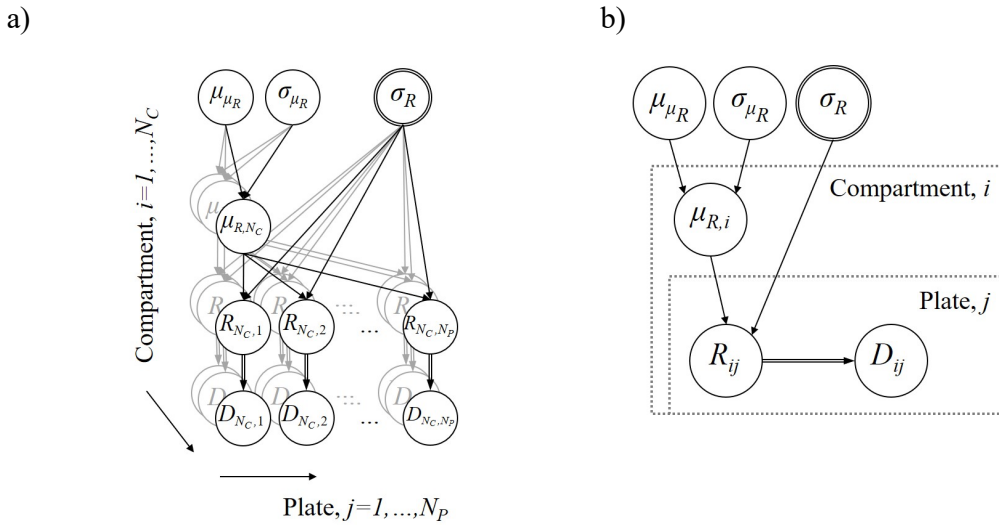


Figure C.1. Example of a hierarchical Bayesian deterioration model (D : deterioration, R : corrosion rate, μ : mean, σ : standard deviation) using (a) explicit and (b) hierarchical representations.

A main goal in the analysis of hierarchical Bayesian models is the estimation of the hyperparameters' posterior distribution. The hyperparameters are assumed to be globally valid, hence they allow one to transfer information from ships (or structures, systems) with inspection data to other ships belonging to the same population. The information contained in observations made at specific elements of a specific ship is used to update the distribution of the hyperparameters. These posterior distributions are then used as prior distributions when inspecting or making predictions of other ships.

C.2.2 Hierarchical structure of the corrosion model

To represent the spatial correlation of corrosion in vessels, several hierarchical levels are defined. The different levels are introduced in the following and illustrated in Figure C.2:

- *Single plate*: Plates are the basic elements at the lowest level of the spatial hierarchy. At this level, the spatial variability of the corrosion loss may be modeled using random fields. In this way, the correlation of corrosion loss among elements can be defined as a function of their distance.
- *Structural Element*: Single plates are grouped according to the structural element class they belong to (e.g. bulkhead, inner bottom, main deck). The reason for this aggregation is that plates from the same structural element type have similar design properties and may exhibit similar corrosion loss. This defines the second level of the hierarchical model.

- *Frame*: Vessels are usually assembled or repaired frame by frame. Plate elements from those frames can therefore have characteristics that are common among them.
- *Compartment*: Plates inside the same compartment are mostly subject to similar environmental and operational conditions. Since these are expected to influence corrosion significantly, compartments define the next level in the hierarchy.
- *Vessel*: This level corresponds to the complete vessel, which groups all compartments of the structure. Vessels are affected by conditions that depend on the characteristics of the structure itself and its operational profile (e.g. stress distribution, loads, temperature, cargo).
- *Fleet*: This is the top level, corresponding to the population of vessels that can be described by the same model (e.g. all vessel of a certain type such as bulk carriers or tankers; or all vessels built according to a similar design with similar materials).

This framework is flexible and it is possible to leave out some levels or define additional levels in the hierarchy, depending on the amount and detailing of the available information. For example, a level between the compartment and structural element levels can be introduced if a certain characteristic (e.g. bottom-middle-upper areas, orientation) provides additional information on the corrosion process. Also the operational characteristics (e.g. cargo type) and the geometry of the vessel can define additional levels between the vessel and fleet levels, helping to distinguish the information from distinct ships in the analysis.

In the following, the corrosion estimation for all plates, as well as every thickness measurement, will be uniquely identified by indices $(i_1, i_2, i_3, i_4, i_5)$ corresponding to the levels in the hierarchy (i.e. i_1 -th vessel, i_2 -th compartment, i_3 -th frame, i_4 -th structural element, and i_5 -th plate). To simplify the index notation, a set of consecutive indices i_1, \dots, i_k is denoted simply as $i_{1:k}$.

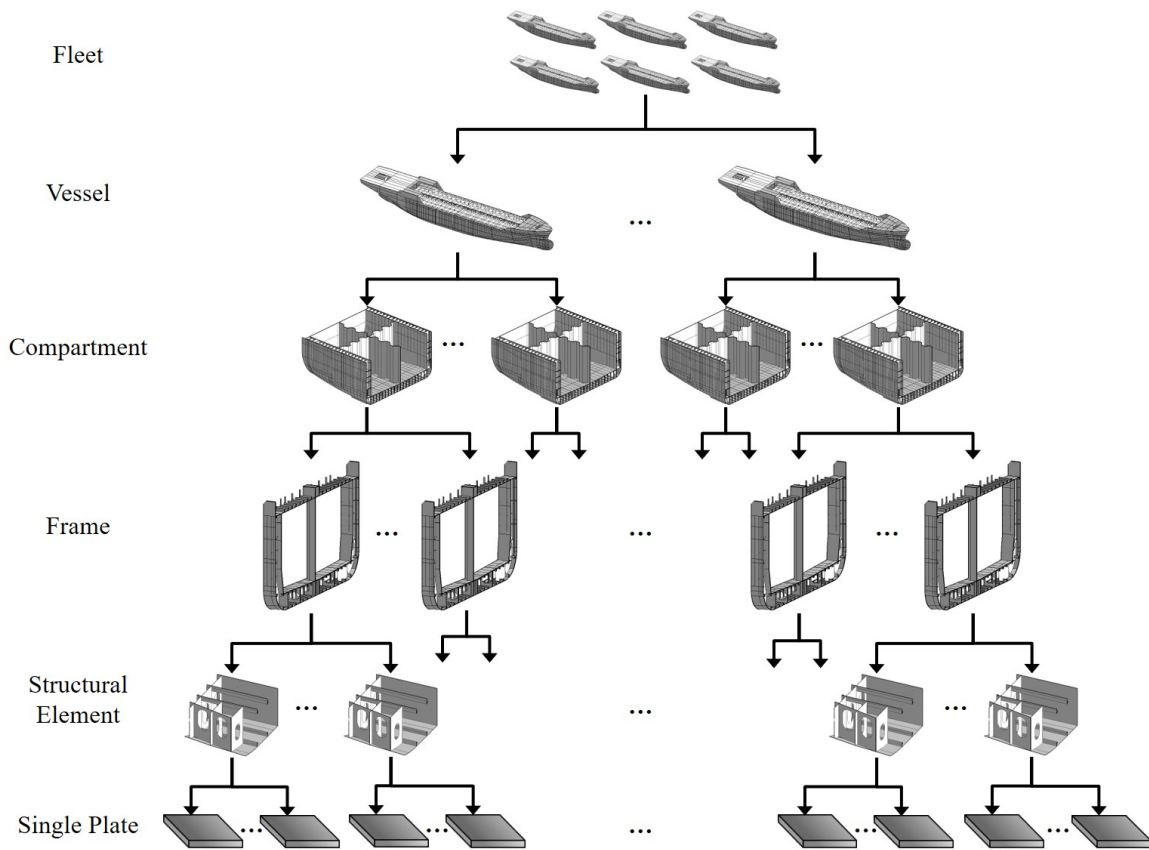


Figure C.2. Hierarchical structure of the spatial corrosion model.

C.2.3 Thickness measurements

The most common inspection method for estimating corrosion loss is to perform thickness measurements at different times and locations. On a plate, the thickness is typically measured at multiple points (e.g. corners and midpoint) and the average is used to represent its current thickness value. The measured corrosion loss of a plate is the difference between its as-built and its current thickness; the corresponding linear corrosion rate is estimated by dividing the corrosion loss by the exposure time of the plate to the corrosive environment.

The direct estimation of the corrosion rate from thickness measurements is hindered by several factors. Firstly, most plate elements are protected against corrosion (usually with a coating paint) and the time when this protection breaks down is not generally known. If the corrosion rate is approximated by dividing the estimated corrosion loss by the vessel age (i.e. without subtracting the coating life) then the corrosion rate might be considerably underestimated. Secondly, measurement campaigns usually contain a non-negligible percentage of plates with measured thickness larger than the thickness reported in plans, producing a negative estimated corrosion loss. The main reason for this obviously unrealistic result is that the originally built-in plates

are thicker than those reported in plans due to reasons of plate fabrication as well as yard building process. The difference between the as-built and gross thickness (i.e. value given in plans) is called thickness margin. In general, this margin is not known at the moment of making thickness measurements and it can cause biased corrosion estimates.

Both coating life and thickness margin directly affect the estimation of the corrosion rate based on measurements. If any of them is not considered, the corrosion rate will be underestimated. For this reason, coating life and thickness margin are important parameters that are included in the proposed spatial hierarchical Bayesian model of corrosion loss.

C.2.4 Corrosion model

A corrosion function (example models are presented in Table C.1) is combined with the proposed spatial Bayesian hierarchical model. It is assumed that the corrosion loss is zero before the coating breaks; this occurs when reaching the stochastic coating life C . If the time-dependent corrosion model f with parameters $\boldsymbol{\theta} = [\theta_1, \dots, \theta_{n_p}]$ defines the corrosion loss, where n_p is the number of model parameters, then the resulting corrosion loss D as a function of time t is:

$$D(t) = \begin{cases} 0 & \text{if } t \leq C \\ f(t - C; \boldsymbol{\theta}) & \text{if } t > C \end{cases} \quad (\text{C.1})$$

Let \hat{w} be the plate gross thickness reported in plans, and M is the thickness margin. The actual plate thickness W at time t is:

$$W(t) = \hat{w} + M - D(t) \quad (\text{C.2})$$

The parameters $\boldsymbol{\theta}$ of the corrosion model f (e.g. the corrosion rate R in the linear corrosion model), coating life C , and thickness margin M are modeled as random variables, which vary from plate to plate depending on their spatial location. In the following sections, these random variables and their hierarchical structure are defined in detail.

C.2.5 Thickness margin

To arrive at a prior probabilistic model for the thickness margin of a plate element, the following considerations and assumptions are made. The thickness margin is defined as a non-negative

random variable. Standards do allow small negative margins (up to 0.6 mm for plates thinner than 25 mm) depending on the quality of the class (Germanischer Lloyd Group 2009) but this possibility is neglected here. Large margins are less likely than small margins, mainly due to the cost of steel. To account for the possible correlation among margins within a frame (plates are typically renewed by frame), a common uncertain mean margin $\mu_{M,i_{1:4}}$ is defined for all structural elements of the same type within a frame. The distribution of $\mu_{M,i_{1:4}}$ is as the exponential distribution with mean μ_{μ_M} . The plate margin $M_{i_{1:5}}$ is modeled as lognormal distributed with mean $\mu_{M,i_{1:4}}$ and coefficient of variation δ_M . The thickness margin of each plate is constant in time and assumed to be independent of the spatial location of the plate inside the frame. The hierarchical probabilistic model of the margin is depicted in Figure C.3, where $F_{\mu_{\mu_M}}$ and F_{δ_M} are the prior distributions of the hyperparameters.

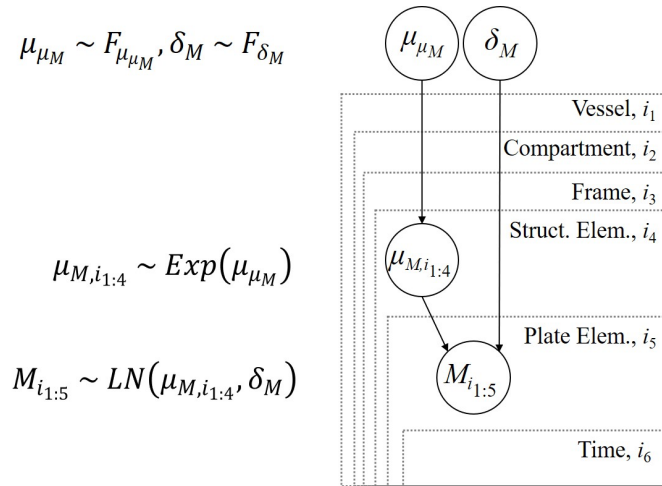


Figure C.3. Hierarchical representation of the thickness margin.

C.2.6 Coating life

All plate elements in the i_1 -th vessel and i_2 -th compartment are modeled with the same mean coating life $\mu_{C,i_{1:2}}$ and standard deviation σ_C . The latter parameter is defined as independent of the compartment (i.e. it is a hyperparameter) and it represents the variability of the coating life among plates within one compartment. The mean coating life $\mu_{C,i_{1:2}}$ is modeled as a lognormal random variable, whose mean μ_{μ_C} and standard deviation σ_{μ_C} are hyperparameters. Figure C.4 summarizes the hierarchical modeling of the coating life. Here, $F_{\mu_{\mu_C}}$, $F_{\sigma_{\mu_C}}$ and F_{σ_C} are the prior distributions of the hyperparameters.

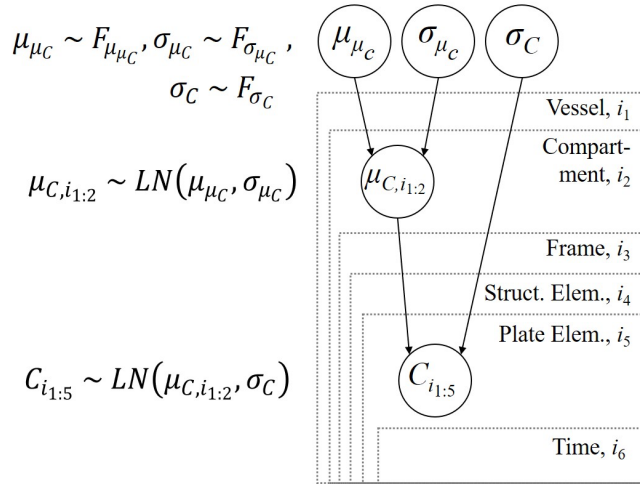


Figure C.4. Hierarchical representation of the coating life.

C.2.7 Parameters of the corrosion model

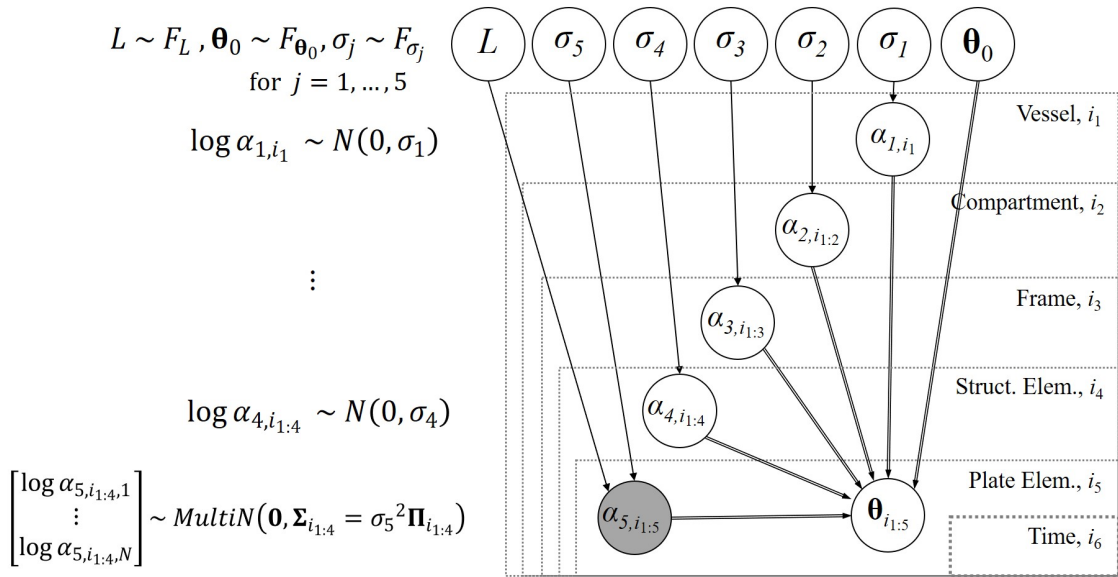
The parameters $\boldsymbol{\theta} = [\theta_1, \dots, \theta_{n_p}]$ of the corrosion model f for a single plate are modeled as constant during the life of the plate, which is the common approach in corrosion modeling. The spatial variability of parameters $\boldsymbol{\theta}$ is hierarchically defined using variability factors $\alpha_1, \alpha_2, \alpha_3, \alpha_4$ and α_5 and a set of base parameters $\boldsymbol{\theta}_0 = [\theta_{1,0}, \dots, \theta_{n_p,0}]$. The idea behind this definition is to distinguish between the uncertainty in the mean (modeled with the base parameters) and the variance (modeled with the variability factors) of the deterioration model parameters. Model parameters $\boldsymbol{\theta}$ in a specific plate at location $i_{1:5}$ are defined as a product of the corresponding variability factors with the base parameters $\boldsymbol{\theta}_0$:

$$\boldsymbol{\theta}_{i_{1:5}} = \alpha_{1,i_1} \alpha_{2,i_{1:2}} \alpha_{3,i_{1:3}} \alpha_{4,i_{1:4}} \alpha_{5,i_{1:5}} \boldsymbol{\theta}_0 \quad (\text{C.3})$$

Factors $\alpha_{1,i_1}, \alpha_{2,i_{1:2}}, \alpha_{3,i_{1:3}}, \alpha_{4,i_{1:4}},$ and $\alpha_{5,i_{1:5}}$ correspond to vessel, compartment, frame, structural element, and plate element levels. These factors are modeled as lognormal random variables with parameters $\mu_{\log \alpha_j} = 0$ and $\sigma_{\log \alpha_j} = \sigma_j$ for $j = 1, \dots, 5$, and they are independent of the corrosion model parameters. It is noted that the choice of the $\mu_{\log \alpha_j}$ is irrelevant, since these parameters are redundant with $\boldsymbol{\theta}_0$ (increasing $\mu_{\log \alpha_j}$ by Δ will lead to a decrease of $\ln \boldsymbol{\theta}_0$ by Δ). Hence the $\mu_{\log \alpha_j}$ are set to zero and not learnt with the data. The standard deviations $\sigma_1, \dots, \sigma_5$ and the base parameters $\boldsymbol{\theta}_0 = [\theta_{1,0}, \dots, \theta_{n_p,0}]$ are defined as hyperparameters and are independent of the position of the plate.

For given location indices $i_{1:4}$ (i.e. for a particular vessel, compartment, frame and structural element type), the set of N variability factors $\alpha_{5,i_{1:4},1}, \dots, \alpha_{5,i_{1:4},N}$ in the lower hierarchical level is modeled through a random field. The correlation among the logarithm of their values is represented by the correlation matrix $\mathbf{\Pi}_{i_{1:4}}$. This matrix is defined through a correlation model, based on the distance between points. The characteristic parameters are the correlation lengths L_x and L_y in x- and y-direction (Vanmarcke 2010). Here, an isotropic correlation function is used, which depends only on the total distance between two points, and hence the only hyperparameter defining the correlation matrix is the correlation length L .

Figure C.5 presents the hierarchical structure among the variability factors $\alpha_{1,i_1}, \alpha_{2,i_{1:2}}, \alpha_{3,i_{1:3}}, \alpha_{4,i_{1:4}}, \alpha_{5,i_{1:5}}$, the base parameters θ_0 , and corrosion model parameters $\theta_{i_{1:5}}$. As mentioned before, gray nodes depict a random field in the model.



$$\theta_{i_{1:5}} = \alpha_{1,i_1} \cdot \alpha_{2,i_{1:2}} \cdot \alpha_{3,i_{1:3}} \cdot \alpha_{4,i_{1:4}} \cdot \alpha_{5,i_{1:5}} \cdot \theta_0$$

Figure C.5. Hierarchical representation of the corrosion model parameters.

Since the variability factors are lognormal distributed, the logarithms of the corrosion model parameters, $\log \theta_{k,i_{1:5}}, k = 1, \dots, n_p$, are normal distributed given the hyperparameters $\sigma_1, \dots, \sigma_5$ and θ_0 , with mean and variance as follows:

$$\mu_{\log \theta_{k,i_{1:5}}} = \log \theta_{k,0} \quad (C.4)$$

$$\sigma_{\log \theta_{k,i_{1:5}}}^2 = \sigma_1^2 + \sigma_2^2 + \sigma_3^2 + \sigma_4^2 + \sigma_5^2 \quad (\text{C.5})$$

where σ_j is the standard deviation of the logarithm of the variability factor α_j , $j = 1, \dots, 5$ and $\sigma_{\log \theta_{k,0}}^2$ is the variance of the logarithm of the base parameter $\theta_{k,0}$. Through Eq. (C.3) and Eq. (C.5), the conditional correlation (given the hyperparameters) between the logarithm of the same deterioration model parameter at two different plates can be obtained as follows:

$$\gamma_q = \frac{\sum_{k=1}^q \sigma_k^2}{\sum_{k=1}^5 \sigma_k^2} \quad (\text{C.6})$$

where q is the lowest level of hierarchy that is common to two plates. For example, if two plates are in the same vessel but in different compartments, i.e. they share the same index i_1 and $i_2 \neq i_2^*$, then $q = 1$ and the correlation between their model parameters is:

$$\rho(\log \theta_{k,i_1,i_{2:5}}, \log \theta_{k,i_1,i_{2:5}^*}) = \frac{\sigma_1^2}{\sigma_1^2 + \sigma_2^2 + \sigma_3^2 + \sigma_4^2 + \sigma_5^2} = \gamma_1 \quad (\text{C.7})$$

If two plates are from the same vessel, compartment, frame and structural element (i.e. they share the same indexes $i_{1:4}$), the correlation between their deterioration model parameters is also affected by the correlation structure defined by the matrix $\mathbf{\Pi}_{i_{1:4}}$ and is obtained as follows:

$$\begin{aligned} \rho(\log \theta_{k,i_{1:4},i_5}, \log \theta_{k,i_{1:4},i_5^*}) &= \frac{\sigma_1^2 + \sigma_2^2 + \sigma_3^2 + \sigma_4^2 + \sigma_5^2 \cdot \mathbf{\Pi}_{i_{1:4}}(i_5, i_5^*)}{\sigma_1^2 + \sigma_2^2 + \sigma_3^2 + \sigma_4^2 + \sigma_5^2} \\ &= (1 - \gamma_4) \cdot \mathbf{\Pi}_{i_{1:4}}(i_5, i_5^*) + \gamma_4 \end{aligned} \quad (\text{C.8})$$

Knowledge of the correlation among different plates can help deciding whether or not to inspect a location, based on a set of measurements from other locations.

Note: the expressions given above for the variance and the correlation coefficients are for given hyperparameters. The uncertainty on hyperparameters, which is a purely statistical uncertainty, introduces additional correlation, which decreases as the amount of data for learning the model increases.

C.2.8 Measurement model

Thickness measurements are described by an additive error model. The measured thickness $Z_{i_{1:6}}$ at time t is equal to the actual current thickness $W_{i_{1:6}}$ plus a measurement error with zero mean and standard deviation σ_e , where t is defined as an additional hierarchical level (i.e. i_6). This measurement error aggregates all sources of errors, of which human and device are the most common types. The outcomes of thickness measurements are included in the Bayesian model as the variables $Z_{i_{1:6}}$, which are normally distributed random variables with mean value $W_{i_{1:6}}$ and standard deviation σ_e , i.e. $Z_{i_{1:6}} \sim N(W_{i_{1:6}}, \sigma_e)$. The distribution of the measurement error is assumed to be independent of the measurement location.

C.2.9 Complete hierarchical corrosion model

By combining the hierarchical definitions for the individual model parameters, the complete hierarchical corrosion model is obtained, as depicted in Figure C.6.

Previous analyses reported in the literature provide estimates of percentiles of the corrosion rate and coating life (Sone et al. 2003). These values can be used as prior information in the proposed hierarchical Bayesian model. If these sources have used information from different fleets, then it must be reflected through the variability of the parameters from vessel to vessel. If no previous information is available, then weakly informative prior distributions should be used.

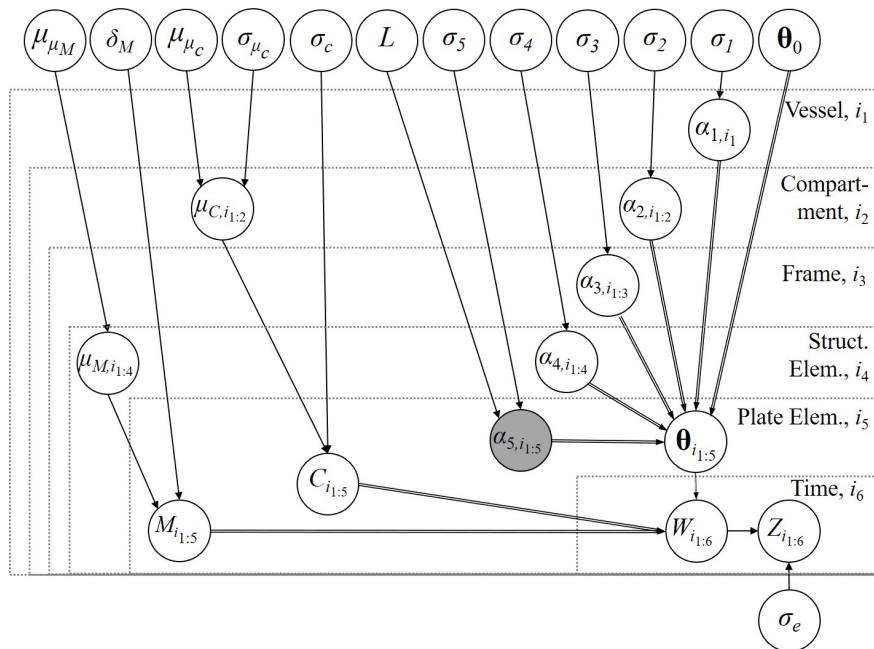


Figure C.6. Hierarchical representation of the full corrosion model, including measurements.

C.2.10 Parameter estimation

The parameters of the proposed hierarchical corrosion model are learnt from data (here: thickness measurements) using Bayesian analysis. We thereby distinguish between (a) learning the hyperparameters, which describe the fleet-wide model, and (b) learning the parameters that are specific to a vessel, a compartment or any lower-level hierarchical element. Part (a) is referred to as general estimation and it is based on records of measurements from multiple vessels. Part (b) corresponds to the analysis of a specific vessel. Here, the estimated probability distributions obtained in part (a) from the analysis of other vessels are used as prior distributions in part (b), which are updated with the new measurements from the specific vessel. The differentiation between part (a) and (b) is motivated purely by practical reasons, since it allows analyzing each vessel individually. The Bayesian methodology itself does not require one to make this distinction; rather, a joint model of all vessels can and should be developed. Ideally, whenever a new measurement in any of the vessels is available, the entire model of all vessels should be updated.

For parameter learning, Bayesian analysis is implemented and solved using Markov Chain Monte Carlo (MCMC). MCMC is a simulation-based method that generates samples of the posterior distribution through a Markov chain, whose stationary distribution is the sought posterior distribution (Gilks et al. 1996, Gamerman and Lopes 2006).

C.3 Numerical investigations

In the following sections, two case studies are presented. The first one presents a hypothetical study using simulated data, which allows assessing the performance of the model and the parameter learning against an assumed “true” model. The second case study presents the learning of the model with thickness measurements from a set of sister tankers (i.e. vessels with virtually identical design). Based on the learned model, a spatial probabilistic prediction of corrosion in a specific tanker is presented.

For simplicity, the linear corrosion model from Table C.1 with a single parameter (i.e. the corrosion rate R) is used as the corrosion function, which is combined with the coating life (Eq. (C.1)). However, the probabilistic framework can be applied in combination with more advanced corrosion functions.

The Bayesian estimation is carried out with OpenBUGS, which is open-source software for performing Bayesian inference (Lunn et al. 2009). The MCMC analysis is carried out with a burn-in period of 1,000. A total of 50,000 samples are generated to estimate the joint PDF of the model parameters. The estimated mean values, standard deviations, 95% credible intervals and posterior distributions of the parameters are presented for each case study, where credible intervals were obtained as the 2.5 and 97.5 percentiles of the posterior distribution.

C.3.1 Case study 1: Simulated scenario

To assess the quality of the Bayesian parameter estimation for the proposed hierarchical model, a first example with synthetic data is presented.

The number of hypothetical vessels, compartments, frames, structural elements, measured plates and measurement campaigns are summarized in Table C.2. Here, several model parameters are assumed to be deterministic with values as given in Table C.3. The resulting hierarchical model is shown in Figure C.7, where the deterministic parameters are represented by double circle nodes. Note that the choice of a correlation length $L = 0$ implies that no conditional (i.e. given the hyperparameters) spatial correlation of the plates within a compartment is considered.

Table C.2. Number of elements at the different hierarchical levels.

Number of vessels	10
Compartments per vessel	5
Frames per compartment	5
Structural elements per frame	3
Plates per structural element	10
Measurement campaigns after	5, 8, 10, 12 years

Table C.3. Deterministic parameters.

Margin variability σ_M [mm]	0.08
Coating variability among compartments σ_{μ_c} [mm]	1.5
Coating variability inside compartments σ_c [mm]	0.5
Frame variability σ_3	0
Correlation length L (i.e. correlation matrices $\mathbf{\Pi}_{i:4} = \mathbf{I}_{10 \times 10}$)	0
Measurement error σ_e [mm]	1

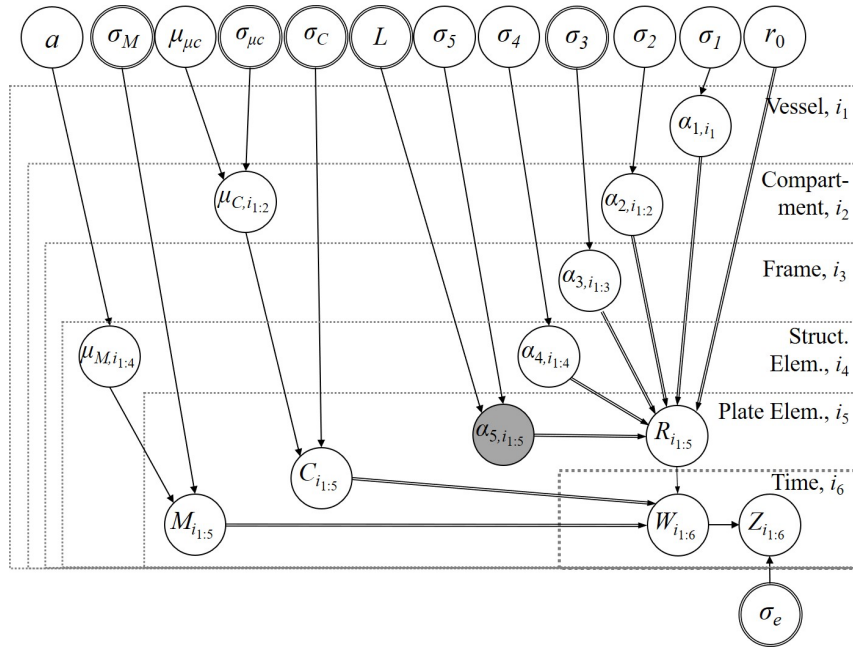


Figure C.7. Hierarchical representation of the simulated example.

Weakly informative priors are used for the hyperparameters, i.e. probability distributions with large uncertainty, e.g. $N(\mu = 0, \sigma = 10^3)$ or $Gamma(\lambda = 10^{-3}, k = 10^{-3})$ are taken as prior distributions.

Good agreement between the original and the estimated values for most of the parameters is obtained (Table C.4 and Figure C.8). The variability factor σ_5 is the only variable in which the true value is not inside the 95% credible interval obtained in the Bayesian analysis.

As more data becomes available, the uncertainty in the estimations will decrease (i.e. the posterior distributions become narrower). Using Bayesian analysis one can estimate the distribution of each random variable in the model and use this information for estimating the deterioration in both the complete fleet and a particular vessel.

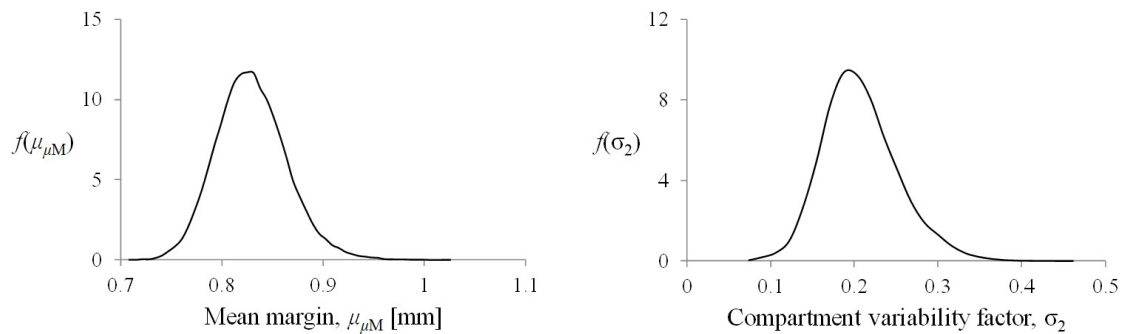


Figure C.8. Exemplary estimated marginal PDFs of model parameters.

Table C.4. Statistics of the stochastic parameters of the model.

	Original (true) Value	Estimates		
		Mean	StDev	95% Credible Interval
<i>Margin</i>				
Mean μ_{μ_M} , [mm]	0.8	0.824	0.032	(0.76,0.89)
<i>Coating</i>				
Mean μ_{μ_C} , [years]	7	6.91	0.255	(6.4,7.4)
<i>Corrosion rate and variability factors</i>				
Vessel variability σ_1	0.3	0.389	0.118	(0.22,0.68)
Compartment variability σ_2	0.2	0.214	0.048	(0.14,0.32)
Struct. element variability σ_4	0.3	0.289	0.0149	(0.26,0.32)
Plate variability σ_5	0.1	0.129	0.0123	(0.11,0.16)
Base corrosion rate r_0 , [mm/yr]	0.3	0.249	0.034	(0.19,0.32)

C.3.2 Case study 2: Corrosion in tanker floors

This case study is based on thickness measurements of floor plates from four inspected tankers. All tankers in the database have the same structural design (i.e. the spatial locations of plates, structural elements and compartments are the same for all vessels) and similar operational characteristics. The inspections were performed when the tankers were between 14 and 18 years old and included many different structural elements from different locations. The reason for studying the floor plates in this analysis is that these belong to the few structural elements for which data is available from two inspection campaigns. All inspected tankers had a major repair when they were 10 years old, which is considered in the model by subtracting 10 years from the inspection time. The underlying assumption is that following the repair all plates were as-built. Main characteristics of the thickness measurements are summarized in Table C.5.

Table C.5. Characteristics of the thickness measurements used for the case study 2.

Tanker	Inspection time [years]	Structural element	Number of compartments	Number of measurements
T1	15.0 / 16.5	Floor	12	128 / 436
T2	14.7 / ----	Floor	12	92 / ----
T3	14.9 / 17.8	Floor	12	127 / 178
T4	14.9 / 17.9	Floor	12	128 / 172

The compartment numbers correspond to the numbering of the cargo tanks that are above the floor plates. This means that floor plates from different compartments might not be physically

separated but they can still be affected by different conditions (e.g. stress distribution due to different cargo tanks above floor plates). Figure C.9 shows the location of floor plates in all 4 tankers and the spatial distribution of the thickness measurements of one inspection campaign as an example.

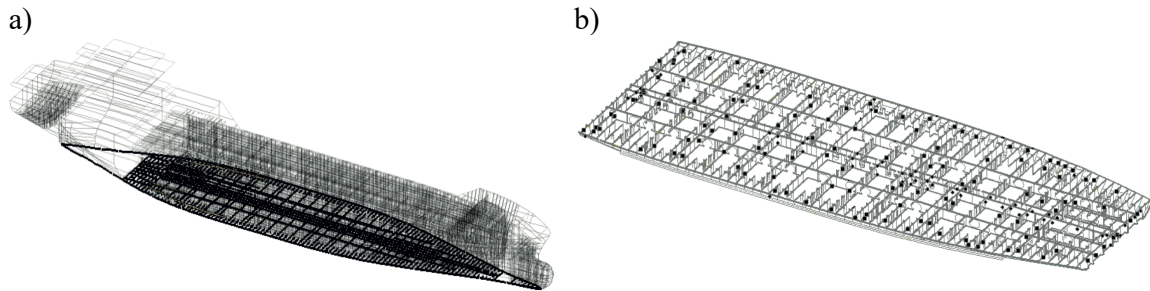


Figure C.9. a) Location of the structural element Floor in tankers; b) locations of thickness measurements in one of the measurement campaigns.

In this example, the vessel-specific factor is omitted (i.e. $\sigma_1 = 0$) and corrosion rates are assumed to be independent of the frame (i.e. $\sigma_3 = 0$). Moreover, because of the small number of inspection campaigns per vessel, the number of possible combinations of corrosion rate, coating life, and thickness margin that give the same observed corrosion loss is not unique. For this reason, the parameters related to the coating life are not learned but taken from Sone et al. (2003) and fixed to $\mu_{\mu_c} = 6$ years, $\sigma_{\mu_c} = 0$, $\sigma_c = 5$ years. The measurement error has a standard deviation of $\sigma_e = 1$ mm.

In order to see how the corrosion estimates from this database compare with results from the literature, weakly informative distributions with large uncertainty were used as prior distributions of the hyperparameters, as in the case study 1. The estimated median of the corrosion loss for vessels with 20 years is approximately 0.26 mm. This is in good agreement with Sone et al. (2003), where the median of corrosion loss in floor plates in single side skin bulk carriers after 20 years is reported as 0.42 mm. The estimated posterior distributions and statistics of the parameters based on the measurements are shown in Table C.6 and Figure C.10.

Analyzing the estimated parameters from Table C.6, one can observe that the variation of the corrosion rate among compartments is larger than the variation within. This result is in agreement with the fact that conditions affecting corrosion are more even among plates within a compartment than between compartments. It is also noted that the estimated mean thickness margin of 0.315 mm represents a non-negligible value, given the low corrosion rate observed

in floor plates. Uncertainty in the estimation of the corrosion rate would decrease if the correct initial thicknesses were reported.

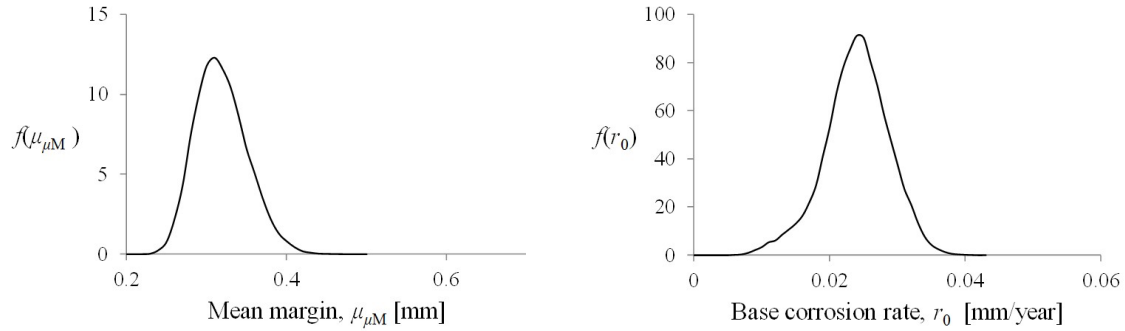


Figure C.10. Exemplary posterior distribution of parameters of the corrosion model for the tankers example.

Table C.6. Statistics of the stochastic parameters of the model.

	Estimations			
	Mean	StDev	MC error	95% Credible Interval
<i>Margin</i>				
Mean margin μ_{μ_M} [mm]	0.315	0.041	1.3e-3	(0.24,0.4)
Coefficient of variation δ_M	0.05	0.0214	8.4e-4	(0.021,0.1)
<i>Corrosion rate and variability factors</i>				
Compartment variability σ_2	0.81	0.205	6.96e-3	(0.5,1.28)
Plate variability σ_5	0.247	0.151	3.87e-3	(0.039,0.55)
Base corrosion rate r_0	0.021	0.006	2.2e-4	(0.009,0.32)

C.3.3 Analysis of a specific vessel

Once a first estimate of the hyperparameters for the entire population of vessels (here: tankers) is available, it can be used as a prior probabilistic model for the analysis of a specific vessel. In the following, the results presented in Table C.6 are used as prior distributions and two inspection campaigns of an additional tanker at years 15 and 17 are included as observations. The measurements and results available for this tanker also serve to illustrate some of the general issues encountered with all data sets.

In one of the inspection campaigns, 27% of measurements of floor plates result in a positive thickness diminution (i.e. the measured thickness is smaller than gross thickness), 14% result in no diminution, and 59% of measurements correspond to a negative diminution (i.e. the measured thickness is larger than the reported gross thickness). As discussed earlier, negative diminutions are due to thickness margins that are not reported in plans or due to measurement

errors. The percentage of measurements with negative diminution in tanker 5 is almost double of that encountered in the general population (33% of measurements). Therefore, the posterior distribution of the thickness margin for this vessel is expected to significantly differ from the prior. Figure C.11 shows the locations of the measured plates and the measured thickness differences. It can be clearly seen how measurements from the same frame (i.e. vertical lines) are correlated. Since frames are defined as a level in the hierarchical model, this dependence is reflected in the resulting estimates. This dependence cannot come from the corrosion rates (due to the assumption of $\sigma_3 = 0$) or the coating life (in the model, mean coating life is independent of the frame) but from the mean thickness margin $\mu_{M,i,1,4}$, which varies from structural elements in one frame to those in another frame. If the effect of the frame in the corrosion rate is to be estimated, then the frame variability hyperparameter σ_3 must be included in the model.

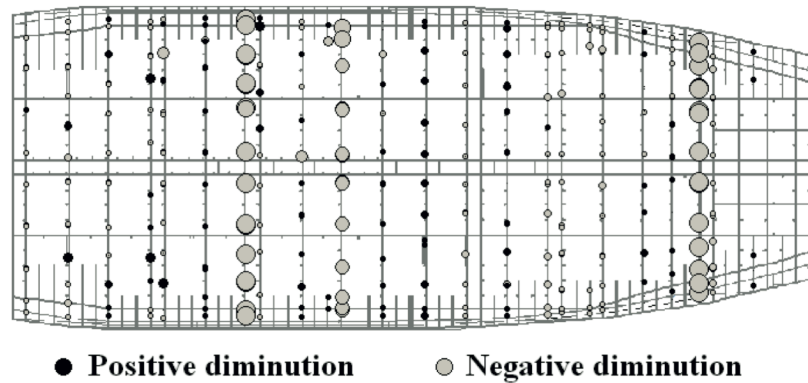


Figure C.11. Measurement campaign in tanker 5 at year 17 used for model updating (the diameter of the circle is proportional to the measured thickness diminution).

It is pointed out that in traditional statistical analyses of corrosion loss in ships, the measurements with a negative thickness diminution are commonly neglected, which reduces the number of available measurements and introduces a bias. In this study, all measurements are included in the estimation of the corrosion rate, coating life and thickness margin. The updated means and standard deviations of all parameters are presented in Table C.7 and the PDFs of the mean margin and base corrosion rate in Figure C.12.

Major differences between the prior and updated (posterior) distributions are observed for the mean margin μ_{μ_M} and the base corrosion rate r_0 . This difference is mainly due to the small number of available tankers in the database. With increasing the number of tankers available in the database, the uncertainty in the hyperparameters will reduce. Any additional measurements will thus lead to smaller changes in the distribution.

Table C.7. Parameters update.

	Prior distribution		Posterior estimates	
	Mean	StDev	Mean	StDev
<i>Margin</i>				
Mean margin μ_{μ_M} [mm]	0.315	0.041	0.43	0.041
Coefficient of variation δ_M	0.05	0.0214	0.044	0.013
<i>Corrosion rate and variability factors</i>				
Compartment variability σ_2	0.81	0.205	0.75	0.167
Plate variability σ_5	0.247	0.151	0.151	0.081
Base corrosion rate r_0 [mm/yr]	0.021	0.006	0.014	3.6e-3

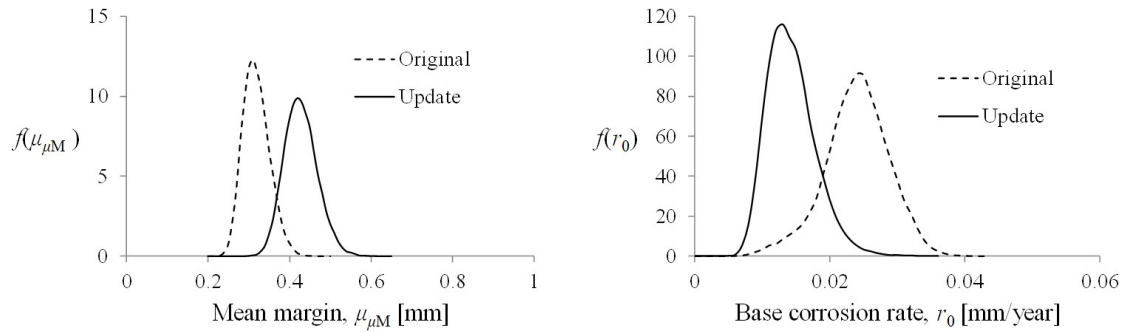


Figure C.12. Comparison between the original (prior) and the updated (posterior) distribution.

To estimate the particular deterioration process of tanker 5, the nodes inside the hierarchical BN (i.e. below the hyperparameters) have to be considered. The spatial distribution of the margin, coating life and corrosion rate can be obtained for each location through their posterior PDF. The expected value of these variables is presented in Figure C.13 for every measured plate, but it can also be estimated for plates without measurements, due to the spatial hierarchy of the model. The resulting mean of the expected margin, coating life and corrosion rate of all measured locations in the ship are 0.6 mm, 5.9 years, and 0.012 mm/year, respectively.

The results in Figure C.13 show how each random variable is affected by the spatial location of the plate. The spatial pattern is particularly obvious for thickness margins (dependence on the frame) and for corrosion rates (dependence on compartments). Negative diminutions observed in the measurement campaigns (Figure C.11) are explained due to fabrication thickness margins for those plates. Using the proposed model, it is possible to obtain corrosion rates also from those measurements with negative diminutions, thus enabling the consistent use of all available information.

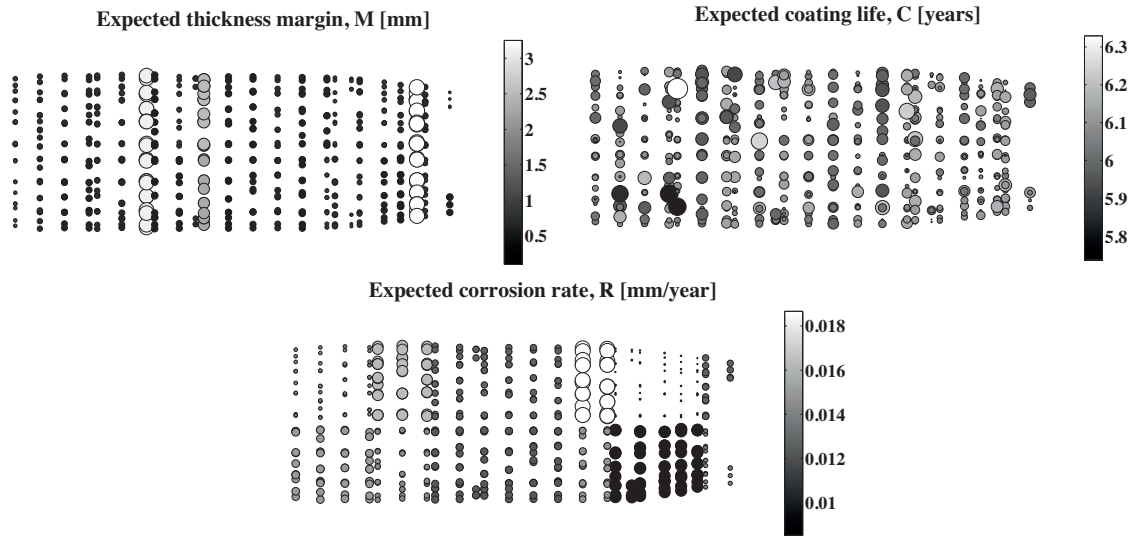


Figure C.13. Spatial distribution of the expected margin, coating life and corrosion rate per measured location. The color of a circle represents the mean estimate and the size of a circle reflects the deviation of the value at this location from the total mean value (i.e. from all measured points). The larger circles are values in the tails of the distribution.

C.4 Discussion

The proposed spatio-temporal corrosion modeling framework probabilistically quantifies the dependence of the deterioration process among different locations in the structure. It provides a systematic and effective way of making the best use of all available information from inspection and measurement campaigns. In the following, important aspects of the model are analyzed in more detail, and some extensions are discussed.

The spatio-temporal Bayesian model is learnt from data using MCMC. It allows the estimation of the posterior PDFs of the hyperparameters (as presented in the previous section), but the remaining parameters (e.g. the mean coating life of a specific compartment) are also learned without additional computations. Once the hyperparameters are estimated, it is possible to extrapolate inspection results to locations without inspections (due to the dependence structure defined with the hierarchical model) and predictions can be made about future corrosion performance (based on the corrosion function used in the model). Moreover, a failure criterion can be defined at any level of the structure (e.g. plate or cross section failure) and the probability of failure as a function of time can be calculated through structural reliability methods.

The homogeneity of the systems and locations from which inspections are obtained (i.e. similarity in the operational characteristics and design of the vessels in the fleet) impacts the accuracy of the model results. In the optimal case, the measurement data contains multiple

inspection campaigns at different times and the fleet has vessels with similar characteristics. In general, the larger the number of inspection times and the more homogeneous the fleet is, the smaller the uncertainty in the estimated parameters will be. However, this does not imply that information from different types of vessels cannot be used in the same analysis. The hierarchical approach allows the model to identify whether or not the data sources have similar characteristics. If measurements from inhomogeneous sources are used in the analysis, then the hierarchical Bayesian model will result in distributions with high dispersion. For example, a large variance σ_1 of variability factor α_1 will indicate that there is a substantial difference in the deterioration process among vessels. If the results obtained from vessels with different characteristics are used as prior distribution in the analysis of a specific vessel, the effect of this information is rapidly reduced (due to the large initial variance) as new measurements of the analyzed vessel itself are obtained. It can be beneficial to include additional hierarchical levels related to known characteristics of vessels (such as cargo type) when measurements come from an inhomogeneous fleet.

At the lowest level of the hierarchy (plates), we propose the use of a random field model, whose main parameter is the correlation length L . In this paper, L is assumed to be fixed and equal to zero, which implies that the spatial dependence represented by the random field is neglected. Even though the correlation length can in principle be estimated directly using the developed Bayesian framework, such an approach requires sufficient number of measurements from components of the same type within the same frame. It is pointed out that L does not affect the correlation beyond the random field (see Eqs. (C.6) and (C.7)), and the overall accuracy of the corrosion estimates is not compromised.

Another model aspect that is treated in a simplifying manner is the relation between the variability factors and the model parameters. At present, the variability factors are defined as being the same for all the deterioration model parameters (see Eq. (C.3)), e.g. the variability factor per compartment α_{i_2} is the same for all parameters $\theta_1, \theta_2, \dots$ in the corrosion model. For the implementations presented here, this has no effect, as the linear corrosion rate is the only parameter. When extending this to models with multiple parameters, the spatial variability of all parameters will not be generally the same. The extension of the model is straightforward, by defining a set of variability factors $\alpha_{i_1,k}, \dots, \alpha_{i_5,k}$ per model parameter θ_k , $k = 1, \dots, n_p$. However, the implementation will be feasible only if sufficient data is available to learn the

additional parameters. Otherwise the statistical uncertainty will outweigh the benefit of having a more flexible model.

The proposed approach hinges upon the systematic availability of large amounts of data from in-service inspections. These are – in principle – available at owners and classification societies. However, efforts are needed to bring the data to a format that is needed to make them accessible. We are convinced that such efforts will pay off in the long run, as the models for estimating corrosion will continuously improve with the inclusion of more data. The Bayesian approach offers the necessary flexibility for this, and the associated computational challenges can – as demonstrated in this paper – be handled well. The improved models will enable a much more targeted scheduling of inspections and maintenance activities.

C.5 Conclusions

A spatio-temporal probabilistic model based on a hierarchical approach is developed for analyzing the dependence of the corrosion process at different locations in a ship structure using data from inspection campaigns. The deterioration model parameters are modeled as separate random variables for each plate element. The dependence of the deterioration process among different locations is modeled by a hierarchical structure, whereby plate elements are grouped according to their structural element type, and the frame, compartment and vessel they belong to. These hierarchical levels are related through common factors and conditions that affect the corrosion process. The model can be used to estimate multiple parameters of the deterioration process (such as corrosion rate and coating life) based on thickness measurements. The flexibility of the model allows changing the levels in the hierarchy, the corrosion type (e.g. general or pitting corrosion), the model type (e.g. linear or nonlinear), and additional relevant variables to be estimated (e.g. thickness margin). With the hierarchical Bayesian model, it is possible to identify current locations with high corrosion rates, areas with ineffective coatings, and to estimate which points are more likely to have problems in future years. During the last years, Classification Societies and the International Maritime Organization have worked on incorporating risk-based methods into rules and regulations. The proposed hierarchical Bayesian model serves as a step towards achieving this goal.

8 Paper D

Risk-based optimal inspection strategies for structural systems using dynamic Bayesian networks

Jesus Luque & Daniel Straub

Engineering Risk Analysis Group, Technische Universität München (jesus.luque@tum.de, straub@tum.de, www.era.bgu.tum.de)

Abstract

In most structural systems, it is neither possible nor optimal to inspect all system components regularly. An optimal inspection-repair strategy controls deterioration in structural systems efficiently with limited cost and acceptable reliability. At present, an integral risk-based optimization procedure for entire structural systems is not available; existing risk-based inspection methods are limited to optimizing inspections component by component. The challenges to an integral approach lie in the large number of optimization parameters in the inspection-repair process of a structural system, and the need to perform probabilistic inference for the entire system at once to address interdependencies among all components. In this paper, we outline a methodology for an integral risk-based optimization of inspections in structural systems, which utilizes a heuristic approach to formulating the optimization problem. It takes basis in a recently developed dynamic Bayesian network (DBN) framework for rapid computation of the system reliability conditional on inspection results. The optimization problem is solved by nesting the DBN inside a Monte-Carlo simulation for computing the expected cost associated with a system-wide inspection strategy. The proposed methodology is applied to a structural system subject to fatigue deterioration and it is demonstrated that it enables an integral risk-based inspection planning for structural systems.

Keywords

Deterioration; inspection planning; reliability; Bayesian networks; optimization

D.1 Introduction

Deterioration processes in engineering structures lead to a reduction of service life and can affect the safety of the structures. Accurate modeling of deterioration remains a challenge today, due to the complexity of the processes and their inherent uncertainties. To address explicitly the prediction uncertainties, probabilistic approaches are suitable for deterioration modeling in an engineering context (Lin and Yang 1985, Ellingwood and Mori 1993, Melchers 1999, Qin and Cui 2003, Melchers and Jeffrey 2007, Kumar et al. 2015).

To reduce the uncertainty in deterioration processes, regular inspections are common practice for most engineering structures. An optimal inspection strategy balances the cost of inspections with the achieved risk reduction. An inspection strategy defines (Faber 2002): (a) what to inspect for (e.g., thickness diminution due to corrosion or erosion, fatigue cracks), (b) how to inspect (the inspection technique), (c) when to inspect, and (d) where to inspect (which components). Each combination of these factors defines an inspection strategy, among which the optimal one is sought.

Methods for risk-based optimization of inspections on structural systems have been developed during the past 40 years (Yang and Trapp 1974, 1975, Thoft-Christensen and Sørensen 1987, Madsen et al. 1989, Sørensen et al. 1991, Straub and Faber 2005, Straub and Faber 2006, Nielsen and Sørensen 2015). The scientific literature also documents industrial applications of inspection planning on offshore structures, aircrafts, bridges or ships (e.g., Skjong and Torhaug 1991, Pedersen et al. 1992, Faber et al. 1992b, Lotsberg et al. 2000, Faber et al. 2005, Moan 2005, Dong and Frangopol 2015). The theory and the applications have focused almost exclusively on the optimization at the component level, with a simplified treatment of the system (Straub and Faber 2005). Only limited research efforts have been directed towards optimization procedures for entire systems, accounting for the statistical dependence among the deterioration states of individual structural details (Straub and Faber 2004a, Straub and Faber 2005, Straub et al. 2009, Papakonstantinou and Shinozuka 2014, Memarzadeh and Pozzi 2015).

Risk-based optimization of inspection-repair strategies for large engineering systems is challenging in practice. Firstly, the interdependence among stochastic deterioration processes for all the system components must be modeled. The two common approaches to such an integral probabilistic deterioration modeling are random fields (Guedes Soares and Garbatov 1998, Vrouwenvelder 2004, Stewart and Mullard 2007, Ying and Vrouwenvelder 2007, Keßler et al. 2014) and hierarchical models (e.g. Maes and Dann 2007, Maes et al. 2008, Qin and Faber 2012, Banerjee et al. 2015, Luque et al. 2017). Secondly, Bayesian updating is required for

computing the probability of failure of all components and the system conditional on a potentially large number of inspection results. This is a computationally challenging problem in itself (e.g. Schneider et al. 2017). In the context of inspection planning, these computations must be performed multiple times for the optimization of the inspection strategies. Thirdly, the inspection optimization must consider system-wide strategies, which – in the general case – leads to a number of optimization parameters that is exponentially increasing with the number of components (Straub and Faber 2005).

Bayesian methods enable incorporating information from inspections into probabilistic deterioration models to quantify the reduction in uncertainty and to update the reliability estimate (Tang 1973, Madsen 1987, Moan et al. 2000, Straub et al. 2016). Bayesian Networks (BNs) can facilitate such analyses. BNs have been applied to engineering risk analysis problems during the last two decades (Torres-Toledano and Sucar 1998, Friis-Hansen 2001, Mahadevan et al. 2001, Faber et al. 2002, Grêt-Regamey and Straub 2006, Nielsen and Sørensen 2010, Fenton and Neil 2012, Weber et al. 2012, Bensi et al. 2013). Conditional independence among model parameters encoded in the graphical structure of the BN can facilitate the Bayesian updating. In addition, if a process can be represented by discrete random variables (e.g. by discretizing all continuous random variables), exact inference algorithms can provide fast and robust solutions to the Bayesian updating. These properties have been exploited in Straub (2009) and Luque and Straub (2016), where dynamic Bayesian networks (DBNs) are utilized to evaluate deterioration at the component and system level. Bespoke exact inference algorithms ensure rapid computation of the conditional probability of system failure given all inspection results, which is essential for solving the optimal inspection problem.

In this paper, we propose a heuristic approach to finding the optimal inspection strategy in structural systems. In contrast to existing methods, the approach can simultaneously account for system effects arising from (a) the dependence among the deterioration at different components, (b) the joint effect of deterioration at multiple components on the system reliability, and (c) the interaction among inspection costs, i.e. the reduction in the marginal cost of an inspection if these are grouped in larger inspection campaigns. This is achieved with the proposed heuristic approach to the optimization, which enables the definition of a system-wide inspection plan with just a few parameters. The optimization criterion is the total expected life-cycle cost, whose computation is made feasible by a novel two-level approach, in which the system DBN algorithm of Luque and Straub (2016) is nested within a Monte-Carlo simulation that addresses the uncertainty on the inspection outcomes. The DBN algorithm allows to compute the conditional probability of system failure given inspection outcomes.

The proposed methodology is demonstrated and investigated by application to a Daniels system, an idealized redundant structural system, whose components are subject to fatigue deterioration.

D.2 Methodology

D.2.1 The inspection optimization problem

An inspection strategy for a structural system defines when, where, what and how to inspect. In general, static inspection regimes are not optimal; instead, one should account for results from previous inspections and maintenance activities when deciding upon new inspections. For this reason, the optimal inspection-planning problem belongs to the class of sequential decision problems (Arrow et al. 1949; Kochenderfer 2015).

The sequential inspection planning problem is visualized in the decision tree of Figure D.1. Branches following a circular node represent random outcomes (e.g. the deterioration state of the system, or the inspection outcomes) and branches after a square node represent possible decision alternatives (e.g. if and where to inspect or repair). This decision tree is equally applicable to single components or entire systems. When considering systems, the outcome space of the random variables and the number of decision alternatives increase exponentially with the number of components. This is one of the main reasons why previous work on risk-based inspection planning has focused mainly on individual components.

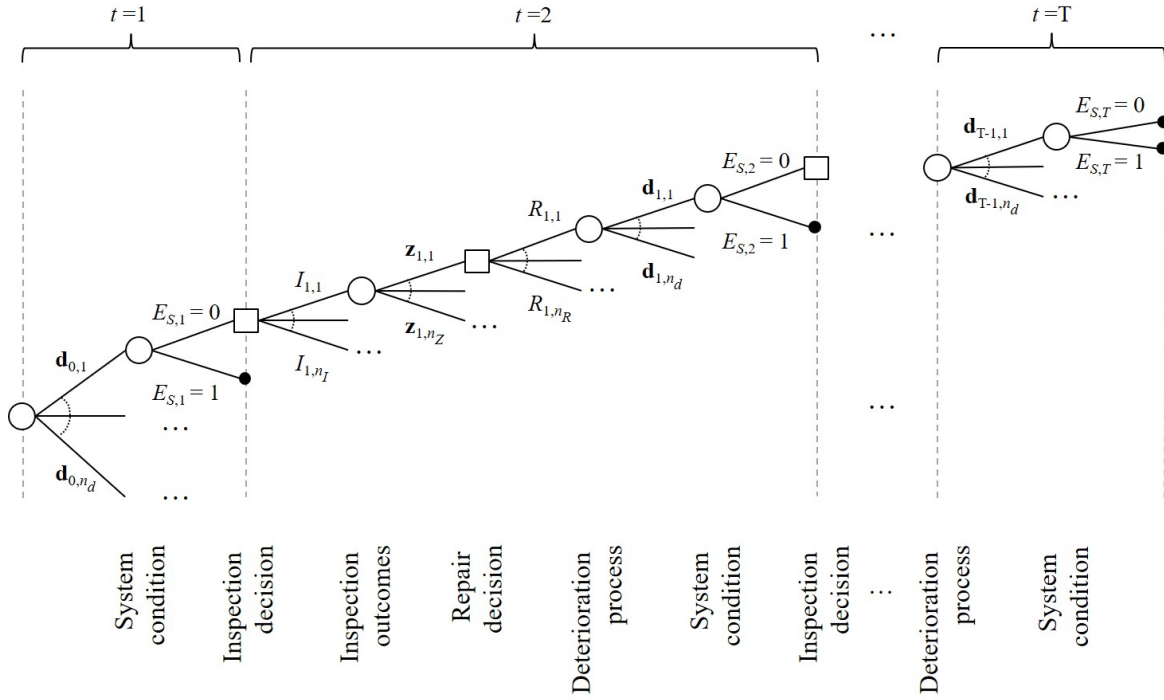


Figure D.1. Example of a decision tree with deterioration vector $\mathbf{D}_{t,i}$ for all system components, the system performance $E_{s,t}$ (0: safe, 1: fail), inspection and repair decisions at each time step $t = 1, \dots, T$, and a set of observations $\mathbf{Z}_{t,i}$ after each inspection decision. A black dot marks the end of a branch, which corresponds to either a system failure or the end of service life.

Solutions to sequential decision problems can be found through the definition of policies. Here, a policy for a decision at time t defines where, what and how to inspect and repair, taking into account the full history of the structure up to t , i.e. past inspection outcomes and repair actions. The set of policies at all times t is the strategy \mathcal{S} . If the policies are the same for all t , the strategy is stationary (Jensen and Nielsen 2007).

For a structural system with N components subject to deterioration, the inspection optimization problem of Figure D.1 can be formalized as follows. The joint deterioration state \mathbf{D} of all components is represented through a probabilistic system deterioration model with random parameters \mathbf{X}_D . Each component can be inspected and/or repaired at discrete times t from 0 to the end of service life T . The strategy \mathcal{S} defines for each component at each time step if and how that component is inspected and repaired, based on all previous inspection outcomes \mathbf{Z} and the repair history of the structure.

Inspections, repairs and system failure are associated with consequences. These are quantified by the present value of total life-cycle cost C_T in function of the strategy \mathcal{S} and the inspection outcomes \mathbf{Z} . It is defined as the sum of the life-time inspection cost C_I , repair cost C_R , and failure risk R_F :

$$C_T(\mathcal{S}, \mathbf{Z}) = C_I(\mathcal{S}, \mathbf{Z}) + C_R(\mathcal{S}, \mathbf{Z}) + R_F(\mathcal{S}, \mathbf{Z}) \quad (\text{D.1})$$

For a given strategy \mathcal{S} and inspection outcomes \mathbf{Z} , the inspection and repair actions are fixed. Hence, $C_I(\mathcal{S}, \mathbf{Z})$ and $C_R(\mathcal{S}, \mathbf{Z})$ can be directly evaluated in function of the cost of individual inspections and repairs, and the relevant discount rate.

The failure risk R_F is defined as:

$$\begin{aligned} R_F(\mathcal{S}, \mathbf{Z}) &= \sum_{t=1}^T c_F \cdot \gamma(t) \cdot \Pr(F_t | \mathbf{Z}_{0:t-1}) \\ &= c_F \cdot \sum_{t=1}^T \gamma(t) \cdot [\Pr(E_{S,t} = \text{Fail} | \mathbf{Z}_{0:t-1}) - \Pr(E_{S,t-1} = \text{Fail} | \mathbf{Z}_{0:t-1})] \end{aligned} \quad (\text{D.2})$$

where c_F is the undiscounted cost of a system failure event, $\gamma(t)$ is a discount factor, F_t is the event of a system failure during time step t , and $E_{S,t}$ is the system condition at time step t .

The conditional probability $\Pr(E_{S,t} = \text{Fail} | \mathbf{Z}_{0:t-1})$ is the probability of a system failure up to time t for given inspection outcomes $\mathbf{Z}_{0:t-1}$. Its computation is a structural reliability problem, which can be formulated as an integral over all random variables \mathbf{X} of the problem (which include the deterioration parameters \mathbf{X}_D , but also load parameters):

$$\Pr(E_{S,t} = \text{Fail} | \mathbf{Z}_{0:t-1}) = \int_{\Omega_{\mathbf{X}}} I[g_{S,t}(\mathbf{x}) \leq 0] \cdot f_{\mathbf{X} | \mathbf{Z}_{0:t-1}}(\mathbf{x}) \, d\mathbf{x} \quad (\text{D.3})$$

$g_{S,t}(\mathbf{x}) \leq 0$ is the limit state function describing system failure up to t , $I[\cdot]$ is the indicator function and $f_{\mathbf{X} | \mathbf{Z}_{0:t-1}}$ is the conditional probability density function of \mathbf{X} given inspection outcomes $\mathbf{Z}_{0:t-1}$.

The solution of Eq. (D.3) is non-trivial, in particular if the system size and the number of observations are large. First Order Reliability Method- (FORM) and sampling-based solutions to this problem are available (Straub 2011a, Straub et. al 2016, Schneider et al. 2017). In inspection planning, the conditional probability must be evaluated many times, and an efficient and robust solution of Eq. (3) is thus required. For this reason, we apply DBNs to solve Eq. (D.3) following Luque and Straub (2016).

Because the inspection outcomes \mathbf{Z} are random variables themselves and are not known in advance, the total cost is also a random variable. If $f_{\mathbf{Z}}$ is the probability distribution of the vector of inspection outcomes, whose support $\Omega_{\mathbf{Z}(\mathcal{S})}$ depends on the strategy \mathcal{S} , then the expected total life-cycle cost associated with the strategy \mathcal{S} is obtained as

$$E_{\mathbf{Z}}[C_T(\mathcal{S}, \mathbf{Z})] = \int_{\Omega_{\mathbf{Z}(\mathcal{S})}} C_T(\mathcal{S}, \mathbf{z}) f_{\mathbf{Z}}(\mathbf{z}) d\mathbf{z} \quad (\text{D.4})$$

The optimal strategy \mathcal{S}^* is defined as the one that minimizes the expected total cost:

$$\mathcal{S}^* = \arg \min_{\mathcal{S}} E_{\mathbf{Z}}[C_T(\mathcal{S}, \mathbf{Z})] \quad (\text{D.5})$$

This optimization is commonly subject to constraints on the minimum reliability and the maximum budget for inspections.

The two main challenges in finding the optimal strategy through Eq. (D.5) are (a) the large number of possible inspection strategies \mathcal{S} , which increases exponentially with time steps and number of components (Figure D.1), and (b) the expectation operations in Eqs. (D.3) and (D.5). These challenges are already non-trivial for single components. For this reason, we first review existing approaches at the component level to solve the optimization problem defined by Eq. (D.5) (Section D.2.2), before presenting a solution at the system level (Section D.2.3). The approach employs the DBN framework for computing the conditional probabilities $\Pr(E_{S,t} = \textit{Fail} | \mathbf{Z}_{0:t-1})$, which is summarized in Section D.2.4.

D.2.2 Optimization at the component level

Risk-based optimization of inspection planning for individual components has been studied extensively (e.g. Straub and Faber 2006, Nielsen and Sørensen 2015). In the following, we briefly review the solutions based on influence diagrams, Markov decision processes, and stationary strategies.

D.2.2.1 Influence diagrams

An influence diagram (ID) is an extension of Bayesian networks, which includes decision and utility nodes (Jensen and Nielsen 2007). An example ID is shown in Figure D.2.

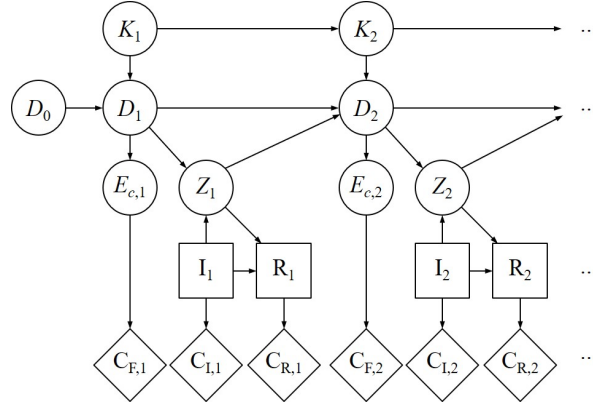


Figure D.2. Example influence diagram for inspection planning of a single component. Circular nodes are random variables, square nodes are decisions and diamond-shaped nodes are costs. Node D_t represents the component deterioration state at time step t as a function of the previous deterioration D_{t-1} and a time-dependent parameter K_t ; $E_{c,t}$ represents the condition (e.g. safe or failed) of the component; Z_t is the inspection outcome; I_t and R_t are the inspection and repair decisions; $C_{F,t}$, $C_{I,t}$, $C_{R,t}$ are the failure, inspection and repair cost nodes.

The ID is a graphical representation of a decision problem, not a solution method. The classical ID is based on the no-forgetting principle, i.e. when making a decision, it is conditional on all previously available information. The solution of such a general ID therefore faces the same exponential complexity as described earlier for the decision tree of Figure D.1. A common approach for approximating the optimal solution is to consider only a subset of the past observations (e.g. the n most recent ones) at each decision step. This approach is known as limited memory influence diagram (LIMID) (Lauritzen and Nilsson 2001, Jensen and Nielsen 2007). A widely-used algorithm to approximate the optimal solution is the single-policy-updating algorithm (Lauritzen and Nilsson 2001). This algorithm considers a strategy \mathcal{S} as (locally) optimal if changing only one its policies (i.e. the set of rules at only one decision node) does not lead to a better strategy in terms of the cost function. This approach has been used to estimate the optimal solution at the component level, e.g. in Nielsen and Sørensen (2011) and Luque and Straub (2013). However, these applications were limited to simplified deterioration models at the component level, because the available optimization algorithms require many evaluations of the expectations in Eqs. (D.3) and (D.5), including the solution of conditional reliability problems.

D.2.2.2 Markov decision processes

If deterioration can be described by a Markov process, the optimal inspection problem can be solved by means of Markov decision processes (MDPs). Markov chains (discrete time Markov processes) have been frequently used for modeling deterioration processes in engineering applications (Rocha and Schuëller 1996, Mishalani and Madanat 2002). Even non-Markovian

processes can be translated into Markov chains by state-space augmentation (Straub 2009). MDPs have been proposed and applied by a series of authors for obtaining the optimal strategy of engineering components or systems described by simple deterioration models (Tao et al. 1995, Robelin and Madanat 2007).

One distinguishes between fully and partially observable decision processes, depending on the type of available information. If all parameters of the deterioration process are directly observable, the process is fully observable. This is applicable only to simple, typically empirical deterioration models. In reality, the full deterioration process is observable only indirectly or incompletely; partially observable Markov decision processes (POMDPs) are then applied. The model of Figure D.2 is a POMDP, in which the state of the component is represented by the three random variables K_t , D_t and $E_{C,t}$ and Z_t is the (potential) inspection outcome. The partial observability implies that not only Z_t , but all past inspection outcomes Z_1, \dots, Z_{t-1} have an effect on the probability distribution of K_t , D_t and $E_{C,t}$. For this reason, the POMDP is solved by introducing a so-called belief state, which represents the knowledge of the decision maker at each point in time, summarizing the past inspection history (Kochenderfer 2015).

POMDPs have been used to find the optimal strategy at the component level (Nielsen and Sørensen 2015, Schöbi and Chatzi 2016) and at the system level (Papakonstantinou and Shinozuka 2014, Memarzadeh and Pozzi 2015), but their application to larger systems is still computationally challenging. In addition, a main limitation of these approaches for their application to structural systems as considered in this paper is that they cannot handle problems in which the costs at the system level are a non-linear function of the costs at the component level. This is however the case when the failure of the system is described by a structural model in function of component states.

D.2.2.3 Heuristic strategies

The most common approach to risk-based inspection planning for components consists of limiting the set of possible strategies \mathcal{S} to a small number of parametrized stationary strategies, based on simple heuristics. The two most commonly applied heuristics are briefly summarized in the following.

Probability threshold: The stationary strategy is specified by a threshold on the probability of component failure p_{th} . An inspection is required in any time step before the probability of failure (conditional on previous inspection results) exceeds p_{th} , as illustrated in Figure D.3.

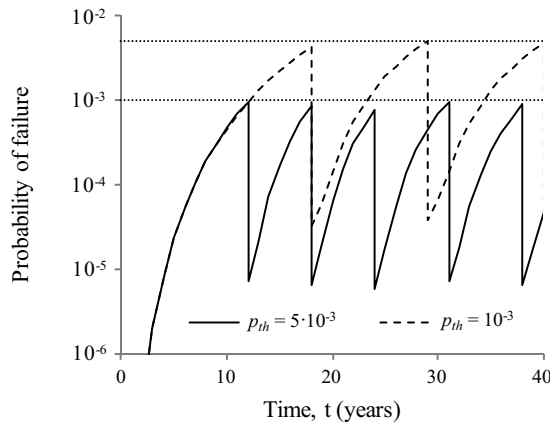


Figure D.3. Probability of failure of a structural element using the probability threshold heuristic with $p_{th} = 10^{-3}$ and $p_{th} = 5 \cdot 10^{-3}$. An inspection is performed prior to exceeding the threshold. The probability of failure shown here is conditional on not having identified any defect in past inspections.

Fixed-interval (periodic) inspections: Inspections are performed at fixed regular intervals Δt_I , e.g. inspections every ten years (Figure D.4). This approach is commonly used in practice because it is easier to incorporate into the overall asset integrity management of a structure.

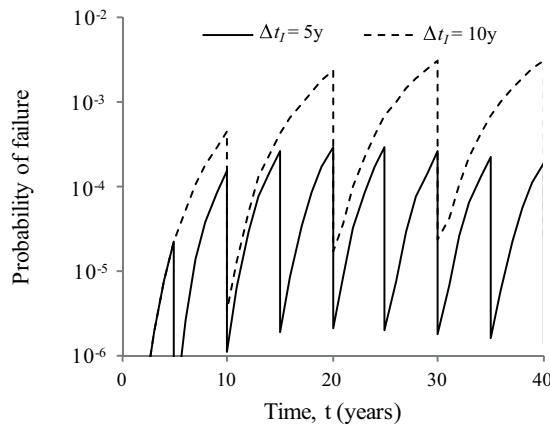


Figure D.4. Probability of failure of a structural element using periodic inspections every 5 and 10 years. The probability of failure shown here is conditional on not having identified any defect in past inspections.

In both heuristics, the repair policy can be fixed in advance. In most applications, it is required that any identified damage is immediately repaired. In this case, the optimization of Eq. (D.5) reduces to finding either the optimal value of p_{th} or the optimal interval between inspections Δt_I . Alternatively, it is also possible to add a parameter for the repair criterion, in which case two optimization parameters have to be considered (Nielsen and Sørensen 2014). By assuming that a repaired component performs like a new component, it is possible to reduce the number

of evaluations of the conditional probability of failure of Eq. (D.3), following Straub and Faber (2006).

It has been demonstrated that heuristic approaches give a good approximation of the optimal solution in risk-based inspection planning, with orders of magnitude less computation effort than other approaches like LIMIDs or POMDPs (Nielsen and Sørensen 2011, Luque and Straub 2013). Figure D.5 shows a comparison between the optimal inspection strategy of a single component using LIMIDs and heuristic approaches (periodic inspections and probability threshold) from a theoretical example investigated in Luque and Straub (2013). The expected inspection, repair, and failure costs of the optimal solutions are compared in Figure D.6.

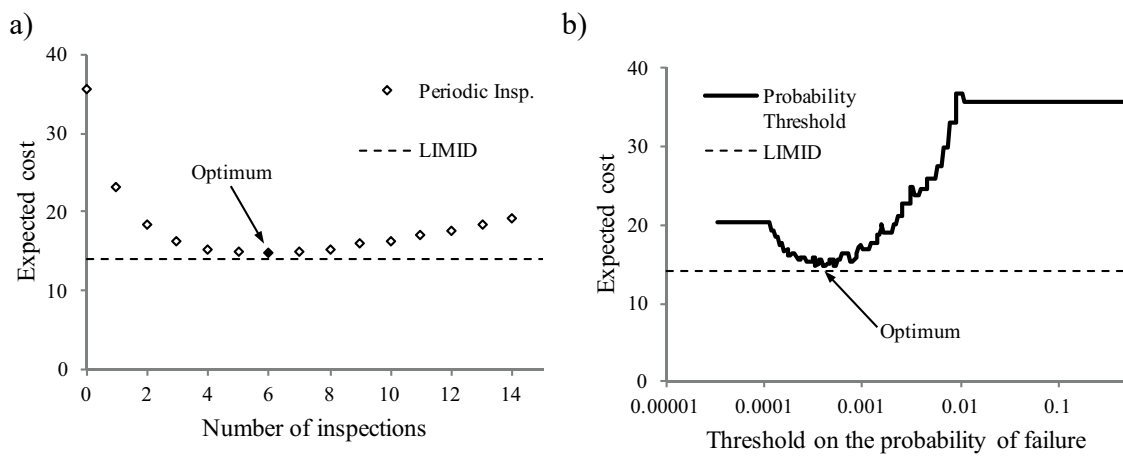


Figure D.5. Comparison between a) the LIMID solution and the Periodic Inspection heuristic; and b) the LIMID solution and the Probability Threshold heuristic (Luque and Straub 2013).

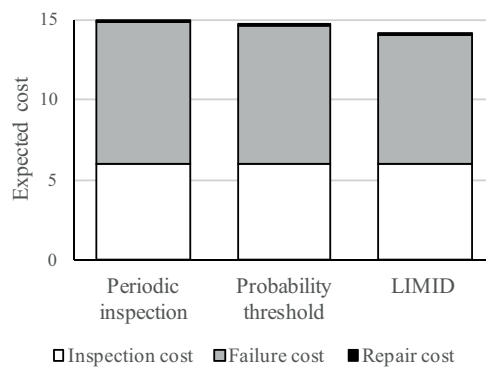


Figure D.6. Expected costs associated with the optimal strategies by periodic inspection, probability threshold, and LIMID approaches obtained at the component level (Luque and Straub 2013)

D.2.3 Optimization at the system level

The identification of the optimal inspection strategy is significantly more challenging for structural systems than for individual components. The number of possible inspection strategies \mathcal{S} in Eq. (D.5) increases exponentially with the number of components, and the computation of the conditional reliabilities in Eq. (D.3) are much more demanding. This is because inspection results and deterioration failure events from the entire structure must be considered in a single integral computation. Given the difficulties one encounters already in solving the optimization problem at the component level, it appears that heuristics are the most promising, if not the only practically feasible, approach to optimizing inspections at the system level. In the following Section D.2.3.1, we present such a heuristic for the system-level inspection planning.

Even with a heuristic approach to defining inspection-repair strategies, to solve the optimization problem at the system level necessitates a computationally efficient and robust algorithm for computing conditional probabilities of failure (Eq. (D.3)). The DBN framework developed in Luque and Straub (2016) provides such an algorithm; it is presented in Section D.2.4.

D.2.3.1 Heuristic strategy at the system level

At the system level, identifying heuristics is less straightforward than at the component level, mainly because it is not only necessary to identify the timing, but also the locations of inspections (Straub and Faber 2005). Nevertheless, we find that the heuristics applied at the component level can be extended to the system level. Our proposed heuristic takes into account that it is typically cheaper to bundle component inspections in campaigns and that regular inspection intervals are preferred for organizational purposes.

The proposed heuristic distinguishes between inspection campaigns (when to inspect?) and individual inspections (where to inspect?). It can be summarized as follows:

1. Inspection campaigns are performed at regular time intervals, in analogy to the fixed-interval heuristic for single components. The time between regular campaigns is Δt_I .
2. The initial number of inspected components during each inspection campaign is fixed at n_I .
3. The components to inspect during a campaign are determined based on the value of information (VoI) (Raiffa and Schlaifer 1961) associated with the component inspection, following the idea of Straub and Faber (2005). Exact computation of the VoI is difficult, hence a proxy must be identified that provides a similar ranking than the VoI. This is further elaborated for the specific structural system considered in Section D.3.4.

4. Whenever the updated system probability of failure exceeds a threshold value p_{th} , additional inspections must be carried out, either within the existing campaign or through an additional inspection campaign.
5. Repairs are performed according to a fixed repair criterion, e.g., any identified defect with a size larger than d_R is repaired.

Adjustments to these rules can and should be made according to the operational environment and constraints. In summary, the heuristic strategy \mathcal{S}_k is a combination of the above stationary rules and is defined by the following parameters:

- the frequency of regular inspections Δt_I ,
- the failure probability threshold p_{th} ,
- the number of components to inspect n_I ,
- the repair criterion d_R .

The optimal combination of these parameters is found by solving Eq. (D.5). This requires the computation of the expected cost associated with a strategy $\mathcal{S}_k = (\Delta t_I, p_{th}, n_I, d_R)$.

D.2.3.2 Computation of the expected cost of a strategy

A Monte Carlo approach is employed to estimate the total expected life-cycle cost of a strategy \mathcal{S}_k defined according to Eq. (D.4). The expected value is approximated as

$$E_{\mathbf{Z}}[C_T(\mathcal{S}_k, \mathbf{Z})] \approx \frac{1}{n_s} \sum_{j=1}^{n_s} C_T(\mathcal{S}_k, \mathbf{z}_{k,j}) \quad (\text{D.6})$$

where $\{\mathbf{z}_{k,1}, \mathbf{z}_{k,2}, \dots, \mathbf{z}_{k,n_s}\}$ are Monte Carlo samples of inspection outcomes, and n_s is the number of samples. To obtain these samples, one first generates random samples of the deterioration history of the entire structure, and then generates random inspection results conditional on these deterioration histories. The total cost C_T is computed according to Eq. (D.1).

The number of samples n_s required to ensure sufficient accuracy is a function of the coefficient of variation of the total cost δ_{C_T} . To ensure a relative error in the estimate of less than ε with a confidence of $1 - \alpha$, the required number of samples is

$$n_s \geq \left[\frac{\Phi^{-1}\left(\frac{\alpha}{2}\right)}{\varepsilon} \delta_{C_T} \right]^2 \quad (\text{D.7})$$

In all cases we investigated, the value of δ_{C_T} was around 1.5. If one requires a relative error less than 10% (i.e. $\varepsilon = 0.1$) with a confidence of 95% (i.e. $\alpha = 0.05$), the required number of samples is $n_s \geq 384\delta_{C_T}^2 = 864$. Typically, the requirements on the accuracy of the estimated total expected life-cycle cost are not as strict, and a number of samples in the order of 200 is expected to be sufficient for most practical applications. Note that the reason for this relatively small number lies in the fact that the conditional probability of failure is computed within each MC sample through the DBN.

D.2.4 DBN framework

A key element in the proposed procedure is an efficient computation of the updated probabilities of failure at the component and the system level given inspection results, i.e. a fast solution to Eq. (D.3). At the component level, Straub (2009) developed a DBN framework for stochastically modeling deterioration processes and updating the failure probability, which was shown to be efficient and robust. In contrast to other Bayesian analysis methods, the DBN combined with exact inference algorithms has the advantage that its performance does not deteriorate with increasing amount of inspection data. Recently, Luque and Straub (2016) extended this framework to the system level through a hierarchical definition of the deterioration model parameters. Its main characteristics are summarized in the following.

The framework developed in Straub (2009) enables translating commonly employed probabilistic deterioration models into a DBN. The probability of failure conditional on inspection results is computed by an adaptation of general purpose inference algorithms for DBNs (Murphy 2002). The approach requires a discretization of continuous random variables, but very good accuracy can be achieved for standard deterioration models (Straub 2009). Other researchers have implemented this framework at the component level (e.g. Nielsen and Sørensen 2010, Zhu and Collette 2015).

The framework by Luque and Straub (2016) extends the DBN to the structural system level, accounting for dependence among deterioration parameters of different components through a hierarchical approach. To model the correlation structure among the deterioration parameters, a set of hyperparameters α is included in the DBN model. These hyperparameters are the link among time-independent parameters θ (e.g. material properties), time-dependent parameters ω (e.g. temperature), and deterioration state \mathbf{D} in all components (Figure D.7). Through the hyperparameters, any inspection result \mathbf{Z} at a component will affect the reliability estimates of

the other components. The system reliability is evaluated through the binary nodes $E_{S,t}$ (with $E_{S,t} = fail$ representing system failure at time t), in function of the component conditions $E_{C,i,t}$. In the DBN model of Figure D.7 there are no links from $E_{S,t}$ to $E_{S,t+1}$. This is an approximation, because a structure that has failed at time t ($E_{S,t} = Fail$) will also be in a failed state in year $t + 1$ ($E_{S,t+1} = Fail$). The probability $\Pr(E_{S,t+1} = Fail)$ computed with the DBN of Figure D.7 without these links is therefore an underestimation of the true probability of failure. However, introducing this link would significantly increase computational costs of the DBN. The approximation error is small if the dominant contribution to the probability of system failure is from the deterioration. This must be checked for a specific application. Alternatively, an upper bound to the probability of failure can be obtained from the DBN by considering the failure events in different time steps as independent events; this upper bound has been used frequently in the literature, e.g. (Val et al. 2000).

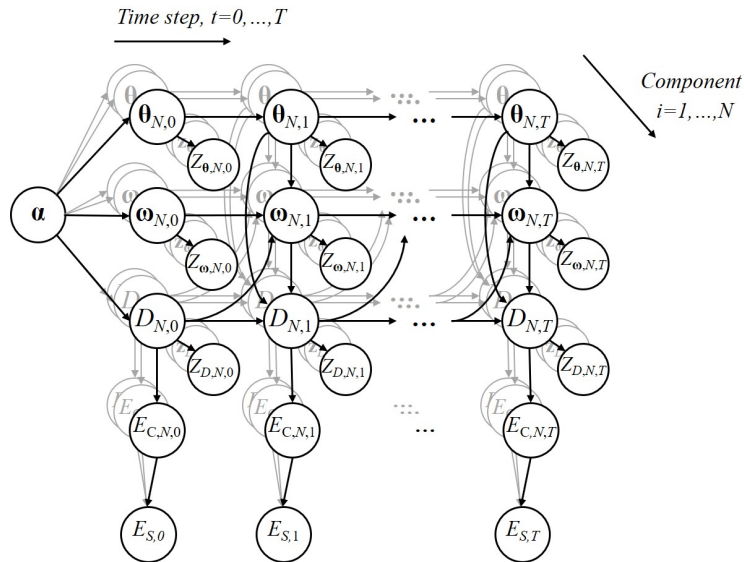


Figure D.7. Hierarchical DBN system deterioration model (Luque and Straub, 2016). Node $D_{i,t}$ represents the deterioration state of the i -th component at time step t as function of the previous deterioration $D_{i,t-1}$, the time-independent parameter $\theta_{i,t}$, and the time-dependent parameter $\omega_{i,t}$; observations $Z_{\theta,i,t}$, $Z_{\omega,i,t}$, and $Z_{D,i,t}$; $E_{C,i,t}$ and $E_{S,t}$ represent the condition (e.g. safe or failed) of the component and the system; α is the set of hyperparameters that links all components.

An exact inference algorithm for solving the hierarchical DBN is available from Luque and Straub (2016). Because of the hierarchical structure of the model, the computation time increases approximately linearly with the number of components. The algorithm also facilitates the use of parallel computation. The following is a short summary of the algorithm, for details on the method, the reader is referred to (Luque and Straub 2016).

In a first step of the algorithm, for all components the joint probability distribution of component i is updated with inspection results from component i , for given hyperparameter values α . In the hierarchical DBN, the deterioration states are statistically independent among components for fixed hyperparameters, i.e.

$$p(d_{i_1,t}, d_{i_2,t} | \alpha) = p(d_{i_1,t} | \alpha) \cdot p(d_{i_2,t} | \alpha) \quad (\text{D.8})$$

for all components $i_1, i_2 = 1, \dots, N$ with $i_1 \neq i_2$. This independence property can be exploited to parallelize the computations of the conditional probabilities given inspection results for individual components in the first step.

In the second step, the joint distribution of the hyperparameters α is updated with the inspection results from all components. Finally, the results of the first and the second step are combined to obtain the probability distributions of all components i conditional on all inspection results in the system.

To speed up computation, it is possible to partly reuse updated probability distributions. If the sampled inspection results for a component i are identical among two samples j_1 and j_2 , the first step in the computation can be avoided, and the previously computed probabilities can be utilized. Additionally, for time steps t prior to the first inspection campaign, the system reliability will be identical among all samples j and has to be calculated only once. Further computational savings may be possible for specific cases, e.g. if components have the same deterioration model.

D.2.5 Summary of the proposed methodology

The proposed procedure for integral optimization of inspections in a structural system consists of the following steps:

1. Define system-wide inspection strategies \mathcal{S}_k through the heuristic of Section D.2.3.1, with optimization parameters Δt_I , p_{th} , n_I , and d_R . Alter the proposed heuristic if necessary to account for operational constraints.
2. Choose an optimization algorithm to identify the solution of Eq. (D.5). The algorithm must be able to handle numerical noise, because the objective function is evaluated with MCS. Perform steps 3–5 to determine the expected total cost associated with a strategy.
3. For every strategy \mathcal{S}_k (i.e. combination of optimization parameter values), generate n_s Monte Carlo samples of inspection outcomes \mathbf{z}_{kj} , where $j = 1, \dots, n_s$. These define the

times and locations of inspections and their outcomes. n_s must be chosen sufficiently high (see Eq. (D.7)).

4. For every strategy \mathcal{S}_k and inspection sample \mathbf{z}_{kj} :
 - a. Compute the conditional probabilities of system failure over the service life (Eq. (D.3)) by means of the DBN.
 - b. Compute the failure risk (Eq. (D.2)).
 - c. Compute the total cost (Eq. (D.1)).
5. Estimate the total expected life-cycle cost of each strategy \mathcal{S}_k by means of Eq. (D.6).

The procedure deals with the two main challenges outlined in the last paragraph of Section 2.1 by (a) extending the heuristic approach from the component level to the system level, through the use of suitable system-wide heuristics, and (b) by computing the expected risk and cost through nesting a DBN computation insight a MCS that integrates over future inspection outcomes.

D.3 Numerical investigations

The proposed methodology is applied to optimize the inspection-repair strategy of a Daniels system subject to fatigue deterioration. This system facilitates the numerical investigation of the effect of system wide inspection strategies.

D.3.1 System definition

A Daniels system consists of a set of N load-sharing elements with independent and identically distributed random capacities R_i , $i = 1, \dots, N$, and an external random load L (Daniels 1945). The system is illustrated in Figure D.8 and its parameters are summarized in Table D.1. The Daniels system facilitates studying the characteristics of load-sharing among the elements in redundant structural systems (Gollwitzer and Rackwitz 1990).

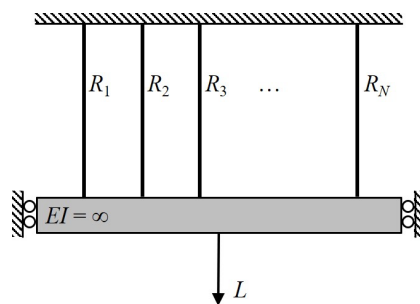


Figure D.8. Daniels system with N elements.

Table D.1. Parameters of the Daniels system, following Luque and Straub (2016).

Parameter	Type	Mean	Std. deviation	Correlation
L	Lognormal	μ_L	$\sigma_L = 0.25 \cdot \mu_L$	
R_i	Normal	μ_{R_i}	$\sigma_{R_i} = 0.15 \cdot \mu_{R_i}$	0
N	Deterministic	10		
Mean safety factor	Deterministic	$N \cdot \mu_{R_i} / \mu_L = 2.9$		

The examples presented in this paper are for a system of $N = 10$ components.

In this study, the components of the Daniel system are affected by fatigue deterioration (Section D.3.2). At the system level, this deterioration is represented by a binary model, in which the component i either has its full capacity (prior to fatigue failure) or zero capacity (after fatigue failure). We neglect any interaction between the extreme load L and the fatigue deterioration.

Because of the exchangeability of components in the Daniels system, the system reliability is a function only of the number of components that have failed because of fatigue, $N_{f,N,t}$. The conditional system failure probability $\Pr(E_{S,t} = fail | N_{f,N,t} = n)$ is presented in (Luque and Straub 2016).

D.3.2 Deterioration and inspection model

All components of the Daniels system are affected by a fatigue deterioration process D . Based on the case study presented in Straub (2009) and Luque and Straub (2016), a simple fracture-mechanics based fatigue model is used to describe the crack depth D_i at component i of the Daniels system at time t :

$$\frac{dD_i(t)}{dt} = \nu C_i \left[\Delta S_{e,i} \sqrt{\pi D_i(t)} \right]^{M_i} \quad (D.9)$$

where ν is the stress cycle rate; $\Delta S_{e,i} = \left(E[\Delta S_i^{M_i}] \right)^{\frac{1}{M_i}}$ is the equivalent stress range per cycle with $E[\cdot]$ being the expectation operator and ΔS_i the stress range per cycle, and C_i, M_i are material parameters.

With $D_{i,0}$ being the initial crack depth of component i at time $t = 0$, an analytical expression for the crack depth at time t is found from Eq. (D.9):

$$D_i(t) = \left[\left(1 - \frac{M_i}{2} \right) C_i \Delta S_{e,i}^{M_i} \pi^{M_i/2} \nu t + D_{i,0}^{1-M_i/2} \right]^{(1-M_i/2)^{-1}} \quad (D.10)$$

The service life of the structure is discretized in $t = 0, 1, 2, \dots, T$ time steps.

To represent dependence of the deterioration process among components, a set of hyperparameters $\alpha = \{\alpha_M, \alpha_K, \alpha_D\}$ is used to link material parameters, stress parameters, and initial crack depths. More details on the definition of the hyperparameters and their application in the DBN model can be found in Luque and Straub (2016).

The component condition at each time step, $E_{C,i,t}$, is either safe or fail. A safe component has its full capacity, whereas a failed component has zero remaining capacity. The failure event is defined through a critical crack depth d_c as $\{E_{C,i,t} = fail\} = \{D_{i,t} \geq d_c\}$.

The inspection $Z_{D,i,t}$ of the i -th component at time step t has two possible outcomes: (a) detection, or (b) no detection (of a fatigue crack). The probability of each outcome is a function of the crack depth $D_{i,t}$ and is represented here with an exponential probability of detection (PoD) model with parameter ξ :

$$\Pr(Z_{D,i,t} = 1 | D_{i,t} = d) = \text{PoD}(d) = 1 - \exp\left(-\frac{d}{\xi}\right) \quad (\text{D.11})$$

The deterioration state after the inspection, $D_{i,t}^*$, is a (stochastic) function of the deterioration state $D_{i,t}$ before inspection, the inspection outcome $Z_{D,i,t}$, and the repair policy. Here, we postulate that all detected cracks are repaired ($d_R = 0$), and the condition of a repaired component is as new. If no crack is found at the inspection, it is simply $D_{i,t}^* = D_{i,t}$.

The parameters and random variables of the hierarchical DBN and deterioration model, the discretization scheme, and the corresponding influence diagram of the DBN model are presented in Table D.2, Table D.3, and Figure D.9. The analysis is performed for an anticipated service life time of $T = 40$ years.

Table D.2. Parameters of the DBN deterioration model, following Luque and Straub (2016).

Parameter	Units	Type	Mean	Std. deviation	Correlation
N	-	Deterministic	10		
T	year	Deterministic	40		
ν	stress cycles per year	Deterministic	$5 \cdot 10^6$		
$\alpha_M, \alpha_D, \alpha_K$	-	Normal	0	1	
$D_{i,0}$	mm	Exponential	1	1	0.5
$M_{i,0}$	-	Normal	3.5	0.3	0.6
$M_{i,t}$	-	Function		$M_{i,t} = M_{i,t-1}$	
$\ln C_{i,t}$	corresponding to N and mm	Function		$\ln C_{i,t} = -3.34M_{i,t} - 15.84$	
$\Delta S_{i,t}$	N	Weibull	scale parameter $K_{i,t}$	shape parameter $\lambda = 0.8$	
$\Delta S_{e,i,t}$	N	Function		$\Delta S_{e,i,t} = K_{i,t} \Gamma \left(1 + \frac{M_{i,t}}{\lambda} \right)^{\frac{1}{M_{i,t}}}$	
$K_{i,0}$	N/mm ²	Lognormal	1.6	0.22	0.8
$K_{i,t}$	N/mm ²	Function		$K_{i,t} = K_{i,t-1}$	
d_C	mm	Deterministic	50		
ξ	mm	Deterministic	10		

$\Gamma(\cdot)$: Gamma function

Table D.3. Discretization scheme.

Random variable	Number of states	Final interval boundaries
$\alpha_{D_0}, \alpha_M, \alpha_K$	5	$\Phi^{-1}(0: 0.2: 1)$
D [mm]	80	$0, \exp\{\ln(0.01) : [\ln(50) - \ln(0.01)]/78 : \ln(50)\}, \infty$
M [-]	20	$0, \ln\{\exp(2.2) : [\exp(4.8) - \exp(2.2)]/18 : \exp(4.8)\}, \infty$
K [N/mm ²]	20	$0, \{0.86 : (2.83 - 0.86)/18 : 2.83\}, \infty$

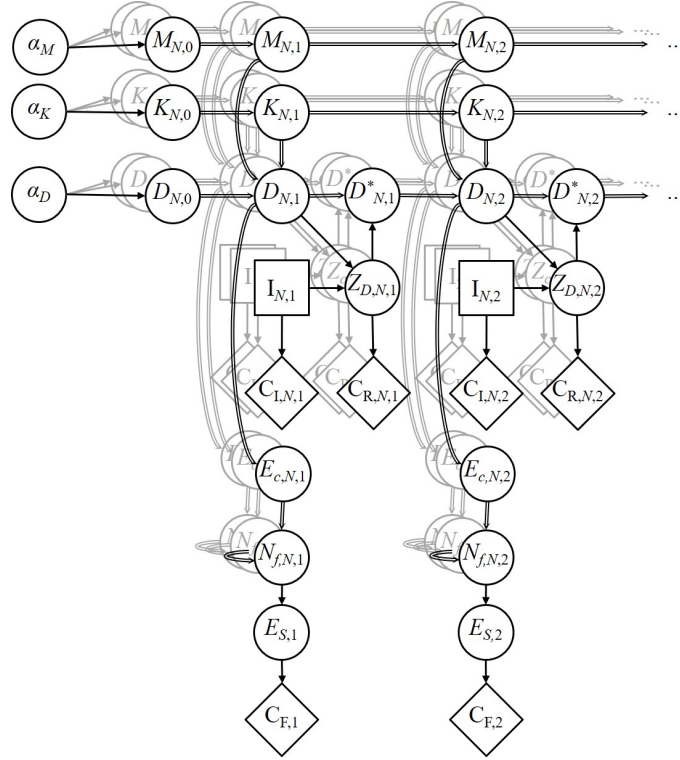


Figure D.9. Influence diagram of the Daniels system. Nodes M , K , and D are the material parameter, the scale parameter of the stress range distribution, and the fatigue crack depth with hyperparameters $\alpha = \{\alpha_M, \alpha_K, \alpha_D\}$. I is the inspection decision, Z_D is the inspection outcome, and D^* the crack depth after a possible repair. E_c , N_f , and E_S are the component condition, the number of failed components, and the system condition. C_I , C_R , and C_F are the inspection, repair, and system failure costs.

The effect of the approximation made by omitting links between $E_{S,t}$ and $E_{S,t+1}$ in the DBN is investigated through a MCS analysis for the unconditional case. We find that the DBN underestimates the probability of failure by a factor of 2, hence the DBN results are adjusted by this factor.

D.3.3 Costs and failure risk

Inspection campaigns have a fixed cost c_c independent of the number of components to be inspected. This is the mobilization cost of personnel and equipment and the cost of interrupting operations. Individual inspections and repairs per component have costs c_I and c_R . The consequences of system failure are represented by the failure cost c_F . All costs in Eqs. (D.1) and (D.2) are discounted to their present value through the following discounting factor based on the real interest rate r (i.e. the interest rate after allowing for inflation):

$$\gamma(t) = \frac{1}{(1+r)^t} \quad (\text{D.12})$$

The ratio of inspection and repair to failure costs can vary significantly among different systems. Two cost cases are considered in this example, summarized in Table D.4. The first case corresponds to a structure with high mobilization costs, such as an offshore structure, and potentially large consequences of failure. The second case corresponds to a case with lower failure costs relative to the inspection campaign, and is motivated by the situation of metallic bridge structures subject to fatigue.

Table D.4. Inspection, repair and failure cost for two different cases.

Cost	Case 1 (offshore structure)	Case 2 (bridge structure)
Inspection campaign, c_C	1	1
Component inspection, c_I	0.1	0.1
Component repair, c_R	0.3	1
System failure, c_F	$3 \cdot 10^4$	10^3
Discount rate, r	0.02	0.02

D.3.4 Optimization

Following Section D.2.3.1, the inspection strategy \mathcal{S}_k is defined through the optimization parameters: Δt_I , the time between regular (i.e. fixed-interval) inspections; p_{th} , the failure probability threshold at which additional inspections are performed; n_I , the pre-defined number of components to inspect during a campaign; d_R , the repair criterion, which is here set to 0.

The optimization is performed through an exhaustive search among a discrete set of parameter values according to Table D.5.

Table D.5. Parameters defining the heuristic strategies.

Parameter	Values
Time between campaigns, Δt_I [year]	{5,10}
PoF threshold, p_{th}	$\{2 \cdot 10^{-5}, 6 \cdot 10^{-5}, 2 \cdot 10^{-4}\}$
Number of inspected components, n_I	{1,2,3, ...,10}
Repair criterion, d_R	0

Following the heuristic, in each campaign the components with the largest VoI are inspected first. Because of the exchangeability of the components in a Daniels system, and because the dependence among all components is the identical (at least a-priori), the VoI is a direct function of the probability of failure (PoF) of the component. A component with a higher PoF has a larger impact on the system reliability; it also has larger uncertainty, hence the learning effect is higher for such a component. Therefore, components are selected for inspection according to

their PoF. Because components are repaired upon detection of a damage, this implies that non-inspected components will be prioritized.

D.3.5 Results

Based on Equation (7), the strategies \mathcal{S}_k are evaluated with $n_s = 1000$ samples to compute the associated total expected life-cycle cost through Eq. (D.4). (As discussed in Section 2.3.2, a smaller number of samples would be sufficient for most practical purposes.) Each sample j corresponds to a possible future inspection history \mathbf{z}_{kj} . To illustrate the workings of the algorithm, results for single inspection histories are presented first, followed by the evaluation and optimization of the total expected cost. In Section D.3.5.3, the results are compared to those obtained with classical component-based inspection planning.

D.3.5.1 Illustrative results for a single inspection sample

A sample inspection outcome \mathbf{z}_{kj} for a strategy \mathcal{S}_k defined by ($\Delta t_I = 10\text{yr}$, $p_T = 2 \cdot 10^{-5}$, $n_I = 3$) is summarized in Table D.6. Figure D.10 presents the component and system failure probabilities associated with this inspection history.

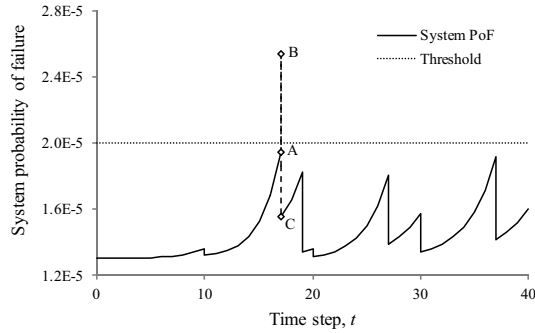
Table D.6. Sample inspection outcome, for a strategy with regular inspections interval $\Delta t_I = 10\text{yr}$, probability threshold $p_T = 2 \cdot 10^{-5}$, and $n_I = 3$ planned component inspections per campaign. Additional inspection campaigns at years 17, 19, 27 and 37 are necessary because of a threshold exceedance. In year 17, two additional component inspections are required during the campaign because of the identified defects.

Component	Time step of inspection						
	10	17*	19*	20	27*	30	37*
1	✓		✓			✓	
2	✓			✓		✓	
3	✓			✓			✓
4		✗					
5		✓		✗			
6		✗					
7		✓*			✓		✓
8		✓*			✓		✓
9			✓		✓		
10			✓			✓	

✓: Inspected without detection of a crack, ✗: Inspected with detection of a crack

* Extraordinary inspection campaign or additional inspected component due to a threshold exceedance

a) System



b) Components

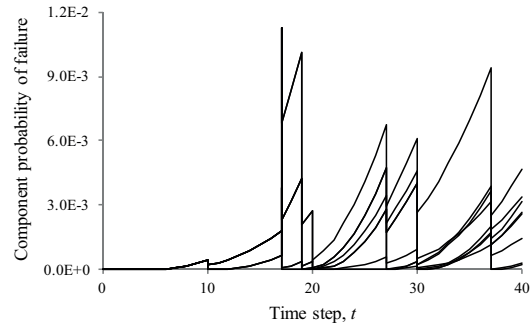


Figure D.10. Probability of failure of the (a) system and (b) individual components conditional on the sample inspection outcome from Table D.6. Point A represents the PoF before the inspection at $t = 17$ yr; B represents the PoF after inspecting the originally planned components (4, 5, and 6); C represents the PoF after inspecting two additional components (7 and 8) to comply with the threshold.

The system PoF associated with all 1000 samples of inspection histories are shown in Figure D.11.

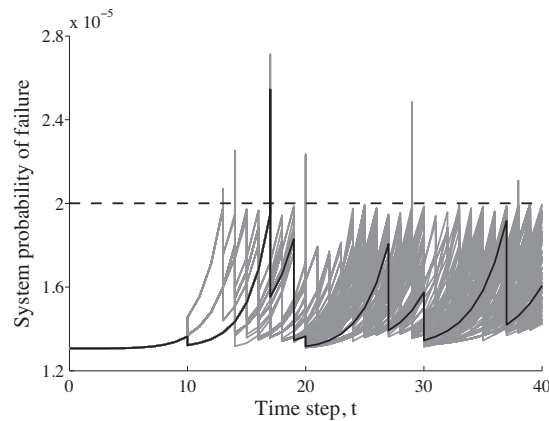


Figure D.11. System probability of failure for all sampled inspection histories. The dark curve corresponds to the outcome defined in Table D.6 and plotted in Figure D.10a.

The total life-cycle cost associated with an inspection history is computed according to Eqs. (1-3). For the inspection history of Table D.6 and cost case 1 (Table D.4), the present value (discounted to $t = 0$) of the costs are $C_I = 4.51 + 1.50 = 6.01$ for the inspection campaign and component inspections, $C_R = 0.63$ for component repairs and $R_F = 0.44$ for failure risk. This amounts to a total present value life-cycle cost of $C_T = 7.08$. The breakdown of these present values over the service life is shown in Figure D.12. This analysis is repeated for all $n_S = 1000$ samples, enabling the MCS estimation of the total expected life-cycle cost following Eq. (D.6).

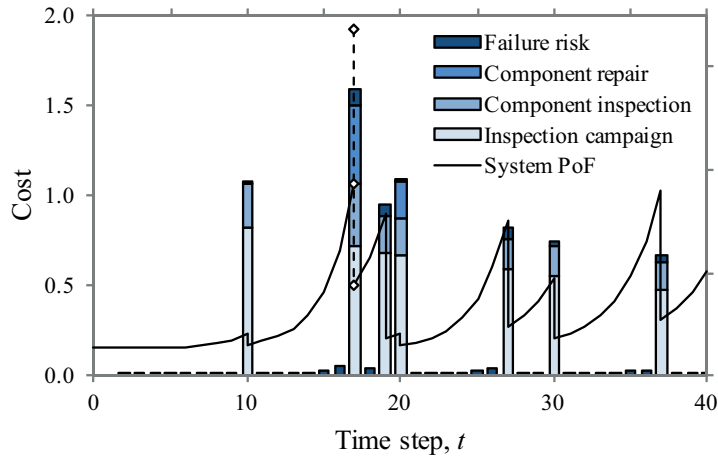


Figure D.12. Expected present values (discounted to $t = 0$) of costs for the inspection outcome from Table D.6. The system PoF from Figure D.10a is included as a reference.

D.3.5.2 Expected costs and optimal inspection strategy

The expected costs of the strategies defined in Table D.5 are shown in Figure D.13 for cost case 1 and Figure D.14 for cost case 2.

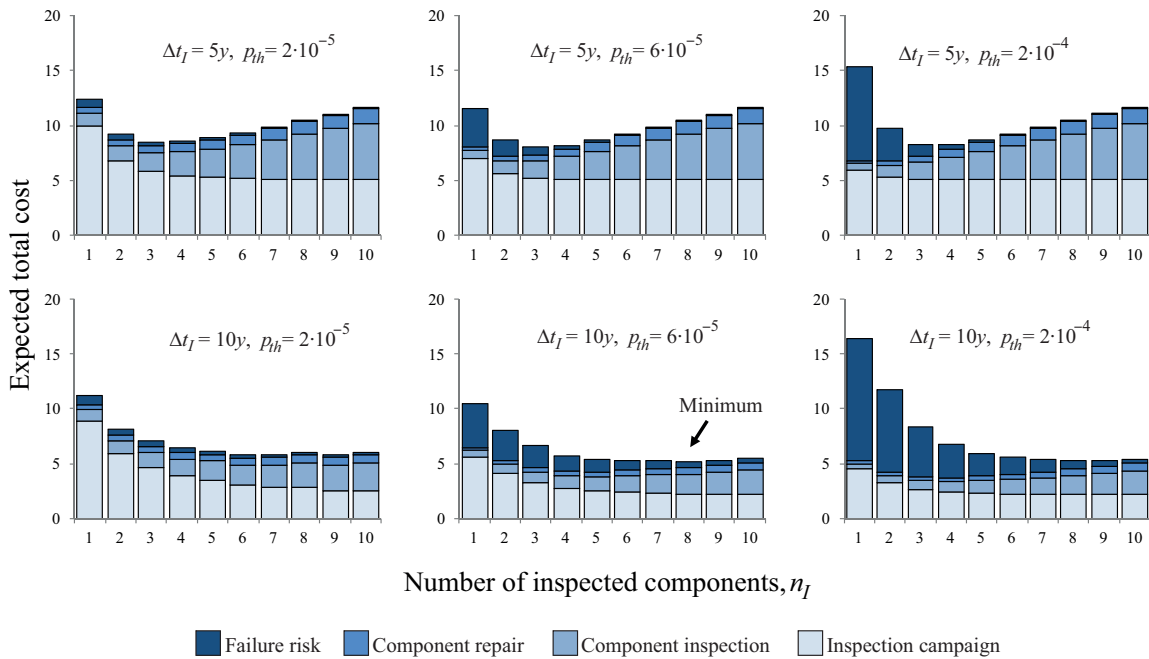


Figure D.13. Comparison of the expected total cost (case 1) varying the number of inspected components n_I , the probability threshold p_{th} , and the regular inspections periodicity Δt_I . The first row corresponds to $\Delta t_I = 5y$ and the second row to $\Delta t_I = 10y$. The columns correspond to the probability thresholds $2 \cdot 10^{-5}$, $6 \cdot 10^{-5}$, and $2 \cdot 10^{-4}$.

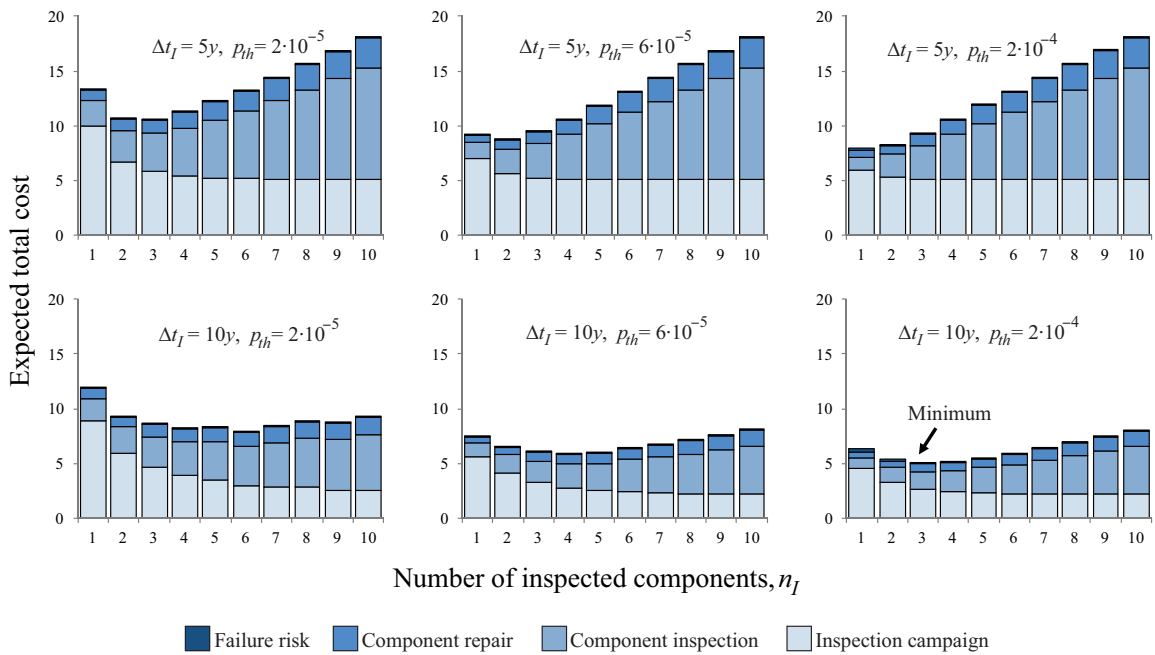


Figure D.14. Comparison of the expected total cost (case 2) varying the number of inspected components n_I , the probability threshold p_{th} , and the regular inspections periodicity Δt_I . The first row corresponds to $\Delta t_I = 5y$ and the second row to $\Delta t_I = 10y$. The columns correspond to the probability thresholds $2 \cdot 10^{-5}$, $6 \cdot 10^{-5}$, and $2 \cdot 10^{-4}$.

Among the strategies presented here, the optimal strategy for cost model 1 is to perform an inspection campaign every 10 years with inspection of 8 elements, following a probability threshold of $6 \cdot 10^{-5}$. For cost model 2, the optimal strategy is to perform an inspection campaign every 10 years with inspection of 3 elements, following a probability threshold of $2 \cdot 10^{-4}$.

D.3.5.3 Comparison to component-based inspection planning

For comparison we show the results of a classical component-based inspection planning for the considered Daniels system. The analysis follows the procedure outlined in Straub and Faber (2006).

Because all components are identical in terms of their probabilistic deterioration model and their effect on the system integrity, the optimal inspection plan will be the same for all components a-priori. Figure D.3 shows the component probability of failure associated with different reliability thresholds and Figure D.4 shows the one associated with periodic inspections.

To estimate the cost of a component failure, one has to account for the effect of a component failure on the system reliability. In risk-based inspection planning, the system redundancy with

respect to failure of component i is typically expressed by the change in the probability of system failure when removing component i (Moan 2005, Faber et al. 2005). This can be measured in terms of the single element importance measure (Straub and Der Kiureghian 2011), which is defined as

$$SEI_i = \Pr(\text{System failure} | \text{fatigue failure of component } i) - \Pr(\text{System failure} | \text{no fatigue failures}) \quad (\text{D.13})$$

For the considered Daniels system, it is $SEI_i = 4.2 \cdot 10^{-5} - 6.5 \cdot 10^{-6} = 3.6 \cdot 10^{-5}$.

When computing the component-based optimal inspection plan with these inputs, the resulting plan is not to perform any inspection. The reason lies in the underestimation of the consequence of a failure in the component-based approach. These are estimated as $C_F \cdot SEI_i$, which with cost model 1 results in a component failure cost of $3 \cdot 10^4 \cdot 3.6 \cdot 10^{-5} = 1.08$, and with cost model 2 in $10^3 \cdot 3.6 \cdot 10^{-5} = 0.036$. With such low failure consequences, inspections are not cost-effective. The problem with the SEI_i measure is that it neglects the possibility of two or more simultaneous component failures. For redundant system this underestimates the true risk, in some cases severely, as shown in (Straub and Der Kiureghian 2011).

Table D.7 presents the comparison of the total expected life-cycle cost associated with not performing any inspection with the cost of the inspection plan obtained by the proposed system RBI planning. Clearly, the component-based approach is not suitable to determine optimal inspection plans for this structural system. It is noted that in practice such a plan would not be implemented and a minimum number of inspections would be performed, based on reliability constraints on the components. Furthermore, an improved redundancy measure (e.g. following Straub and Der Kiureghian 2011) could provide more realistic estimates of the consequences of component failures. Nevertheless, the integral system-based optimization will outperform any purely component-based optimization.

Table D.7. Expected costs associated with the optimal strategies identified with component-based and the proposed system-wide optimization approach, for cost case 1. Note that the system-wide solution is not the global optimum; it is the optimum among the investigated strategies following Table D.5 and Figure D.13.

Optimization algorithm	Component-based	Proposed system-wide
Expected cost for inspections C_I	0	3.56
Expected cost for repairs C_R	0	0.47
Risk R	117.3	1.54
Total expected cost C_T	117.3	5.57

D.4 Discussion

The proposed framework determines optimal inspection-repair strategies for structural systems in an integral manner considering interdependences among component deterioration states and among the information from inspections. It also explicitly includes the interaction between the reliability of components and the structural system. By applying the DBN framework to computing the conditional reliability given inspection results, the method has a computational cost that is suitable for applications in practice.

To manage the complexity of the decision problem underlying the optimal inspection planning, the approach employs heuristics for defining possible system-wide inspection strategies. The heuristic approach results in inspection plans that are likely close to but not identical to the globally optimal plans. Because it is not actually possible to compute the optimal plan even for simple structures such as the Daniels system studied in this paper, there is no reference against which to evaluate goodness of the results. However, the computation of the expected cost for a fixed strategy is accurate (bare the Monte Carlo error and approximations in the deterioration model); it is therefore possible to compare the proposed inspection strategies against any other proposal.

The results also show that – in analogy to the optimization of inspections for components – the total expected life-cycle cost of different inspection strategies is rather flat around the optimum (see Figure D.13 and Figure D.14). For this reason, it is sufficient to restrict the optimization to investigating a discrete set of values of the optimization parameters, taking into account operational constraints.

In practice, inspection planning is commonly performed following a reliability-based rather than risk-based approach, i.e. instead of optimizing the total expected life-cycle cost one aims at minimizing inspection and repair cost while ensuring a minimum level of reliability. The proposed framework is also applicable in this context, by fixing the probability threshold at the system reliability level, and then optimizing the number of inspection campaigns and the number of inspections per campaign. For example, if the minimum reliability is associated with a probability of structural failure of 10^{-5} per year, then the optimum strategies change following Figure D.13 and Figure D.14. The advantage of the proposed approach is also that it correctly computes the system reliability, which component-based inspection planning can get wrong completely (see Section D.3.5.3).

In the numerical investigation presented in this paper, we apply the framework to an idealized structure and an idealized deterioration model, which are chosen for demonstration purposes.

In real-life applications, these models will be more sophisticated, which leads to additional challenges, but does not affect the main findings of this paper. It is rather straightforward to include more sophisticated deterioration models into the DBN, as long as the number of random variables in each time step is limited. This can be achieved in most cases by grouping random variables in the DBN (see Straub 2009 for an example). The extension of the DBN model to more complex structural systems is discussed in (Luque and Straub 2016) and an application of the system RBI framework to such a system is presented in (Bismut et al. 2017).

With respect to the optimization procedure, the presented Daniels system is simplified in that all elements have the same structural importance and the fatigue performance is assumed to be the same for all elements. This allows using a simple proxy for the VoI, because the learning potential is a function of the element probability of failure only. It remains to be investigated what is a good proxy for the VoI in structural systems whose elements have different degrees of importance. The optimization problem presented in this paper is also further complicated when deciding among multiple types of inspection techniques, or when considering structural health monitoring to complement inspections. These aspects are left for future investigation.

D.5 Conclusions

A framework to determine optimal inspection-repair strategies for deteriorating structural systems subject to reliability constraints is proposed. The framework – for the first time – enables a system-wide optimization, which accounts for (a) the interaction among element deterioration states, (b) the relation between the reliability of the structural elements and the structural system, and (c) the effect of information obtained on one element of the structure on the remaining elements and the overall system. The framework also enables the use of state-of-the-art deterioration models for the individual elements. To tackle the computational challenges associated with this complex pre-posterior optimization problem, we propose heuristics for planning inspections, which are informed by practical constraints commonly encountered in the asset integrity management of engineering structures. To compute the expected cost of a system-wide inspection strategy, we nest a dynamic Bayesian network (DBN) algorithm inside a Monte Carlo analysis that accounts for uncertain inspection outcomes. The numerical investigation demonstrates the effectiveness of the proposed framework.

9 Concluding remarks

This chapter discusses the advantages and limitations of the proposed DBN framework and makes some recommendations for implementing it. Then it continues with some suggestions for extending the results of the thesis and ends with the thesis' main conclusion.

9.1 Discussion

Based on the results of the case studies presented in Chapter 4, the main advantages and limitations of the DBN deterioration framework proposed in this thesis are discussed.

Advantages of the framework

Firstly, the DBN framework explicitly considers the spatial and temporal dependence of deterioration processes among multiple locations in the structure. The temporal dependence is modeled using dynamic Bayesian networks and the spatial dependence is represented through hierarchical levels, which allow accounting for the effect of common influencing factors. Such an approach facilitates the representation of complex deterioration processes in the proposed framework and the interpretation of the model parameters when the model is learned.

Secondly, the exact inference algorithm specifically developed for the DBN framework leads to considerably small computation times that are orders of magnitude lower than other approaches, such as MCMC. Although a direct comparison of computation time has only a limited value due to the differences in software used for their implementation, the difference in computational complexity is noticeable. In particular, the performance of MCMC deteriorates when increasing the amount of inspection and monitoring results. This is not the case of the exact inference algorithm, whose complexity is independent of the amount of data used. Additionally, except for the step when the system probability of failure is updated in the model, the inference algorithm has almost linear complexity with respect to the number of components and time steps. Finally, because of the hierarchical definition of the DBN model, it can be run in parallel for each component, significantly decreasing the total computation time.

To handle the complexity of the optimal inspection planning problem, the proposed framework uses a heuristic approach that not only simplifies the solution of the problem, but also makes the framework more applicable to real-life cases because of the easiness to interpret its solution

and relatively fast computation. The heuristic approach defines a set of possible system-wide inspection strategies, which can be easily characterized by a reduced number of parameters that are easy to interpret. Even though the heuristic approach results in inspection plans that are likely close to (but not identical to) the globally optimal plans, it offers a feasible manner to approximate the solution of the RBI problem.

One can also speed up the computation of the optimization methodology through partly reusing updated probability distributions. For example, if the simulated inspection results for a component i are identical among two samples j_1 and j_2 , then the first step of the inference algorithm (i.e. updating each component using only observations from that component) can be avoided, and the previously computed probabilities can be reutilized. Another example is reusing the computed component and system probabilities of failure for time steps before the first inspection campaign is performed, which must be the same for every simulated sample. Further computational savings are also possible for specific cases, e.g. when components have the same deterioration model and the computed results of one can be reused in another one before observations are included.

Finally, one of the main advantages of the proposed risk-based approach is that it correctly computes the system reliability, which component-based inspection planning cannot do. Component-based approaches may produce inspection plans that are far from the real optimal solution (see Section D.3.5.3). The main reason for this is that they neglect the possibility of two or more simultaneous component failures. Improved redundancy measures (e.g. following Straub and Der Kiureghian 2011) could provide more realistic estimates of the consequences of component failures such as considered in Mendoza et al. (2021). Nevertheless, the integral system-based optimization will outperform any purely component-based optimization.

Limitations of the framework

A limitation of the proposed algorithm is the required effort in pre-processing. The choice of the discretization scheme and its implementation lead to an increased effort by the analyst. For this reason, the DBN framework is mainly of use when computations must be performed repetitively, as in the solution of the RBI problem where multiple function evaluations must be performed.

An important consideration is the complexity of the inference algorithm with respect to the size of the discretization scheme (i.e. the number of states generated after discretizing continuous variables). The computational complexity is a linear or quadratic function of the number of

states used for discretizing the random variables. Therefore, the number of random variables that can be included explicitly in the DBN model is limited. While the deterioration models considered in this thesis include less than five random variables, published state-of-the-art models often include more. Nevertheless, the problem is less critical as it may seem at first glance. The number of random variables can often be reduced by combining multiple random variables to a single random variable, as shown in Straub (2009). In addition, in models with many random variables it is often possible to consider some as deterministic with limited loss of accuracy.

Another aspect to take into account when discretizing random variables is the location of the discrete states (i.e. the values from the original variable domain that are used to represent the discrete states). The number and location of the discrete intervals have an impact on the computation time and accuracy of the approximation. There exist several algorithms that obtain the optimal intervals based on a specific estimation, typically the probability of failure. In this thesis heuristic principles to define the discretization scheme are used, which have shown accurate results when compared to other inference algorithms with the original continuous random variables. However, this situation is case dependent and must be checked before applying the methodology outlined here for risk-based inspection planning.

Finally, the DBN model developed in the proposed framework makes a subtle but strong simplification in the consideration of the system condition. As pointed out in Paper D, the node that represents the system condition $E_{S,t}$ has no direct link to its previous or following condition, $E_{S,t-1}$ and $E_{S,t+1}$. Introducing these links would break the independence among components given the hyperparameters, which would significantly increase the computational cost of the inference algorithm. This is an approximation because a structure that has failed at time t should also be in a failed state at time $t + 1$. Therefore, the probability $\Pr(E_{S,t} = Fail)$ computed with the DBN model without these links is therefore an underestimation of the true system probability of failure. The approximation error is small if the dominant contribution to the system probability of failure is from the deterioration (and not from, e.g., external extreme loads), but this must be checked for a specific application. This aspect is discussed in detail in Straub et al. (2020). Alternatively, an upper bound to the probability of failure can be obtained by considering the failure events in different time steps as independent events as shown in Paper D and applied to the case study from Section 4.5.

Practical recommendations:

This section contains suggestions that can be used to better understand and interpret the results of the model when implemented in real-life cases.

In the numerical investigations presented here, the DBN framework is applied to idealized structures and with idealized deterioration models, which are chosen for demonstration purposes. In real-life applications, these models might be more sophisticated, which would lead to additional challenges, but does not affect the main findings from this thesis. It is rather straightforward to include more elaborated deterioration models into the DBN, as long as the number of random variables in each time step is limited. As mentioned in the previous section, this can be achieved in most cases by grouping random variables or replacing less important ones with deterministic parameters in the DBN.

After the deterioration model is chosen, one can define the discretization scheme. As mentioned above, the discretization of continuous random variables in the proposed framework introduces a tradeoff between accuracy and computational cost (including memory allocation and computational complexity) that must be balanced when solving the RBI problem. An adequate discretization scheme can be obtained either from heuristic rules (as in this thesis) or using more sophisticated methods (e.g. Zwirgmaier and Straub 2016). In general, the optimal discretization is case dependent and it is recommendable to compare more than one discretization scheme to prevent potential major errors when estimating system probabilities of failure and the optimal inspection strategy.

Using the optimization parameters of this framework in a different manner allows one to apply it to other problem settings. For example, the framework is applicable to solve reliability-based inspection planning, i.e. instead of optimizing the total expected life-cycle cost one aims at minimizing inspection and repair cost while ensuring a minimum level of reliability. To do this in the proposed framework, one only needs to fix the probability threshold at the system reliability level, and then optimizing the rest of the parameters that define the strategy. Another example is when deciding among multiple types of inspection techniques (e.g. visual inspection, ultrasonic devices, etc.). To solve this problem, one can include one additional optimization parameter that indicates the inspection technique to be used. Then one simply needs to find the expected total cost for each combination of parameters for each value of the inspection technique parameter. As a remark, there is no constraint in how the optimal inspection technique is evaluated in the model. It is possible to have a set of different optimization parameters for each inspection technique (for example, when measurement observations require a different

model or are related to different nodes in the DBN) and then choosing the technique with the combination of parameters that have the smallest expected total cost.

It is also possible to include observations from monitoring systems and sensors in the DBN framework. As already mentioned, the computation time of the inference algorithm is not affected by the amount of observed data. However, it is sensitive to the number of time steps. Therefore, including raw sensor/monitoring data (which can be available in periodicities from minutes to milliseconds) would increase considerably the number of time steps, making the optimization methodology infeasible. As a possibility, one can summarize the sensor or monitoring data and represent it in the DBN model through, for example some basic statistics (e.g. mean, median, standard deviation, minimum, maximum, percentiles) or other aggregated values (frequencies, natural frequencies, equivalent stress ranges for the case of loads) at each time step, so the inference algorithm takes a similar time to update the probabilities as the original setting (Schneider 2019, Kamariotis et al. 2020). As a remark, sensor and monitoring data must be kept in the model at the component level. This means, sensors cannot be associated to a system property (e.g. structure's natural frequency). This constraint comes from the construction of the inference algorithm for the DBN model that requires independence among components given the hyperparameters. If one includes system-level observations (either from sensors or from inspections), then the independence of components given the hyperparameters does not occur, and the exact inference algorithm developed here is not applicable.

Finally, the proposed optimization methodology can also be extended to more complex structural systems. For example, Bismut et al. (2017) obtains the optimal inspection and maintenance strategy for the Zayas frame. In this case, they propose a prioritization index as a proxy of the value of information for inspecting components. The main results of Bismut et al. (2017) confirm the computational efficiency and effectiveness of the DBN framework to solve the optimal inspection planning problem when applied to more real-life cases.

9.2 Future research

This section contains possible extensions of the DBN framework that can improve its applicability to more complex structural systems or deterioration processes. In some cases, the presented extensions might need a small change in the current methodology; in other cases, they could require strong modifications in the assumptions of the framework, making their feasibility a bit uncertain. These are ideas that have arisen during the development of this research as potential continuations of the results obtained here.

Varying initial correlations

The DBN framework assumes that the correlation among the initial deterioration \mathbf{D}_0 , time-dependent parameters $\boldsymbol{\omega}_0$, or time-independent parameters $\boldsymbol{\theta}_0$ (see Figure 8) does not vary among components in the system. This assumption keeps the complexity and computational cost of the inference algorithm at a feasible level. If different correlations among components are present, then it is recommendable to separate the original structural system into subsystems, where the components of each subsystem are equi-correlated. If subsystems are assumed independent, then the solution of the problem would not require any modification of the framework. If dependence among subsystems is to be included, then an additional hierarchical level can be included with a new set of hyperparameters that links them as demonstrated in Paper C. The original inference algorithm would require obtaining the conditional probabilities given all hyperparameters (i.e. original hyperparameters linking components plus additional hyperparameters linking subsystems). Theoretically this is possible, and the complexity of the inference algorithm with respect to the total number of hyperparameter states is linear (see Section B.3.5). However, the size of the conditional probability tables will considerably increase, generating potential memory issues. As stated at the end of Section B.3.2, another alternative is to use the Dunnett-Sobel class (Thoft-Christensen and Murotsu 1986, Kang and Song 2009), which would keep the computational effort at the same level.

Including monitoring and sensor information

As already mentioned in the practical recommendations of Section 9.1, the most critical aspect of including monitoring and sensor data in the DBN framework is its near real-time observability. This information must be summarized, e.g., through some of its statistics, so that the number of time steps in the model is not increased and consequently the computation time remains constant. The optimization problem implies simulating outcomes of monitoring and sensor systems, which requires more detailed and thorough probabilistic models to generate realistic samples than for the inspection case. Further analysis must also be done to calculate the number of samples required to estimate the expected total cost with a given confidence. Finally and most important, one must develop a model to relate the monitor and sensor data to the deterioration amount of the component (e.g. how the observed natural frequency of the component or system is related to the condition of the component). Depending on the type of

observed data, such model will most likely be based on the outcome of a numerical structural analysis made for multiple system configurations.

Defining a more general proxy for the value of information

As mentioned in Section 3.3.1, the heuristic rule for defining which components to inspect first is based on the value of information (VoI). This value is not straightforward to compute. Depending on the structural system, a proxy for the VoI must be defined and its computation should be considerably easier and faster than the VoI. Case study 4.5 and Bismut et al. (2017) define proxies applied to the Daniels system and Zayas frame, respectively. However, other proxies for the VoI could lead to inspection strategies with lower expected costs.

Number of system configurations

In general, the ultimate capacity of a structural system is a function of the capacity of its components. Each combination of possible component capacities defines a different system configuration. In the simple case when a component can have either its full capacity or zero capacity (because of failure), a system with N components can have a total of 2^N different configurations. Considering explicitly all system configurations is in most cases prohibitively expensive for computing the conditional system reliability given the observed data. In some cases, as demonstrated in case study 4.2, components can be grouped, and it is sufficient to consider their cumulative effect on the system condition. In other cases, it is possible to pursue a hierarchical modeling approach also for the mechanical models; such a strategy is utilized in case study 4.3. Alternatively, approximate models of system behavior may be applied (e.g. the model proposed in Straub and Der Kiureghian 2011, which requires only the marginal effect of component failure on the system reliability as an input) or other types of surrogate models. Another possible alternative is to reduce the number of system configurations to consider based on their contribution to the probability of failure (Kim et al. 2013). If an alternative representation of the system configuration is not possible or not convenient, it is also possible to combine the proposed exact algorithm with sampling-based methods. After learning the model using the exact inference algorithm of the DBN framework, one could generate samples of the deterioration conditions in the components and then evaluate the condition of the system to estimate its probability of failure. One can use efficient simulation methods to estimate the low probability of failure, for example sequential importance sampling (Papaioannou et al.

2016). In this way, one would avoid the large computation time of MCMC approaches to learn the model and generate samples of system failures given the data.

Redistribution of stresses and sequential failure

As mentioned in Sections 4.2 and 4.3, the model developed in this thesis for the Daniels' system and Zayas frame considers neither redistribution of stresses after component failures nor sequential failure. The immediate way to include redistribution of stresses to the model is adding links between component states and stresses. However, these new links break the d-separability of the components' layers when the hyperparameters are given and, in consequence, the inference algorithm of the DBN framework does not apply anymore. This would imply making some assumptions to keep the d-separability or developing a new inference algorithm for this extended model. For the case of sequential failure, some approaches have been developed for estimating the sequences that have the largest probability of occurring and producing a system failure (e.g. Kang and Song 2009, Lee and Song 2014). Then, instead of explicitly considering all possible system configurations in the model, one can include these most-likely failure sequences in the model when computing the conditional probability of system failure given component failure. The conditional probability table will not only consider individual component failure, but also those sequences that start with this component failure will be included in the same row. This approximation of the system probability of failure will reduce the number of rows in the conditional table from 2^N (number of system configurations) to $N + 1$ (number of components plus one – no component failure). The main difficulty of this approach is to accurately estimate the sequences with the highest contribution to the system probability of failure (i.e. probability of the sequence times probability of system failure given the sequence) due to the strong impact of stress redistributions in the computation.

Multi-level hierarchical model

The current model utilizes a set of hyperparameters through a one-level hierarchical structure to represent the interdependence among components. This representation assumes that the initial correlation among initial conditions is the same among components. However, this is not always the case for all types of structures. One solution to represent complex structures is to separate the system into several subsystems (e.g. by spatial or operational areas in the structure) and to model each of them separately and independently with the proposed DBN framework. A more accurate approach would be to consider all subsystems as interrelated "components"

through an additional level in the hierarchy of the model (i.e. a second set of hyperparameters that would link all subsystems). Then the inference algorithm would need to be extended and applied to the second hierarchical level because the subsystems, which would keep the property of being independent given the new set of hyperparameters (i.e. the d-separability would be preserved). The extended model implies additional challenges in its development and testing, especially in the direction of computational complexity and applicability of potentially new heuristic rules to keep the computation time at a feasible level.

9.3 Conclusions

This thesis proposes an integral framework to determine optimal inspection-repair strategies for deteriorating structural systems subject to reliability constraints.

At first, a probabilistic multi-hierarchical framework for modeling deterioration is developed, which is able to represent the time dependence and spatial variability of the deterioration process. It accounts for the dependence among corrosion states at different locations due to common influencing factors. In the case study from Section 4.1, this framework is applied to model uniform corrosion deterioration in ship vessels using real thickness measurements obtained during in-service inspection campaigns. Using MCMC as inference algorithm, the posterior distribution of the model parameters is estimated, and the current and future corrosion in the structure. The framework also allows computing probabilities of failure at different levels of the structure (e.g. a single plate failure or a complete cross section failure) using structural reliability methods if a failure criterion is defined. Even though one could use this framework to solve the RBI problem, MCMC can be computationally expensive when solving reliability problems with low probabilities of failure. For this reason, a DBN deterioration framework with a tailor-made inference algorithm is developed to solve the RBI problem more efficiently.

The developed DBN framework – for the first time – enables a system-wide optimization of inspections, which accounts for: a) the interaction among element deterioration states, b) the relation between the reliability of the structural elements and the structural system, and c) the effect of information obtained on one element of the structure on the remaining elements and the overall system. The framework also enables the use of state-of-the-art deterioration models for the individual elements. To tackle the computational challenges associated with this complex pre-posterior optimization problem, a heuristic approach for planning inspections is used, which inspections are informed by practical constraints commonly encountered in the asset integrity management of engineering structures. To compute the expected cost of a

system-wide inspection strategy, a dynamic Bayesian network framework is developed with an accurate, robust, and efficient inference algorithm at the system level to solve the reliability problem for computing probabilities of system failures. The developed inference algorithm is then nested inside a Monte Carlo analysis to account for the uncertainty in the inspection outcomes. The DBN framework was successfully applied in two different case studies (Daniels system and Zayas frame) obtaining fast and accurately probabilities of failure due to fatigue deterioration, and in another case study showing step by step how to solve the optimal inspection planning problem.

References

- Andrade AR and Teixeira PF, (2015). Statistical modelling of railway track geometry degradation using Hierarchical Bayesian models. *Reliability Engineering and System Safety* 142, 169-183.
- Arrow KJ, Blackwell D, Girshick MA, (1949). Bayes and minimax solutions of sequential decision problems. *Econometrica* 17 (3/4): 213-244.
- Ayyub BM, Stambaugh KA, McAllister TA, de Souza GF, Webb D, (2015). Structural Life Expectancy of Marine Vessels: Ultimate Strength, Corrosion, Fatigue, Fracture, and Systems. *ASCE-ASME Journal of Risk and Uncertainty in Engineering Systems, Part B: Mechanical Engineering*, 1(1):011001-011001-13.
- Banerjee S, Carlin BP, Gelfand AE, (2015). Hierarchical modeling and analysis for spatial data. CRC Press, Second Edition.
- Bensi MT, Der Kiureghian A, Straub D, (2013). Efficient Bayesian network modeling of systems. *Reliability Engineering & System Safety*, 112: 200-213.
- Bensi MT, Der Kiureghian A, Straub D, (2011). Bayesian network modeling of correlated random variables drawn from a Gaussian random field. *Structural Safety*, 33(6), pp. 317-332.
- Bismut E and Straub D, (submitted). Optimal Adaptive Inspection and Maintenance Planning for Deteriorating Structural Systems.
- Bismut E, Luque J, Straub D, (2017). Optimal prioritization of inspections in structural systems considering component interactions and interdependence. *Proceedings ICOSAR 2017, Vienna*
- Brownjohn JMW, (2007). Structural health monitoring of civil infrastructure. *Philosophical transactions of the Royal Society. Mathematical, Physical and engineering sciences*, 365: 589-622.
- Chang KC and Chen HD, (2005). Efficient inference for hybrid dynamic Bayesian networks. *Proc. SPIE 5429, Signal Processing, Sensor Fusion, and Target Recognition XIII*, 402.
- Daniels HE, (1945). The statistical theory of the strength of bundles of threads, Part I. *Proceedings of the Royal Society of London, Series A*, 183(995), 405-435.
- De Boer PT, Kroese DP, Mannor S, Rubinstein RY, 2005. A tutorial on the cross-entropy method. *Annals of operations research* 134 (1), 19-67.
- Ditlevsen O and Madsen HO, (1996). *Structural reliability methods*, Wiley, New York.
- Dong Y and Frangopol D, (2015). Risk-informed life-cycle optimum inspection and maintenance of ship structures considering corrosion and fatigue. *Ocean Engineering*, 101, 161-171.
- Engelund S, Faber MH, Sørensen JD, Bloch A, (2000). Approximations in inspection planning. In *Proc. 8th ASCE Speciality Conference on Probabilistic Mechanics and Structural Reliability*, Notre Dame, Paris, France.
- Ellingwood BR and Mori Y, (1993). Probabilistic methods for condition assessment and life prediction of concrete structures in nuclear power plants. *Nuclear Engineering and Design*, 142, 155-166
- Faber MH, (2002). Risk Based Inspection - the Framework. *Structural Engineering International*, 12(3): 186-194
- Faber MH, Engelund S, Sørensen JD, Bloch A, (2000). Simplified and generic risk based inspection planning. *Proc. 19th Offshore Mechanics and Arctic Engineering Conference*, ASME.
- Faber MH, Kroon IB, Kragh E, Bayly D, Decosemaeker P, (2002). Risk assessment of decommissioning options using Bayesian networks. *Journal of Offshore Mechanics and Arctic Engineering*, 124(4), 231-238.
- Faber MH and Sørensen JD, (2000). Aspects of Inspection Planning: Quality and Quantity. In *Applications of Statistics and Probability-Civil Engineering Reliability and Risk Analysis: Proceedings of the 8th International Conference on Applications of Statistics and Probability in Civil Engineering*, 739-746.
- Faber MH, Sørensen JD, Kroon IB, (1992a). Optimal inspection strategies for offshore structural systems. In *Proceedings of the 11th International Conference on Offshore Mechanics and Arctic Engineering*, 145-151.
- Faber MH, Sørensen JD, Rackwitz R, Thoft-Christensen P, Lebas G, (1992b). Reliability analysis of an offshore structure: A Case Study - I. *Proceedings OMAE 1992, Calgary, Canada* .
- Faber MH, Sørensen JD, Tychsen J, Straub D, (2005). Field Implementation of RBI for Jacket Structures. In: *Journal of Offshore Mechanics and Arctic Engineering, Trans. ASME*, 127(3): 220-226.
- Faber MH, Straub D, Maes MA, (2006). A computational framework for risk assessment of RC structures using indicators. *Computer-Aided Civil and Infrastructure Engineering* 21(3), 216-230.

- Farrar CR and Worden K, (2007). An introduction to structural health monitoring. *Philosophical transactions of the Royal Society. Mathematical, Physical and engineering sciences*, 365(1851): 303-315.
- Fenton N and Neil M, (2012). *Risk assessment and decision analysis with Bayesian networks*. CRC Press.
- Frangopol DM, Kallen MJ, Van Noortwijk JM, (2004). Probabilistic models for life-cycle performance of deteriorating structures: review and future directions. *Progress in Structural Engineering and Materials*, 6(4): 197-212.
- Friis-Hansen A, (2001). *Bayesian Networks as a Decision Support Tool in Marine Applications*. Department of Naval Architecture and Offshore Engineering, PhD thesis, TU Denmark.
- Gamerman D and Lopes HF, (2006). *Markov Chain Monte Carlo, stochastic simulation for Bayesian inference*. 2nd Ed. Chapman & Hall/CRC, Florida, USA.
- Gardiner CP and Melchers RE, (2003). Corrosion analysis of bulk carriers, Part I: operational parameters influencing corrosion rates. *Marine Structures* 16, 547-566.
- Gelman A, Carlin JB, Stern HS, Rubin DB, (2004). *Bayesian Data Analysis*. 2nd ed., Florida, USA: Chapman & Hall/CRC
- Germanischer Lloyd Group, (2009). *Rules for classification and construction: II Materials and welding*. Germanischer Lloyd Aktiengesellschaft, Hamburg.
- Gilks WR, Richardson S, Spiegelhalter DJ, (1996). *Markov Chain Monte Carlo in practice*. Chapman & Hall/CRC.
- Gollwitzer S and Rackwitz R, (1990). On the reliability of Daniels systems. *Structural Safety*, 7(2-4), 229-243.
- Grêt-Regamey A and Straub D, (2006). Spatially explicit avalanche risk assessment linking Bayesian networks to a GIS. *Natural Hazards and Earth System Sciences*, 6(6), pp. 911-926.
- Guedes Soares C, (1988). *Reliability of Marine Structures*. Reliability Engineering, Kluwer Academic Publishers, pp. 513-559.
- Guedes Soares C and Garbatov Y, (1999). Reliability of maintained, corrosion protected plates subjected to non-linear corrosion and compressive loads. *Marine Structures* 12, pp. 425-45.
- Guedes Soares C and Garbatov Y, (1997). Reliability assessment of maintained ship hulls with correlated corroded elements. *Marine Structures* 10, pp. 629-653.
- Hanea A, Kurowicka D, Cooke R, (2006). Hybrid method for quantifying and analyzing Bayesian belief nets. *Quality and Reliability Engineering International* 22(6), 613-729.
- Hergenröder M and Rackwitz R, (1992). Maintenance strategy for RC-elements under normal outdoor exposure conditions. *Bridge Rehabilitation. Proceedings of the 3rd International Workshop on Bridge Rehabilitation*.
- Herzberg E, Chan T, Chang P, Kelly A, Kumaran M, O'Meara N, (2010). The annual cost of corrosion for navy ships. Report MEC81T3.
- Jensen FV and Nielsen TD, (2007). *Bayesian networks and decision graphs*. Second Edition. New York, NY, Springer (Information Science and Statistics).
- Jordaan IJ, (2005). *Decisions under uncertainty. Probabilistic analysis for engineering decisions*. Cambridge: Cambridge University Press.
- Kamariotis A, Straub D, Chatzi E, 2020. Optimal maintenance decisions supported by SHM: A benchmark study. IALCCE 2020: The Seventh International Symposium on Life-Cycle Civil Engineering.
- Kang WH and Song J, (2010). Evaluation of multivariate normal integrals for general systems by sequential compounding. *Structural Safety* 32(1), pp 35-41.
- Kang WH and Song J, (2009). Efficient reliability analysis of general systems by sequential compounding using Dunnett-Sobel correlation model. *Proc. 10th International Conference on Structural Safety and Reliability (ICOSSAR2009)*, Osaka, Japan.
- Keßler S, Fischer J, Straub D, Gehlen C, (2014). Updating of service life prediction of reinforced concrete structures with potential mapping. *Cement and Concrete Composites*, 47, 47-52.
- Kim DS, Ok SY, Song J, Koh HM, (2013). System reliability analysis using dominant failure modes identified by selective searching technique. *Reliability Engineering & System Safety*, 119, 316-331.
- Kochenderfer MJ, (2015). *Decision making under uncertainty: Theory and application*. MIT Lincoln Laboratory Series, The MIT Press.

- Kumar R, Cline D, Gardoni P, (2015). A stochastic framework to model deterioration in engineering systems. *Struct Safety*, 53:36–43.
- Langseth H, Nielsen TD, Rumí R., Salmerón A., (2009). Inference in hybrid Bayesian networks. *Reliability Engineering and System Safety*, 94(10), 1499-1509.
- Lauritzen SL and Nilsson D, (2001). Representing and solving decision problems with limited information. *Management Science*, 47(9): 1235-1251.
- Lee YJ and Song J, (2014). System reliability updating of fatigue-induced sequential failures. *Journal of Structural Engineering*, 140(3), 04013074-1~16.
- Lin YK, Yang JN, (1985). A stochastic theory of fatigue crack propagation. *AIAA J.*, 23(1), 117-124.
- Liu PL and Der Kiureghian A, (1986). Multivariate distribution models with prescribed marginals and covariances. *Probabilistic Engineering Mechanics*, 1(2), 105-112.
- Lotsberg I, Sigurdsson G, Wold PT, (2000). Probabilistic inspection planning of the Asgard A FPSO hull structure with respect to fatigue. *Journal of Offshore Mechanics and Arctic Engineering*, 122(2), 134-140.
- Lunn D, Spiegelhalter D, Thomas A, Best N, (2009). The BUGS project: Evolution, critique and future directions (with discussion), *Statistics in Medicine* 28, pp. 3049-3082.
- Luque J and Straub D, (2019). Risk-based optimal inspection strategies for structural systems using dynamic Bayesian networks. *Structural Safety*, 76, 68-80.
- Luque J and Straub D, (2016). Reliability analysis and updating of deteriorating structural systems with dynamic Bayesian networks. *Structural Safety*, 62, 34-46.
- Luque J and Straub D, (2015). Reliability analysis of monitored deteriorating structural systems with dynamic Bayesian networks. *Proc. 12th International Conference on Applications of Statistics and Probability in Civil Engineering*, Vancouver, Canada.
- Luque J and Straub D, (2013). Algorithms for optimal risk-based planning of inspections using influence diagrams. *Proc. 11th International Probabilistic Workshop*, Brno, Czech Republic.
- Luque J, Hamann R, Straub D, (2017). Spatial probabilistic modeling of corrosion in ship structures. *ASCE-ASME Journal of Risk and Uncertainty in Engineering Systems, Part B: Mechanical Engineering*, 3(3): 031001-12.
- Luque J, Hamann R, Straub D, (2014). Spatial model for corrosion in ships and FPSOs. *Proceedings of OMAE, 33rd International Conference on Offshore Mechanics and Arctic Engineering*, San Francisco, CA.
- Madsen HO, (1997). Stochastic modeling of fatigue crack growth and inspection. IN SOARES, C.G. (Ed.) *Probabilistic Methods for Structural Design*. Kluwer Academic Publishers. Printed in the Netherlands.
- Madsen HO, (1987). Model updating in reliability theory. *Proceedings ICASP 5*. Vancouver, Canada.
- Madsen HO, Krenk S, Lind NC, (1985). *Methods of structural safety*. Englewood Cliffs, NJ, Prentice Hall.
- Madsen HO, Sørensen JD, Olesen R, (1989). Optimal inspection planning for fatigue damage of offshore structures. *Proceedings ICOSSAR 1989*, San Francisco, United States.
- Maes MA, (2003). Modelling infrastructure deterioration risks. *International Journal of Modelling and Simulation* 23/1, S. 43-51.
- Maes MA, (2002). Updating performance and reliability of concrete structures using discrete empirical Bayes methods. *Journal of Offshore Mechanics and Arctic Engineering* 124.4: 239-244.
- Maes MA and Dann M, (2007). Hierarchical Bayes methods for systems with spatially varying condition states. *Canadian Journal of Civil Engineering* 34, pp. 1289- 1298
- Maes MA, Dann M, Breitung K, Brehm E, (2008). Hierarchical modeling of stochastic deterioration. Graubner, Schmidt & Proske: *Proceedings of the 6th International Probabilistic Workshop*, Darmstadt.
- Mahadevan S, Zhang R, Smith N, (2001). Bayesian networks for system reliability reassessment. *Structural Safety*, 23(3), 231-251.
- Malioka V, (2009). Condition indicators for the assessment of local and spatial deterioration of concrete structures. Ph.D thesis, ETH Zürich, Switzerland.
- Maljaars J and Vrouwenvelder ACWM, (2014). Probabilistic fatigue life updating accounting for inspections of multiple critical locations. *International Journal of Fatigue* 68, 24-37
- Marquez D, Neil M, Fenton N, (2010). Improved reliability modeling using Bayesian networks and dynamic discretization. *Reliability Engineering and System Safety* 95(4), 412-425.

- Melchers RE, (2003). Modeling of marine immersion corrosion for mild and low-alloy steels-Part 1: Phenomenological model. *Corrosion* Vol. 59, No. 4.
- Melchers RE, (1999). Corrosion uncertainty modeling for steel structures. *Constructional Steel Research* 52, pp. 3-19.
- Melchers RE, (1998). Probabilistic modelling of immersion marine corrosion. In: Shiraishi N, Shinozuka M, Wen Y K, editors. *Structural safety and reliability*, vol. 3. Rotterdam: Balkema, pp. 1143-9.
- Melchers RE, Jeffrey R, (2007). Probabilistic models for steel corrosion loss and pitting of marine infrastructure. *Reliability Engineering and System Safety* 93, pp. 423-432.
- Memarzadeh M and Pozzi M, (2015). Integrated inspection scheduling and maintenance planning for infrastructure systems. *Computer-Aided Civil and Infrastructure Engineering* 31(6), 403-415.
- Memarzadeh M, Pozzi M, Kolter JZ, (2014). Optimal planning and learning in uncertain environments for the management of wind farms. *ASCE J. of Computing in Civil Engineering*, DOI: 10.1061/(ASCE)CP. 1943-5487.0000390.
- Mendoza J, Bismut E, Straub D, Köhler J, (2021). Risk-based fatigue design considering inspections and maintenance. *ASCE-ASME Journal of Risk and Uncertainty in Engineering Systems, Part A: Civil Engineering*, 7(1): 04020055.
- Mishalani RG, Madanat SM, (2002). Computation of infrastructure transition probabilities using stochastic duration models. *Journal of Infrastructure Systems*, 8(4), 139-148.
- Moan T, (2005): Reliability-based management of inspection, maintenance and repair of offshore structures. *Structure and Infrastructure Engineering*, 1(1), 33-62.
- Moan T and Song R, (2000). Implications of inspection updating on system fatigue reliability of offshore structures. *Journal of Offshore Mechanics and Arctic Engineering*, 122, 173-180.
- Moan T, Vardal OT, Heelewig NC, Skjoldli K, (2000). Initial crack depth and POD values inferred from in-service observations of cracks in North Sea jackets. *Journal of Offshore Mechanics and Arctic Engineering*, 122, 157-162.
- Murphy KP, (2002). *Dynamic Bayesian networks: Representation, inference and learning*. Ph.D thesis, Univ. of California, Berkeley, Calif, 268.
- NACE International, (2016). *International measures of prevention, application, and economics of corrosion technologies study*. Houston, TX, USA.
- Neil M, Tailor M, Marquez D, (2007). Inference in hybrid Bayesian networks using dynamic discretization. *Statistics and Computing* 17(3), p. 219-233.
- Nielsen JJ, Sørensen JD, (2015). Risk-based decision making for deterioration processes using POMDP. *Proceedings ICASP12, Vancouver, Canada*.
- Nielsen JJ, Sørensen JD, (2014). Methods for risk-based planning of O&M of wind turbines. *Energies*, 7(10), 6645-6664.
- Nielsen JJ, Sørensen JD, (2011). Risk-based operation and maintenance of offshore wind turbines using bayesian networks. *Proceedings of the 11th International Conference on Applications of Statistics and Probability in Civil Engineering: 311-317, CRC Press LLC*.
- Nielsen JJ, Sørensen JD, (2010). Bayesian networks as a decision tool for O&M of offshore wind turbines. *Proceedings 5th Asranet Conference. Edinburgh, UK*.
- Ntzoufras I, (2009). *Bayesian modeling using WinBUGS*. John Wiley & Sons, Inc. New Jersey, USA.
- Paik JK, Thayamballi AK, Park YI, Hwang JS, (2004). A time-dependent corrosion wastage model for seawater ballast tank structures of ships. *Corrosion Science* 46, pp. 471-486.
- Papaoannou I, Papadimitriou C, Straub D, (2016). Sequential importance sampling for structural reliability analysis. *Structural Safety*, 62, 66-75.
- Papakonstantinou KG, Shinozuka M, (2014). Planning structural inspection and maintenance policies via dynamic programming and Markov processes. Part II: POMDP implementation. *Reliability Engineering and System Safety*.
- Pearl J, (1988). *Probabilistic reasoning in intelligent systems: networks of plausible inference*. The Morgan Kaufmann series in representation and reasoning. San Mateo, Calif., Morgan Kaufmann Publishers.

- Pedersen C, Nielsen JA, Riber HO, Madsen HO, Krenk S, (1992). Reliability based inspection planning for the Tyra field. Proceedings OMAE 1992, Calgary, Canada.
- Qin H, Zhou W, Zhang S, (2015). Bayesian inferences of generation and growth of corrosion defects on energy pipelines based on imperfect inspection data. *Reliability Engineering and System Safety* 144, 334-342.
- Qin J and Faber MH, (2012). Risk management of large RC structures within a spatial information system. *Computer-Aided Civil and Infrastructure Engineering*, 27(6), 385-405.
- Qin S and Cui W, (2003). Effect of corrosion models on the time-dependent reliability of steel plated elements. *Marine Structures* 16, 15-34.
- Raiffa H and Schlaifer R, (1961). *Applied statistical decision theory*. Cambridge, Cambridge University Press.
- Raudenbush SW and Bryk AS, (2008). *Hierarchical linear models, applications and data analysis methods*. 2nd Ed. SAGE Publications, Inc. California, USA.
- Robelin CA and Madanat SM, (2007). History-Dependent Bridge Deck Maintenance and Replacement Optimization with Markov Decision Processes. *Journal of Infrastructure Systems* 13(3), 195-201.
- Rocha MM and Schuëller GI, (1996). A probabilistic criterion for evaluating the goodness of fatigue crack growth models. *Engineering Fracture Mechanics*, 53(5), 707-731.
- Russell SJ and Norvig P, (2003). *Artificial intelligence: A modern approach*. 2nd Ed. Prentice-Hall, Englewood Cliffs, N.J.
- Schneider R, (2019). Time-variant reliability of deteriorating structural systems conditional on inspection and monitoring data. PhD thesis, Technische Universität München.
- Schneider R, Fischer J, Bügler M, Nowak M, Thöns S, Borrmann A, Straub D, (2015). Assessing and updating the reliability of concrete bridges subjected to spatial deterioration - principles and software implementation. *Structural Concrete*, 16(3): 356-365.
- Schneider R, Thöns S, Straub D, (2017). Reliability analysis and updating of structural systems with subset simulation. *Structural Safety*, 64: 20-36.
- Schöbi R and Chatzi EN, (2016). Maintenance planning using continuous-state partially observable Markov decision processes and non-linear action models. *Structure and Infrastructure Engineering*, 12(8): 977-994.
- Shenoy PP and West JC, (2011). Inference in hybrid Bayesian networks using mixtures of polynomials. *International Journal of Approximate Reasoning*, 52(5), 641-657
- Shi W, (1993). In-service Assessment of Ship Structures: Effects of General Corrosion on Ultimate Strength. *Transactions Royal Institution of Naval Architects*, 135, pp. 77-91.
- Shreir FF, (1976). *Corrosion*, Vol. 3. Newnes-Butterworths, London.
- Skjong R and Torhaug R, (1991). Rational methods for fatigue design and inspection planning of offshore structures. *Marine Structures*, 4(4), 381-406.
- Sone H, Magaino A, Yamamoto N, Harada S, (2003). Evaluation of thickness diminution in steel plates for the assessment of structural condition of ships in service. *Nippon Kaiji Kyokai (ClassNK) Tech Bulletin*.
- Sørensen JD, Faber MH, Rackwitz R, Thoft-Christensen P, (1991). Modelling in optimal inspection and repair. *Proc. OMAE 1991*. 10th, Stavanger, Norway.
- Southwell CR, Bultman JD, Hummer Jr CW, (1979). Estimating of service life of steel in seawater. In: Schumacher M, editor. *Seawater corrosion handbook*. New Jersey: Noyes Data Corporation, pp. 374-87.
- Stephens RI, (2001). *Metal fatigue in engineering*. 2. ed. New York, NY, Wiley.
- Stewart MG and Mullard JA, (2007). Spatial time-dependent reliability analysis of corrosion damage and the timing of first repair for RC structures. *Engineering Structures* 29(7), 1457-1464.
- Straub D, (2014). Value of Information Analysis with Structural Reliability Methods. *Structural Safety*, (49): 75-86
- Straub D, (2011a). Reliability updating with equality information. *Probabilistic Engineering Mechanics*, 26(2), pp. 254-258.
- Straub D, (2011b) Reliability updating with inspection and monitoring data in deteriorating reinforced concrete slabs. *Proceedings ICASP11*, Zürich, Switzerland.
- Straub D, (2009). Stochastic modeling of deterioration processes through dynamic Bayesian networks. *Journal of Engineering Mechanics*, *Trans. ASCE*, 135(10), pp. 1089-1099.

- Straub D and Der Kiureghian A, (2011). Reliability Acceptance Criteria for Deteriorating Elements of Structural Systems. *Journal of Structural Engineering*, Trans. ASCE, 137(12), 1573-1582.
- Straub D and Der Kiureghian A, (2010). Bayesian network enhanced with structural reliability methods. Part A: Theory & Part B: Applications. *Journal of Engineering Mechanics*, Trans. ASCE, 136(10), 1248-1270.
- Straub D and Faber MH, (2007). Temporal Variability in Corrosion Modeling and Reliability Updating. *Journal of Offshore Mechanics and Arctic Engineering*, Trans. ASME, 129(4), pp. 265-272.
- Straub D and Faber MH, (2006). Computational aspects of risk based inspection plan-ning. *Computer-Aided Civil and Infrastructure Engineering*, 21(3): 179-192.
- Straub D and Faber MH, (2005): Risk based inspection planning for structural systems. *Structural Safety*, 27(4): 335-355.
- Straub D and Faber MH, (2004a). System Effects in Generic Risk Based Inspection Planning. *Journal of Offshore Mechanics and Arctic Engineering*, Trans. ASME, 126(3): 265-271.
- Straub D and Faber MH, (2004b). On the relation between inspection quantity and quality. In *e-Journal of Nondestructive Testing*, 9(7): 1-14.
- Straub D and Papaioannou I, (2015). Bayesian updating with structural reliability methods. *ASCE Journal of Engineering Mechanics* 141(3), 04014134.
- Straub D, Chatzi E, Bismut E, Courage W, Döhler M, Faber MH, Köhler J, Lombaert G, Omenzetter P, Pozzi M, Thöns S, Val D, Wenzel H, Zonta D, (2017). Value of information: A roadmap to quantifying the benefit of structural health monitoring. *Proc. 12th International Conference on Structural Safety & Reliability ICOSSAR*
- Straub D, Malioka V, Faber MH, (2009). A framework for the asset integrity management of large deteriorating concrete structures. *Structure and Infrastructure Engineering*, 5(3): 199-213.
- Straub D, Papaioannou I, Betz W, (2016). Bayesian analysis of rare events. *Journal of Computational Physics*, 314, 538-556.
- Straub D, Schneider R, Bismut E, Kim H, (2020). Reliability analysis of deteriorating structural systems. *Structural Safety* (82), 101877
- Swanson L, (2001). Linking maintenance strategies to performance. *International Journal of Production Economics*, 70: 237-244.
- Tang WH, (1973). Probabilistic updating of flaw information. *Journal of Testing and Evaluation*, 1(6), 459-467.
- Tao Z, Corotis RB, Ellis JH, (1995). Reliability-Based Structural Design with Markov Decision Processes. *Journal of Structural Engineering* 121(6), 971-980.
- Thoft-Christensen P and Murotsu Y, (1986). *Application of structural systems reliability theory*, Springer.
- Thoft-Christensen P and Sørensen JD, (1987). Optimal Strategy for Inspection and Repair of Structural Systems. *Civil Engineering Systems*, 4(2), 94-100.
- Torres-Toledano JG and Sucar LE, (1998). Bayesian networks for reliability analysis of complex systems. *Ibero-American Conference on Artificial Intelligence*. Springer Berlin Heidelberg.
- Val DV, Stewart MG, Melchers RE, (2000). Life-Cycle Performance of RC Bridges: Probabilistic Approach. *Computer-Aided Civil and Infrastructure Engineering* 15(1), 14-25.
- Vanmarcke EH, 2010. *Random fields. Analysis and synthesis*. World Scientific Publishing Co.
- Vrouwenvelder T, (2004). Spatial correlation aspects in deterioration models. *Proc., 2nd Int. Conf. Lifetime-Oriented Design Concepts*, F. Stangenberg, ed., Ruhr-Universität Bochum, Germany.
- Wang G, Spencer J, Elsayed T, (2003a). Estimation of corrosion rates of structural members in oil tankers. *Proceedings of OMAE, 22nd International Conference on Offshore Mechanics and Arctic Engineering*.
- Wang G, Spencer J, Sun H, (2003b). Assessment of corrosion risks to aging ships using an experience database. *Proceedings of OMAE, 22nd International Conference on Offshore Mechanics and Arctic Engineering*.
- Weber P, Medina-Oliva G, Simon C, Lung B, (2012). Overview on Bayesian networks applications for dependability, risk analysis and maintenance areas. *Eng. Appl. Artif. Intel.*, 25(4), 671-682.
- Wells T and Melchers RE, (2014). An observation-based model for corrosion of concrete sewers under aggressive conditions. *Cement and Concrete Research*, 61, 1-10.
- Yang JN and Trapp WJ, (1975). Inspection frequency optimization for aircraft structures based on reliability analysis. *Journal of Aircraft*, 12(5), 494-496.

- Yang JN and Trapp WJ, (1974). Reliability analysis of aircraft structures under random loading and periodic inspection. *AIAA Journal*, 12(12), 1623-1630.
- Ying L and Vrouwenvelder ACWM, (2007). Service life prediction and repair of concrete structures with spatial variability. *HERON*, 52, No. 4.
- Zayas V, Mahin SA, Popov EP, (1980). Cyclic inelastic behavior of steel offshore structures. Univ. of California, Berkeley, Earthquake Engineering Research Center Report No. UCCB/EERC-80/27.
- Zhang S, Zhou W, Al-Amin M, Kariyawasam S, Wang H, (2014). Time-dependent corrosion growth modeling using multiple ILI data. *Journal of Pressure Vessel Technology* 136, 1-7.
- Zhu J and Collette M, (2015). A dynamic discretization method for reliability inference in Dynamic Bayesian Networks. *Reliability Engineering & System Safety*, 138, 242-252.
- Zwirgmaier K and Straub D, (2016). A discretization procedure for rare events in Bayesian networks. *Reliability Engineering & System Safety*, 153: 96-109.